universität wien

DIPLOMARBEIT

Titel der Diplomarbeit

Targeted Meiotic Recombination in *Arabidopsis thaliana*

angestrebter akademischer Grad

Magister der Naturwissenschaften (Mag. rer. nat.)

Verfasser:	Michael Peter Janisiw
Matrikel-Nummer:	9804391
Studienrichtung (lt. Studienblatt):	A490 Molekulare Biologie
Betreuer:	Dr. Peter Schlögelhofer
	Univ.-Prof. Dr. Dieter Schweizer

Wien, am 4. Mai 2009

Dedicated to Josef, Marieluise and Eva.

Table of Contents

1. Abstract 9
2. Introduction 11
2.1. *Arabidopsis thaliana* - a versatile model organism 11
2.2. The Cell Cycle 12
2.3. Mitotic Cell Division 12
2.4. The Role of Sexual Reproduction in the *Arabidopsis* Life Cycle 15
2.5. Meiotic Cell Division 16
2.5.1. DSB Formation: Initiation of Meiotic Recombination 18
2.5.2. Meiotic Recombination: Early Steps in DSB Repair 20
2.5.3. Meiotic Recombination: Control and Regulation of Crossover Formation 21
2.5.4. Chromosome Synapsis 25
2.5.5. Final Stages of Meiotic Division 27
2.6. Hotspots of Meiotic Recombination 28
2.7. Generation of Artificial Hotspots of Recombination 30
2.8. Polydactyl Zinc-Finger Proteins, Meiosis-specific Nucleases 32
2.9. Aims and Objectives 37
3. Results 39
3.1. General *At*SPO11-1 Fusion Protein Construction Strategy 39
3.2. Generation of *At*SPO11-1-PZF Fusion Proteins 42
3.2.1. Design and Construction of PZF DNA Binding Motifs 42
3.2.2. *In-vitro* Analysis of 4xZF DNA Binding Activity 46
3.2.3. Fusion of *At*SPO11-1 with 4xZF DNA Binding Motifs 47
3.2.4. Fusion of *At*SPO11-1-*CSR1*-ZFP Constructs with *c-Myc* Protein Tags 50
3.3. Complementation Analysis of *At*SPO11-1-PZF Variants 53
3.3.1. Segregation Analysis 58
3.4. Detection of *18xMyc* Constructs in Cell Suspension Culture 62
3.5. Generation of Test Systems to Quantify and Monitor Locus-specific Recombination Events 65
4. Discussion 71
4.1. Generation of *At*SPO11-PZF Fusion Proteins 71
4.2. Complementation Analysis of *At*SPO11-1-ZF Variants 73
4.3. Detection of 18xMyc Constructs in Cell Suspension Culture 74

4.4. Experimental Outlook 75
4.4.1. Detection of *At*SPO11-1-PZF Fusion Protein Expression 75
4.4.2. Extended Analysis of *At*SPO11-1-PZF Variants 76
4.4.3. Confirmation of DNA binding activity of *At*SPO11-1-PZF Fusion Proteins 76
4.4.4. Confirmation of DNA cleavage activity of *At*SPO11-1-PZF Fusion Proteins Quantification of Locus-specific Recombination Events 77
4.4.5. Generation of further *At*SPO11-PZF Fusion Proteins 78
4.4.6. Targeted Meiotic Recombination in Crop Plants 79
5. Materials and Methods 81
5.1. Media and Solutions 81
5.1.1. Bacterial Media 81
5.1.2. Plant Media 81
5.2. Plant Work 82
5.2.1. Seed Sterilization 82
5.2.2. Growth Conditions 82
5.2.3. Transformation of *Agrobacterium tumefaciens* 82
5.2.4. Transformation of *Arabidopsis thaliana* Cell Culture 83
5.2.5. *In-planta* Transformation 83
5.2.6. Selection of Transgenic Plant Seedlings 84
5.2.7. Crossing of Mutant *Arabidopsis* Lines 84
5.2.8. Analysis of Fluorescent Pollen Tetrads 84
5.3. DNA Work 85
5.3.1. DNA Preparation from *E.coli* 85
5.3.2. High-Quality Grade DNA Preparation from *E.coli* 85
5.3.3. DNA Preparation from *Agrobacterium tumefaciens* 86
5.3.4. PCR-Grade DNA Preparation from *Arabidopsis thaliana* 86
5.3.5. High-Quality Grade DNA Preparation from *Arabidopsis thaliana* 86
5.3.6. Restriction Endonuclease Digest 87
5.3.7. DNA Gel-Electrophoresis 87
5.3.8. DNA Gel Extraction and Precipitation 87
5.3.9. DNA Quantification and Plasmid DNA Ligation 88
5.3.10. Transformation of chemically-competent *E. coli* 88
5.3.11. PCR Conditions 89
5.3.12. *Atspo11-1-2* Genotype Determination 90
5.3.13. Sequencing Reactions 90

5.4. Generation of *At*SPO11-1-PZF Fusion Proteins 91
5.4.1. Fusion of *At*SPO11-1 with 4xZF DNA Binding Motifs 91
5.4.2. Fusion of *At*SPO11-1-*CSR1*-ZFP Constructs with 18xMyc Protein Tags 92
5.5. Protein Work 92
5.5.1. Protein Isolation from *Arabidopsis thaliana* Cell Suspension Culture 92
5.5.2. Protein Gel 93
5.5.3. Western Blot 93
6. Supplementary Information 95
6.1. Oligonucleotide Primer 95
6.2. Vectors and Construct Maps 95
6.3. Sequence Information 101
7. References 103
8. Abbreviations 117
9. Acknowledgments 119
10. Curriculum vitae 121
11. Zusammenfassung 125

1. Abstract

Sexually reproducing eukaryotes need to maintain their chromosome number across generations. During meiosis two rounds of chromosome segregation that finally lead to the formation of four haploid gamete precursors follow one round of DNA replication. During this process genetic diversity is increased by recombination of paternal and maternal homologous chromosomes. Moreover, chiasmata form as a consequence of the reciprocal recombination events and are essential for regular chromosome segregation during the first meiotic division.

The key event of this process is controlled DNA double strand break (DSB) formation, which is a prerequisite for subsequent homologous recombination (HR). Sites of DSB induction are not randomly distributed, but preferentially formed at discrete loci within certain genomic regions, the hotspots of meiotic recombination. The central protein of meiotic DNA DSB formation is the conserved enzyme SPO11. In *Arabidopsis thaliana* three different *SPO11* genes exist, of which *AtSPO11-1* and *AtSPO11-2* are involved in meiotic DSB induction.

The major aim of this study was to target the meiotic recombination machinery to specific loci within the *Arabidopsis* genome. My strategy involved the creation of a series of fusion proteins, with *At*SPO11 fused to different C-terminal zinc-finger (ZF) DNA binding proteins. As a consequence, introduced DSBs are anticipated to be generated at the target site of the respective ZF protein. Repair by the HR pathway will lead to exchange of paternal and maternal genetic information at a chosen locus. Different zinc-finger constructs were designed to target an endogenous *Arabidopsis* locus. Introduction of a *c-Myc* epitope enabled biochemical manipulation of transgenic fusion proteins. Successful complementation analysis confirmed that the assessed fusion proteins are functional *in-planta*. Future work will include the generation of *At*SPO11-2-ZF fusion proteins as well.

The *CSR1* locus as a target for the ZF fusion proteins was carefully chosen because of its unique characteristics. Two mutant alleles *crs1-1* and *csr1-2* are available, flanking the ZF target sites, respectively, and conferring resistance to two different classes of herbicides. The naturally given very low intragenic recombination rate between *csr1-1* and *csr1-2* will allow to detect low-level induction of recombination due to SPO11-ZF induced DSB formation.

Furthermore, the different tester lines harboring SPO11-ZF constructs, and visual markers for screening recombination at the ZF target locus have been combined by crossings. Induction of locus-specific meiotic recombination will result in a *trans* to *cis* exchange of marker configuration, which will be scored by fluorescent pollen signal exchange or by occurence of double herbicide resistance in subsequent generations. Apart from stimulating the mere exchange of genetic markers, introduction of locus-specific DSBs might allow for the integration of ectopic homologous DNA sequences, possibly opening new roads in the generation of transgenic organisms.

2. Introduction

2.1. *Arabidopsis thaliana* - a versatile model organism

The small crucifer *Arabidopsis thaliana* is a small flowering annual plant that displays useful characteristics that contribute to the plants utilization as an experimental model organism for the study of plant molecular biology (reviewed in Meyerowitz, 1989; Meinke *et al*., 1998; Somerville *et al*., 2002). The fast-growing, self-fertile weed plant displays a rapid life cycle of four to six weeks from germination to mature seed under continuous illumination with prolific seed production even at cultivation in restricted space (Pruit and Meyerowitz, 1986; Gepstein and Horwitz, 1995).

Arabidopsis has a small genome, consisting of five chromosomes spanning a genome size of 125 Mb, which was fully sequenced by the Arabidopsis Genome Initiative (AGI, 2000). Over the years, extensive genetic and physical maps of all 5 chromosomes have been established, covering and integrating new sets of markers, including mutants (Koornneef *et al*., 1983), restriction fragment length polymorphisms (RFLPs; Chang *et al*., 1988; Hauge *et al*., 1993), cleaved amplified polymorphic sequences (CAPS; Jarvis *et al*., 1994), and microsatellite loci (Bell and Ecker, 1994).

Efficient mutagenesis protocols using chemical mutagens, like the alkylating agent ethylmethanesulfonate (EMS), radiation or insertional mutagenesis with T-DNA have been developed (Koornneef *et al*., 1982; Koncz *et al*., 1990; Feldmann, 1991). In parallel a multinational research community of academic, government and industry laboratories has emerged, establishing a large base of mutants, genetic mapping, gene sequences libraries and online resources in a remarkably short time (Koncz *et al*., 1992; Rhee *et al*., 2003).

Though *Arabidopsis thaliana* is not a valuable crop plant itself, the plant is a member of the *Brassicaceae* family, which includes also cultivated species such as cabbage, radish and canola. By this relationship, genes isolated from *Arabidopsis* can be used to find their homologs in crop plants. Likewise, fundamental mechanisms can be understood in a model plant, and applied to crop plants like *Brassica napus* (Robert *et al*., 1998) and *Brassica oleracea* (Ayele *et al*., 2005) in the future (Gepstein and Horwitz, 1995; Lim *et al*., 2007).

Due to the small genome and the small size of reproductive organs, reservations against cytogenetic meiotic analysis in *Arabidopsis* existed. Proceedings in DNA staining and spreading techniques (reviewed in Koornneef *et al*., 2003) allowed the creation of an extensive light microscopic atlas of meiosis stages (Ross, *et al.*, 1996). This atlas of wild type meiosis provides the basis for cytological analyses of meiotic mutants (section 2.5.4, Figure 7).

2.2. The Cell Cycle

As in all other higher eukaryotic organisms the *Arabidopsis* cell cycle can be divided into four distinct stages. In Gap phase 1 (G1), cell growth and synthesis of DNA replication factors is taking place. DNA replication itself is completed within S phase (S), after which Gap phase 2 (G2) prepares the cell for mitotic / meiotic division, finally taking place in M phase (M). Transition from one phase to another is tightly regulated, mainly by the interaction of temporary expressed cyclins with their respective cyclin-dependend kinases (CDKs) (reviewed in Francis, 2007; Sullivan *et al*., 2007).

Throughout the cell cycle, several checkpoint mechanisms are present which are sensing certain cellular conditions and subsequently regulate cyclin / CDK activity through G1/S and G2/M transitions, as well as the exit from mitosis. As a consequence, cell cycle progression is slowed down or stopped completely. So-called checkpoint kinases inhibit cell cycle progression, for example in response to DNA DSBs (reviewed in De Veylder *et al*., 2003).

The study of mammalian mutants deficient in genomic maintenance is often complicated. Lethality, low viability or infertility, as results of cell cycle delay or apoptosis (programmed-cell-death), are triggered by those genomic aberrations. The small thale cress displays several practical advances over other higher eukaryotic model organism systems to investigate genome maintenance and DNA repair mechanisms. Since plants do not possess a reserved germ line, the gametes arise from undifferentiated meristematic cells. Those cells have undergone several events of somatic growth and division, being continually exposed to potentially mutagenic conditions, either being endogenous or environmental. Though long-lived plants do not show highly elevated mutation rates, somatic genome-maintenance activities are to be as efficient as mammalian counterparts (Klekowski, 1997).

Moreover, plants seem to tolerate genome-maintenance deficiencies that trigger lethal responses in mammals, since null mutations that inactivate proteins involved in repair of DNA lesions have proved to be tolerated by plants. Therefore Arabidopsis has become a powerful model system for elucidation of responses to DNA lesions (reviewed in Hays, 2002).

2.3. Mitotic Cell Division

Mitotic cell division is characterized by an equal distribution of replicated chromosomes, resulting in the formation of two diploid daughter cells that are identical with respect to their genetic material and chromosomal karyotype. The goal of mitotic cell division is the faithful transmission of chromosomes, which is governed by a series of tightly regulated cellular events taking place in four different stages of mitotic progression, termed prophase, metaphase anaphase and telophase, respectively (Figure 1; reviewed in Nasmyth, 1999; Ishiguro and Watanabe, 2007; Decordier *et al*., 2008).

An important aspect of chromosome segregation is the establishment of sister chromatid cohesion, which is required for proper spindle attachement and sister chromatid segregation during late steps of mitotic cell division. The cohesin protein complex mediates sister chromatid cohesion. The mitotic core complex consists of a group of highly conserved *structural maintenance of chromosomes* (SMC) and *sister chromatid cohesion* (SCC) proteins SMC1, SMC3, SCC1 and SCC3, being loaded onto DNA prior to DNA replication in S-Phase (Uhlmann and Nasmyth, 1998). After completed replication the sister chromatids are tethered together by topological interaction through the cohesin molecules (Ivanov and Nasmyth, 2005).

During prophase, the replicated chromosomes begin to condense through the action of *condensins*, which are likewise members of the SMC protein family (SMC proteins reviewed in Hirano, 2006). Cohesion between replicated sister chromatids is maintained until metaphase. However, in higher eukaryotic mitosis, most of the cohesin along the chromosome arms is removed along the so-called Prophase Pathway. This dissociation is due to phosphorylation of cohesin subunit SCC3 by Polo-like kinase (PLK1), without Separase-mediated cleavage of the kleisin subunit SCC1 (Hauf *et al*., 2005). In addition to PLK1, Aurora B may contribute to this process. Centromeric cohesin is protected from prophase pathway-mediated removal by constant dephosphorylation via protein phosphatase PP2A. In mammals the centromeric localization of PP2A is conferred through recruitment by Bub1 and possibly Sgo2, and finally stabilized through Sgo1-PP2A complex formation. However, cohesin remains present at the centromeres and ensures thereby proper chromosomal alignment at the cell equator during metaphase (Rivera *et al*., 2006).

The spindle assembly checkpoint ensures that all replicated sister chromatid pairs display bipolar microtubule attachment (two spindles emanating from opposite spindle poles). Incorrect spindle attachments are sensed through the action of the mitotic checkpoint complex (MCC). After checkpoint activation, some MCC components bind to the CDC20 subunit of the Anaphase Promoting Complex/Cyclosome (APC/C) and render it inactive (Musacchio and Hardwick, 2002). After proper microtubule attachement to the kinetochores, the MCC subsequently breaks up and releases the now active APC/C^{CDC20} complex. The APC/C^{CDC20}complex displays E3 ligase activity, and selectively poly-ubiquitinylates the target substrate Securin, the inhibitory chaperone of Separase as well as other specific targets. After Securin proteolysis through the 26S proteasome, Separase is inactive and cleaves the kleisin subunit SCC1. Previous phosphorylation of SCC1 by PLK1 enhances protein cleavage by Separase and seems to be conserved among eukaryotic organisms. As the cohesin ring is opened, interaction of replicated sister chromatids is lost and triggers the chromosome segregation, which marks the metaphase to anaphase transition (Decordier *et al*., 2008).

Spindle pole movement and microtubule dynamics confer chromosome segregation to opposite poles of the cell. Telophase is characterized by chromosome decondensation and nuclear envelope reformation. Finally, cytokinesis marks the end of mitosis, through reestablishment of cytoplasma separation. Thereby, mitotic division leads to the separation of replicated sister chromatids. Each progenitor cell inherits one copy of each paternal and maternal chromosome, resulting in the formation of two identical cells (Figure 1).

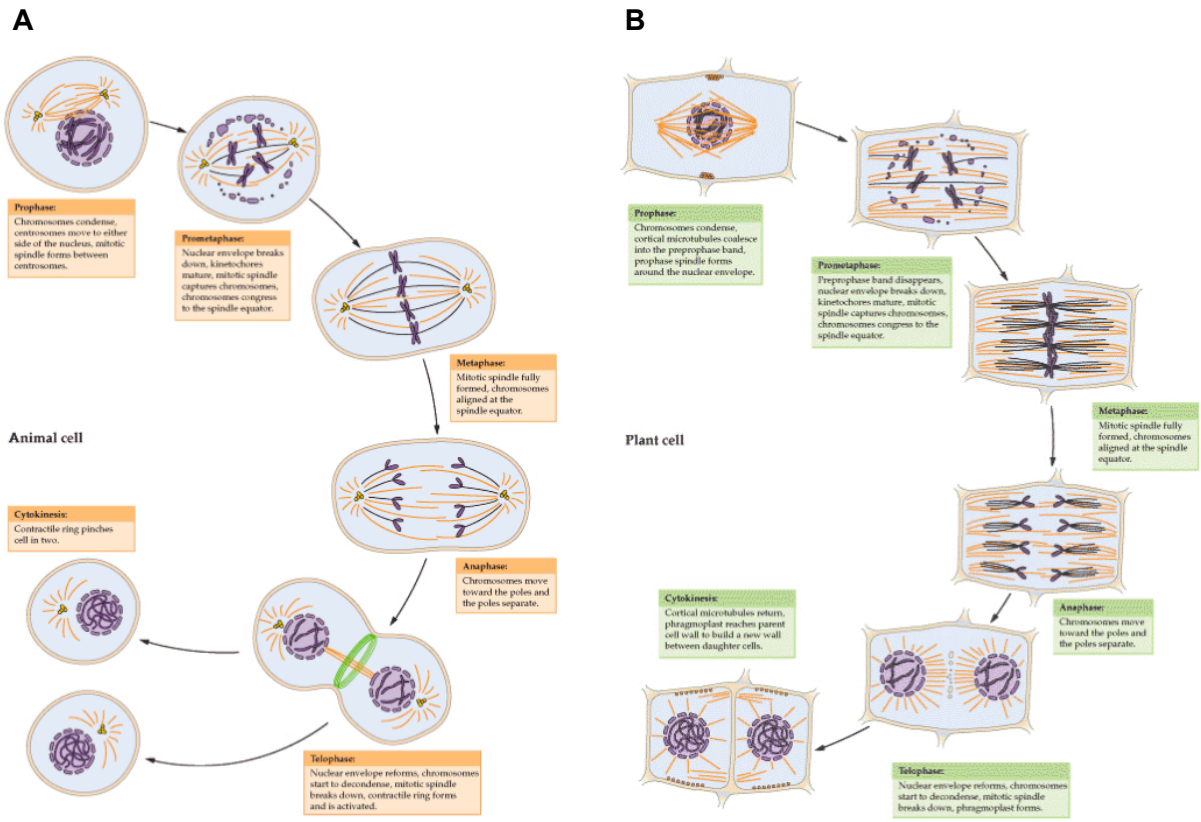

(Alberts, *et al*., 2002)

Figure 1 | Animal vs. Plant Mitosis Overview. (A) Prophase is characterized by fully replicated sister chromatids that are closely linked by topological interaction through cohesin. Other DNA interacting molecules called condensins mediate the condensation of sister chromatids during the prophase.

Prometaphase is characterized by the breakdown of the nuclear envelope, conferred by lamin protein phosphorylation. Chromosomes are condensed but disordered.

Metaphase chromosomes are attached to the microtubules at their kinetochores in random order. Dynamic instability of microtubules confers eventually bipolar spindle attachment whereby the opposite oriented kinetochores are attached to microtubules from different spindle poles. This bipolar attachment generates a spindle pulling force stabilizing the microtubules and finally orientates the condensed chromosomes at the cell equator.

Metaphase to anaphase transition is triggered by cleavage of the mitotic cohesin SCC1 subunit, leading separation of sister chromatids. Sister chromatids are pulled to different cell poles by spindle pole movement and kinetochore microtubule shortening.

During telophase the two sets of sister chromatids arrive at the poles of the spindle and decondense, accompanied by the formation of a new nuclear envelope, marking the end of mitosis.

Finally cytokinesis takes place. In animal cells a contractile ring is formed around the former cell equator. The contraction of the myosin / actin filaments creates two daughter cells and an interphase array of microtubules is reestablished.

Figure 1 | Animal vs. Plant Mitosis Overview (continued). (B) Plant cells differ from animal or fungal cells through a fixed, cytoskeletal-mediated position of their nucleus and through the absence of centrioles. Spindle poles are not point-shaped like animal centrosomes but rather broad and band-shaped. Plant cells contain plastid genomes and are enclosed by a semi-rigid cell wall in contrast to animal cells.

The plant cell is not divided by a contractile ring from the outside-in. Rather the plant cell is partitioned from the inside out by the construction of a new cell plate between the two daughter nuclei. The orientation of the cell plate is not sufficiently determined by the spindle apparatus alone. In G2 phase the cortical array of microtubules disappears and the preprophase band, a circumfencial ring of actin and myosin filaments is formed. This band disappears again as the cell progresses to prophase but has established the plane of the future cell plate.

The assembly of the cell plate begins in late anaphase and is guided by the phragmoblast, the remainders of the overlapping spindle microtubules ends. Small golgi-derived vesicles filled with polysaccharide and glycoproteins are transported along the microtubules to the equator of the phragmoblast with the help of microtubule dependent motor proteins. The vesicles then fuse to form the disc shaped, membrane-enclosed early cell plate which finally reaches the cell wall and is reinforced by the deposition of cellulose microfibrills.

2.4. The Role of Sexual Reproduction in the *Arabidopsis* Life Cycle

Sexual life cycles of eukaryotic organisms involve a cyclic alteration between diploid (2n) and haploid (1n) phases. In higher eukaryotic organisms the germline is well separated from the somatic tissue, either by the separation of pluripotent germ cell primordia or by the temporal development of generative organs, while the latter one is the case in many plant species. In flowering plants like *Arabidopsis* the haploid gametophyte phase is short, corresponding to pollen grain and embryo sac formation on male and female side. Those are residing within the male and female generative organs of the plant, the anthers and gynoetium, respectively.

The sporophyte generation constitutes the diploid phase of the plant life cycle. It starts by fertilization of the haploid egg cell in a flower ovary by a pollen-derived haploid sperm cell. The fertilized egg in the seed subsequently develops into a quiescent embryo. After germination the plant seedling undergoes several stages of organ formation and vegetative growth to finally develop into a mature sporophyte (Figure 2; reviewed in Boavida *et al*., 2005; Coelho *et al*., 2007).

Redistribution of genetic information is mediated by two different cellular events, which take place during the specialized meiotic division. Random distribution of maternal and paternal homologs between daughter cells in meiotic division I (meiosis I) leads to a different mixture of parental chromosomes in each resulting gamete. From this process alone, 2^n genetically different gametes are produced, where n is the haploid number of chromosomes. Additionally, genetic recombination through chromosomal crossing-over takes place during prophase of meiosis I, leading to reciprocal exchange of genetic information between paternal and maternal chromosomes.

Therefore, meiosis and particularly meiotic recombination are important genetic mechanisms that have likely contributed to the enormous success of eukaryotes (Ma, 2006).

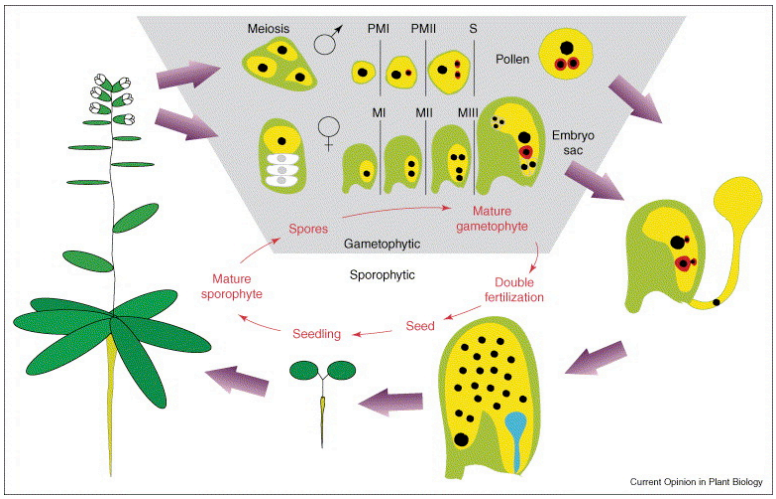

(Berger *et al*. Curr Opin Plant Biol (2006) vol. 9 (6) pp. 664-70)

Figure 2 | *Arabidopsis thaliana* Life Cycle. Under certain growth conditions the sporophyte develops flowers, containing the generative organs of the plant. The anthers are the male generative organs in which diploid germ cell precursors, the microspore mother cells, undergo a specialized type of cell division called meiosis. This meiotic division leads to reduction of ploidy of the resulting products, leading to the formation of four haploid microspores. Those microspores undergo two subsequent mitotic divisions, to form mature gametophytes called pollen. Those are comprised of a large, vegetative cell harbouring the two actual gametes, the haploid sperm cells.

The female generative organ of the plant, the gynoecium, contains several ovules. Within each ovule a diploid megaspore mother cell undergoes meiosis to form four division products. Only one of those cells survives to form the haploid megaspore. These megaspores undergo three subsequent rounds of nuclear divisions followed by cellularization, leading to the formation of the female embryo sac containing one egg cell, two synergids which later on direct the pollen tube growth direction and a double haploid central cell which will form the triploid endosperm after fertilization (the three antipodal cells degenerate in *Arabidopsis thaliana*).

The formation of haploid gametophytes indicates the starting point of the haploid plant life cycle. When pollen lands on the stigma of the gynoecium, pollen tube growth is taking place. In parallel to the pollen tube elongation the vegetative nucleus and the two sperm nuclei are migrating through the tube, finally reaching the embryo sac. Each sperm nucleus either fertilizes the haploid egg cell or the double haploid central cell, resulting in the formation of a diploid zygote and a triploid endosperm and indicating the end of the gametophytic haploid phase of the plant life cycle.

2.5. Meiotic Cell Division

The formation of gametes is taking place after the germ-line restricted meiotic division. A usually diploid (2n) germ cell precursor undergoes one round of DNA replication, followed by two subsequent chromosome alignment and segregation steps, meiosis I and meiosis II, producing finally four haploid (1n) division products. The reductional division of meiosis I is characterized by pairing and subsequent segregation of homologous chromosomes. Thereby, recombination between homologous chromosomes establishes chiasmata that counteract monopolar spindle pulling forces, and allows paired homologous chromosomes to align at the cell equator. The equational division of meiosis II is similar to mitosis as segregation of sister chromatids is taking place. As a consequence the mechanistics of this specialized cell division have to be different from those involved in mitotic cell division (Figure 3).

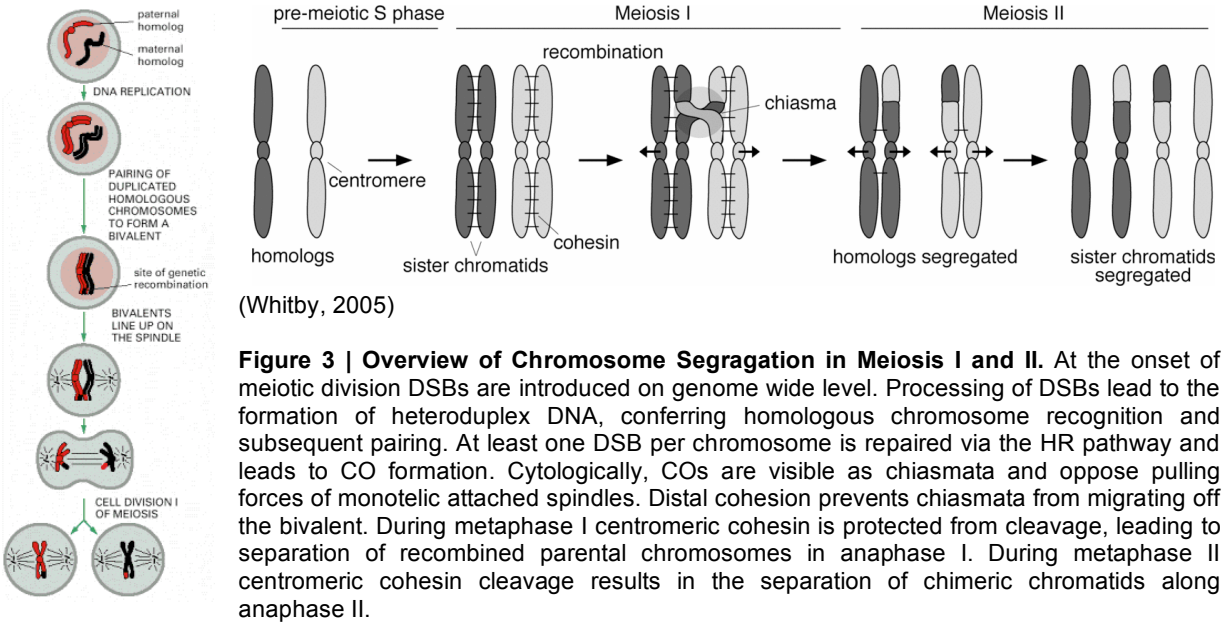

(Whitby, 2005)

Figure 3 | Overview of Chromosome Segragation in Meiosis I and II. At the onset of meiotic division DSBs are introduced on genome wide level. Processing of DSBs lead to the formation of heteroduplex DNA, conferring homologous chromosome recognition and subsequent pairing. At least one DSB per chromosome is repaired via the HR pathway and leads to CO formation. Cytologically, COs are visible as chiasmata and oppose pulling forces of monotelic attached spindles. Distal cohesion prevents chiasmata from migrating off the bivalent. During metaphase I centromeric cohesin is protected from cleavage, leading to separation of recombined parental chromosomes in anaphase I. During metaphase II centromeric cohesin cleavage results in the separation of chimeric chromatids along anaphase II.

(Alberts, *et al.*, 2002)

During meiotic progression, precicely regulated events of DSB formation, recombination, chromosome pairing and synapsis take place to ensure that indeed homologous chromosomes find each other and are faithfully distributed along the chromosome segregation steps of meiosis I. Meiotic progression can be divided into four distinct stages namely prophase, metaphase, anaphase and telophase, as in mitotic cell division (section 2.3). The process of chromosome pairing is essential for segregation and mediated by a complex sequence of events. Therefore, prophase of meiosis I is the longest and most complex stage of the division, and can be divided into five sub-stages (leptotene, zygotene, pachytene, diplotene and diakinesis).

At the beginning of meiotic cell division diploid male microspore and female megaspore mother cells undergo DNA replication in the premeiotic S-phase, which is different in comparison to mitosis and a prerequisite for meiotic DSB formation (reviewed in Baudat *et al.*, 2001; Forsburg, 2002). Cohesin protein complexes similar to their mitotic counterparts are loaded onto paternal and maternal chromosomes at premeiotic S-phase prior to DNA replication. Different from mitosis, meiotic cohesin contains the kleisin subunit REC8 instead of SCC1 (Dong *et al.*, 2001). After completed DNA replication sister chromatids are tethered together as they are both enclosed by the same circular cohesin molecules.

2.5.1. DSB Formation: Initiation of Meiotic Recombination

The occurrence of unrepaired DSBs is a dramatic cellular event. In *Saccharomyces cerevisiae*, the occurrence of a single DSB during mitosis may lead to cell death (Bennett *et al*., 1993). During meiosis however, programmed DSBs are induced genome-wide between leptotene and zygotene to initiate the process of meiotic recombination. In all studied eukaryotic organisms DSBs are introduced by the conserved protein Spo11 (Bergerat *et al*., 1997; Keeney *et al*., 1997). Generally, Spo11 proteins share homology with the archaeal toposiomerase II subunit VIA-like protein (TOPVIA; reviewed in Keeney, 2001).

Genetic screens in *Saccharomyces cerevisiae* have identified nine other proteins aside from Spo11 that are essential in the catalysis of DSB formation (Mre11, Rad50, Xrs2, Rec102, Rec104, Rec114, Mei4, Mer2 and Ski8; Keeney, 2001). Only four of those proteins (Mre11, Rad50, Nbs1 and Ski8) are conserved in plants but have no conserved essential functions at the step of DSB induction (Jolivet *et al*., 2006; Waterworth *et al*., 2007).

Analysis of budding yeast *mre11S*, *rad50S* and *com1*Δ/*sae2*Δ mutants have led to the identification of recombination intermediates, with Spo11 proteins covalently attached to 5’ DNA ends at DSB sites (Alani *et al*., 1990; Keeney and Kleckner, 1995), and Spo11 could be identified as the protein responsible for DSB formation (Keeney *et al*., 1997). These findings and the fact that Spo11 shares TopVIA functional domains implicate that Spo11 is introducing DSBs through a transesterification reaction that is typical for topoisomerase proteins (Bergerat *et al*., 1997; Diaz *et al*., 2002). In a proposed model, Spo11 displays intrinsic DNA binding and nucleolytic activity, the latter one conferred by a conserved catalytic tyrosyl residue. Thereby two Spo11 molecules interact with backbones of both DNA strands through their conserved tyrosine hydroxyl-residues. A nucleophilic attack on the DNA backbone phosphate molecules leads to formation of phosphotyrosyl-ester-bondings. This process leads to the creation of a DSB and two covalently bound Spo11 molecules at the 5’ ends at the breakage site (Figure 4).

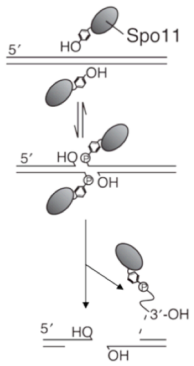

Figure 4 | Spo11-mediated DNA DSB Induction Model. Two molecules of Spo11 act together upon DNA DSB induction. The conserved catalytic Tyrosyl-residues are thereby involved in a nucleophilic attack on a phosphate molecule within the DNA ribose-phosphate backbone. During the course of an irreversible transesterification reaction, two molecules of Spo11 become covalently linked to the 5’ DNA terminin at the breakage site.

Removal of covalently bound Spo11 occurs after nucleolytic processing. The Spo11 protein remains attached to a short stretch of ssDNA, which is consistent with the identification of Spo11-containing recombination intermediate DNA-protein complexes.

(adapted from Neale *et al*., 2005)

Genetic analyses revealed that removal of Spo11 from DNA is dependent on proteins Com1/Sae2, Mre11 and Rad50 (Borde, 2007). Most probably due to Mre11 mediated DNA endonuclease activity, both DNA strands are nicked by asymmetric single-stranded DNA (ssDNA) exonuclease activity, and Spo11 is released from DNA covalently bound to short ssDNA stretches.

In contrast to budding yeast, plants have three Spo11 homologues *At*SPO11-1 to *At*SPO11-3, two of which (*At*SPO11-1 and *At*SPO11-2) are required for meiotic recombination initiation (Grelon *et al*., 2001; Hartung and Puchta, 2000, 2001; Stacey *et al*., 2006). All three *At*SPO11 proteins share 20-30% sequence similarity with other eukaryotic Spo11 proteins. Moreover the same sequence similarity is shared with other TOPVIA protein family members as well (Hartung and Puchta, 2000, 2001). Additional data show that catalytic tyrosyl residues of both *At*SPO11-1 and *At*SPO11-2 are essential for DSB induction and complementation of an *Atspo11-1*; *Atspo11-2* mutant background. The double mutant *Atspo11-1*; *Atspo11-2* does not differ phenotypically from the single mutants (Hartung *et al*., 2007). Each single mutant displays the same severe asynaptic meiotic phenotype, resulting in almost full sterility (Grelon *et al*., 2001; Stacey *et al*., 2006). The lack of functional redundancy suggests that DSB formation is catalyzed by an *At*SPO11-1/*At*SPO11-2 heterodimer and not by a homodimer as thought to occur in other eukaryotes (Hartung *et al*., 2007). This data is supported by budding yeast studies, indicating that meiotic interaction between differentially tagged Spo11 proteins takes place *in-vivo* and does not depend on DSB formation, but is regulated by Rec102 and Rec104 (Sasanuma *et al*., 2007). Taken together, these findings strongly suggest that both catalytic residues of two molecules of Spo11 are involved in DSB induction within a dimeric Spo11 configuration, being it either a Spo11 homodimer or a SPO11-1/SPO11-2 heterodimer in higher plants like *Arabidopsis*. *At*SPO11-3 has recently been identified to interact with a unique, plant-specific *At*TOP6B topoisomerase subunit and is involved in DNA endoreduplication in somatic cells (Hartung *et al*., 2007).

Forward meiotic mutant screening has led to the identification of *At*PRD1, which is essential for DSB formation in *Arabidopsis* and interacts with *At*SPO11-1 in a yeast two hybrid assay, providing the first evidence for the existence of a DSB forming complex in higher eukaryotes (De Muyt *et al*., 2007). Other proteins in this complex remain to be identified. Mutants, defective in DSB induction, are characterized through the presence of univalents at diakinesis stage of meiosis I, which results in the random segregation of chromosomes during the reductional meiotic division. According to this phenotype the *At*SDS gene, encoding a meiosis-specific cyclin-like protein (Azumi *et al*., 2002), was identified, and may belong to the class of DSB induction defective mutants (reviewed in Ma, 2006; Mercier *et al*., 2008; Muyt *et al*., 2009).

2.5.2. Meiotic Recombination: Early Steps in DSB Repair

During DSB formation Spo11 is found covalently linked to generated 5´ DNA ends. Spo11 release from DNA is mediated by the formation of a ssDNA nick next to the DSB site. In budding yeast, this release is dependent on proteins Mre11, Rad50 and Com1/Sae2 (Keeney and Kleckner, 1995; Neale *et al.*, 2005; Prieler *et al*., 2005). Together with Xrs2, Mre11 and Rad50 form the MRX complex. In *Arabidopsis*, this putative complex is formed by proteins *At*MRE11, *At*RAD50 and possibly *At*NBS1 (Daoudal-Cotterell *et al*., 2002; Akutsu *et al*., 2007; Waterworth *et al*., 2007), and was found to be essential for DSB processing together with *At*COM1 (Uanschou *et al*., 2007) but not for DSB formation (Bleuyard *et al*., 2004; Puizina *et al*., 2004; Waterworth *et al*., 2007).

In *Saccharomyces cerevisiae* and *Mus musculus* DSB processing is characterized by asymmetric ssDNA endonuclease activity, leading to Spo11 release from DNA, covalently bound to ssDNA stretches of different distinct length (about 12nt and 30nt, respectively). This asymmetric release might occur chronologically distinct, first by mere dissociation of the shorter fragments, and second by active unwinding of the Spo11-DNA recombination intermediate (Keeney, 2001; Neale *et al*., 2005).

After 3’ ssDNA nicking 5’-3’ DNA end resection is taking place by a yet unidentified nuclease. Thereby stretches of 3’ ssDNA are generated, believed to work as probes for identification of homologous chromosomes. Recent studies in budding yeast identified a two-step mechanism for DSB processing during somatic recombination. First, the Mre11 complex and Sae2 remove a small oligonucleotide from the DNA ends to form an early intermediate. Second, exonuclease Exo1 and/or helicase Sgs1 rapidly process this intermediate to generate extensive tracts of single-stranded DNA (Mimitou *et al*., 2008).

After DNA end processing, generated free 3’ ssDNA overhangs are loaded with DNA strand-exchange protein RecA homologs Rad51 and Dmc1. Both proteins are thought to be involved in active homology search (Shinohara and Shinohara, 2004), promoting homologous chromosome pairing through single end invasion (SEI) of the free 3’ ssDNA end into intact stretches of homologous dsDNA sequences. Notably, Rad51 displays both meiotic and somatic DNA repair functions, while Dmc1 function is meiosis specific. Corresponding *Arabidopsis Atrad51* mutants fail to repair meiotic DSBs (Li *et al*., 2004) while DSBs in *Atdmc1* mutants are repaired, using the sister chromatid as a template (Couteau *et al*., 1999; Siaud *et al*., 2004).

In addition to *At*RAD51 and *At*DMC1, two RAD51 paralogues, *At*RAD51C and *At*XRCC3, are involved in meiotic DSB repair. Moreover, several proteins are thought to assist DMC1/RAD51 in strand invasion: homologues of the breast cancer susceptibility gene BRCA2 product and of the Mnd1/Hop2 complex were identified as key players in meiotic recombination in *Arabidopsis thaliana* together with the recombinases (reviewed in Mercier *et al*., 2008).

2.5.3. Meiotic Recombination: Control and Regulation of Crossover Formation

As previously discussed, 3' ssDNA stretches are generated during meiotic DSB processing. These ends act as DNA homology probes in subsequent *At*RAD51/*At*DMC1 driven strand invasion. Introduced DSBs appear on every chromosome in high number (n=150-250 in mid-zygotene per *Arabidopsis* meiocyte by means of RAD51 foci number estimation (Mercier *et al*., 2003). During single end invasion (SEI) the 3' ssDNA end forms a D-loop with the intact partner chromatid of the homologous chromosome, initiating homologous chromosome pairing.

DNA synthesis is primed from the invading strand using the intact strand of the homologous chromosome as repair template. Branch migration further stabilizes the stretch of heterodupex DNA and therefore chromosome pairing. Invasion of the second broken end and further DNA synthesis yield a Holliday Junction (HJ). Emanating from a (protein-stabilized) HJ structure are four double stranded DNA helices, which are equal concerning their three-dimensional properties. However, directional cutting of two opposite ssDNA stretches may occur at both junction sites of a double-Holliday Junction (dHJ) structure, leading to regulated crossover (CO) or non-crossover (NCO) resolution, respectively, which can be circumscribed as exchange or non-exchange of flanking markers at chromosomal levels. NCOs resemble non-reciprocal DSB repair events and eventually confer gene conversion if the allelic composition of paternal and maternal chromosomes is different around the DSB site. Thereby, only limited exchange of sequence information is taking place, leaving flanking markers adjacent to dHJ structures unchanged (Figure 5).

The working model of meiotic recombination was originally proposed on the basis of biochemical studies on *S. cerevisiae* and animal cells, called the double-strand break repair (DSBR) model (Szostak *et al*., 1983). According to this model, meiotic recombination is initiated by the programmed formation of DSBs during leptotene stage of meiosis I and repaired with a strong bias for the homologous chromosome (Schwacha and Kleckner, 1997). The model predicts that both CO and NCO recombinants derive from dHJ resolution. This is consistent with the activities of known HJ resolvases that would cleave either pair of strands at each HJ with equal probability. However, in recent years, a number of mutations have been found in *S. cerevisiae* that reduce dHJ resolution and CO formation without affecting the formation of DSBs and NCOs (reviewed in Bishop and Zickler, 2004). Recent genetic studies in *Arabidopsis* identified several homologs of those proteins and led to the formation of a revised DSB repair model.

At least three different pathways are involved in the formation of NCO and CO events in plants, which emanate from the common SEI event: the ZMM (Zip, Mer, Msh) protein-dependent pathway similar to the initially proposed canonical Szostak *et al*. DSBR pathway leading to interference sensitive class I COs; the SDSA pathway leading to NCOs; and the Mus81-Eme1 dependent pathway leading to interference insensitive class II COs (Figure 5 for further information). The term interference describes that the occurrence of class I COs inhibits further CO formation within limited distance around the initial CO. Class II COs are randomly distributed, and not affected by the presence of additional CO events in their vicinity (reviewed in Whitby, 2005; Ma, 2006; Cromie and Smith, 2007; Mercier *et al*., 2008; Muyt *et al*., 2009).

SDSA pathway resolution is well investigated and characterized by D-loop disruption, mediated by displacement of the elongated invading strand. Strand reannealing to its prior partner is taking place through pairing of elongated homologous sequence stretches. Flap removal of DNA overhangs, DNA synthesis and ligation are resulting in formation of a NCO resolution event (Allers and Lichten, 2001; Hunter and Kleckner, 2001; Börner *et al*., 2004; McMahill, 2007).

Within the interference sensitive class I CO generating pathway in budding yeast, CO formation is dependent on a series of ZMM Protein family members (Zip1 to Zip4, Msh4, Msh5 and Mer3) as well as on Mlh1 and Mlh3 (Whitby, 2005). Those proteins are recruited to certain DNA DSB sites (Börner *et al*., 2004; Fung *et al*., 2004), promote SEI stability (Börner *et al*., 2004) and subsequent dHJ formation, and ensure that resolution occurs with a bias to generate COs. Without ZMM protein stabilization SEI events remain unstable and are believed to be channeled to the alternative SDSA pathway (Bishop and Zickler, 2004). Three of the ZMM proteins (Mer3, Msh4 and Msh5) are thought to promote SEI stabilization (Börner *et al*., 2004). While the helicase Mer3 is involved in D-loop extension *in-vitro* (Mazina *et al*., 2004), human homologs of the bacterial MutS mismatch repair (MMR) protein hMSH4 and hMSH5 are found to bind specifically to and accumulate at HJ sites (Snowden *et al*., 2004). MutL homologs Msh1and Mlh3 form a complex that works downstream Msh4 and Msh5. Thereby these proteins direct the manner of a yet unknown dHJ resolvase action, ensuring that mainly COs are formed. In mammalian cells Rad51-like proteins Xrcc3 and Rad51C were found to confer HJ resolvase activity (Whitby, 2005).

As in budding yeast (Argueso *et al*., 2004), the existence of two CO pathways was suggested in *Arabidopsis* (Copenhaver *et al*. 2002) and is supported by the identification of several ZMM homologs (Higgins *et al*., 2004; Chen *et al*., 2005; Mercier *et al*., 2005; Chelysheva *et al*., 2007) and two MUS81 homologs (Hartung *et al*., 2006; Berchowitz *et al*., 2007), being critical for late stage meiotic recombination. Putative homologs of Zip2 and Zip 3 remain to be identified.

The *Arabidopsis* class I CO pathway is likewise depending on *At*MSH4 and *At*MER3 (Higgins *et al*., 2004; Mercier *et al*., 2005), but it is not known whether *At*XRCC3 and *At*RAD51C (Bleuyard and White, 2004, Bleuyard *et al*., 2005) are part of this pathway (reviewed in Whitby, 2005; Cromie and Smith, 2007).

The non-interfering class II CO pathway was found to depend on the conserved endonucleae Mus81 that acts together with Mms4 (*Sc*Eme1, *Hs*EME1) (de los Santos *et al*., 2003; Lynn *et al*., 2007). *Arabidopsis* homologs of MUS81 were identified (Hartung *et al*. 2006; Berchowitz *et al*., 2007), while no *At*EME1 homolog has yet been functionally characterized. Mus81 is related to the *Xeroderma Pigmentosum* complementation group F (XPF) family of structure-specific endonucleases and it forms a complex with Mms4/Eme1 that can cleave a variety of branched DNA structures *in-vitro*, including HJs. Detailed analysis of complex specificity and processivity from budding and fission yeast as well as from humans, displayed a much higher complex activity on D-loops and nicked HJs than on intact HJs. These findings sugggest that the complex might act early in the recombination reaction to cleave the D-loop after SEI and the nicked HJ that is formed after second end capture, finally leading to the formation of an obligate CO (Figure 5; reviewed in Whitby, 2005; Cromie and Smith, 2007).

Genetic analysis in various species suggests that the ratio of interfering COs to non-interfering COs differs depending on the organism in which it was studied. In budding yeast, disruption of the class I CO pathway leads to a 70 % total reduction of CO formation, while the remainders do not display interference (de los Santos *et al*., 2003). The proposed model of coexisting Msh4/Msh5 dependend class I and Mus81/Mms4 dependent class II CO pathways had to be revised due to residual CO formation in class I and class II CO pathway disabled mutant backgrounds, suggesting that a third mechanism for CO formation might exist (de los Santos *et al*., 2003; Argueso *et al*., 2004). This pathway is normally inhibited by Msh5, as CO numbers are approx. 3-fold higher in *mlh1; mms4; msh5* triple mutants in comparison to class I and class II CO disabled *mlh1; mms4* double mutants (Argueso *et al*., 2004; reviewed in Whitby 2005; Cromie and Smith, 2007).

In *Arabidopsis*, disruption of ZMM proteins (*At*MSH4/*At*MSH5, *At*MER3) does not alter early meiotic recombination events but results in a drastic decrease in CO formation (Copenhaver *et al*., 2002). The maximum effect on CO formation reduction is never greater than 85% of the wild-type (WT) level, suggesting that at least 15 % of the COs are independent of the ZMM pathway. Total reductions of CO numbers in class I CO pathway disabled *Atmsh4* mutants (75 %) and in class II CO pathway disabled *Atmus81* mutants (10 %) are observed (Berchowitz *et al*., 2007).

Similar to yeast data, the disruption of *Arabidopsis* class I and class II CO pathways does not eliminate overall CO formation, and suggests that a third mechanism for CO formation might exist (reviewed in Mercier *et al*., 2008; Muyt *et al*., 2009).

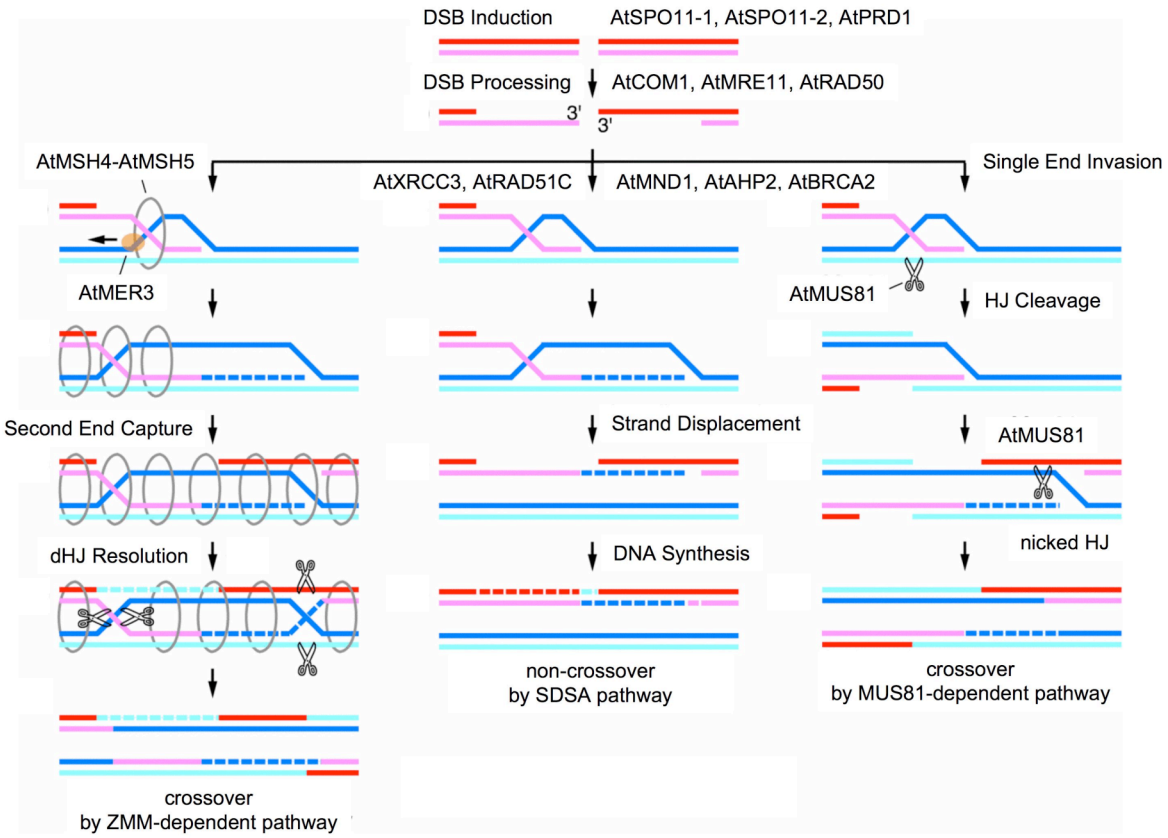

(adapted from Whitby, 2005)

Figure 5 | Current Models for Meiotic DSB Repair. Detailed genetic analysis has led to a modification of the canonical Szostak *et al*. DSB repair model over the years. The model initially proposed that meiotic DSBs are repaired along the HR pathway, and that a dHJ structure might be resolved in different ways, yielding either COs as well as NCO events.

After DNA DSB induction, 5' to 3' DNA end resection leads to the formation of free stretches of 3' ssDNA overhangs. The DNA overhangs serve as homology probes and invade the intact recombination partner to form a D-loop. DNA synthesis, using the homologous chromosome as repair template, extends D-loop formation and further stabilizes the pairing of homologous chromosomes mediated by the stretch of heteroduplex DNA. Genetic studies indicate that CO vs. NCO designation is taking place already at single end invasion (SEI) stage, and that at least three different repair pathways are responsible for CO and NCO resolution.

(ZMM pathway, left) The canonical ZMM protein pathway seems to be the principal pathway of CO formation in most organisms. It is resulting in the formation of interference-sensitive class I COs, ensuring an even-spaced distribution. In the DSBR model, dHJ formation is taking place. The extended ssDNA stretch captures the original 5' DNA end which likewise invaded the D-loop. The second end of free 3' ssDNA is elongated, using the D-loop as repair template and gets ligated to the 5' ssDNA end. Resolution is taking place with a strong bias towards CO formation. These events lead to exchange of chromosomal markers flanking the dHJ, and thereby to the creation of chimeric chromosomes.

(SDSA pathway, middle) In the SDSA model the extended stretch of the invading 3' ssDNA homology probe gets displaced from the D-loop and reanneals to its prior partner, the own complementary strand. After flap removal it is serving as an elongation template for its complementary strand. Strand ligation finally completes the repair process and is always resulting in NCO resolution, which eventually leads to a gene conversion events if the allelic composition of paternal and maternal chromosomes is different at the region of DSB induction. Thereby NCO resolution might also contribute to the exchange of genetic information, however not on genome wide level (McMahill *et al*., 2007).

(Mus81 pathway, right) In budding yeast the Mus81-dependent pathway is regarded as a backup for the ZMM-dependent pathway of CO formation and leading to the formation of non-interferning class II COs. Absence of ZMM proteins at SEI intermediates might either channel them for SDSA-pathway mediated NCO resolution or for Mus81-dependent non-interfering CO resolution.

2.5.4. Chromosome Synapsis

In plants, as in most organisms, recombination, pairing and chromosome synapsis are tightly linked processes. The chronology of DSB induction, synapsis and finally stabilizing synaptonemal complex (SC) formation can be found in the majority of eukaryotic organisms, where the temporal formation of the SC between homologous chromosomes is taking place during meiotic prophase I (Roeder, 1990; reviewed in Kleckner, 2006).

In *Saccharomyces cerevisiae*, DSB induction is a prerequisite for chromosome synapsis, followed by SC formation, while in *Schizosaccharomyces pombe* DSB induction is directly followed by chromosome association and pairing without any SC establishment at all. In *Drosophila melanogaster* and *Caenorhabditis elegans* the process of SC formation is found to be independent of DNA DSB formation (reviewed in Gerton and Hawley, 2005).

In budding yeast, SC assembly is inititated by the formation of the axial element (AE) along each pair of sister chromatids prior to synapsis. The AEs become the lateral elements (LEs) of the SC during the beginning of synapsis of two homologus chromosomes. This process is mediated by interconnection of the LEs through polymerization of transverse filaments (TFs) between them. Finally the common central element (CE) is formed from the heads of the TFs, which are connencted to the LEs (Figure 6).

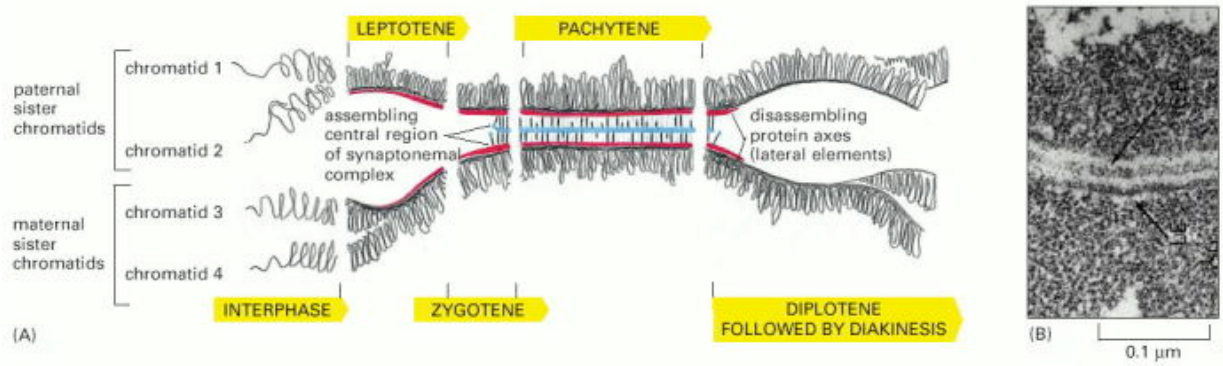

(Alberts, *et al.*, 2002)

Figure 6 | SC Formation during Prometaphase I. The SC is a proteinacous structure formed by lateral elements (LE), a common central element (CE) and transverse filaments, which interconnect the LEs. The LE comprises of meiosis-specific cohesins, structural proteins and HORMA-domain proteins. The latter ones connect the SC scaffold to the chromosome loops.

Stages of meiotic prophase I can be classified according to cytological features of chromosome condensation as well as SC formation and disassembly, and can be accessed cytologically via light microscopy, following DNA staining with the fluorochrome 4',6-Diamidino-2'-phenylindole (DAPI) combined with a spreading procedure (Figure 7 for further information; reviewed in Ross, *et al.*, 1996; Ma, 2006).

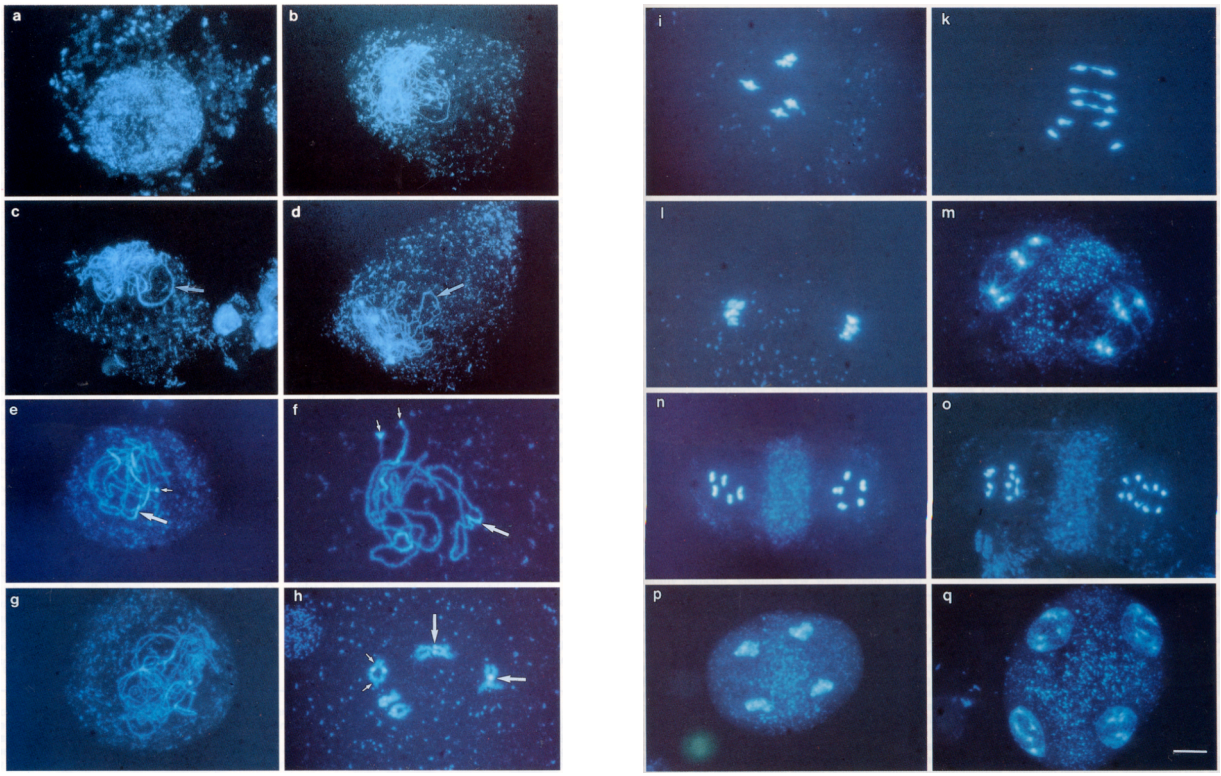

(Ross, *et al.*, 1996)

Figure 7 | Spreadings of DAPI-stained Meiotic Division Stages. (a) Interphase nuclei are characterized by diffuse chromatin. Chromosomes display spatial organization through association of clusterd telomeres around the nucleolus (Armstrong *et al.*, 2001). Leptotene displays beginning condensation of the duplicated homologous chromosomes going along with the formation of the SC axial element. The nucleolus and chromocentres are visible. Meiotic DSBs have been induced in this early stage.

(b-d) Zygotene is characterized by further chromosome condensation and partial synapsis (the beginning of parallel chromosome alignment). The nuclear lamina is degraded, resulting in loop-formation of chromosomes into the cytoplasm. Those loops can be seen as single thread like structures (arrows, panels c and d). Introduced DSBs are now processed, strand invasion, second end capture and ligation take place. However, HJs and COs are cytologically invisible, not until further chromosome condensation is achieved. Synapsis is stabilized by the help of beginning SC formation around sites of homologous recombination.

(e+f) Pachytene shows complete pairing of chromosomes. Pairs of synapsed homologs appear as thick thread-like structures. The SC is fully established and supports the homologous recombination process. HR has taken place, but is not visible yet.

(g) Diplotene stage is characterized by SC disassembly. Chiasmata are visible as the physical consequences of chromosomal HR events due to further chromosome condensation, Further chromosome condensation results in highly compacted bivalents.

(h) Diakinesis chromosomes are almost fully condensed. Bivalents are still attached through distal chiasmata. Opposing pulling forces at paired centromeres with equally oriented kinetochores lead to X-shaped bivalent structures (indicated by arrows) through the action of opposing microtubule-pulling forces. Diakinesis indicates the end of meiotic prophase I, demanding with a duration of approximately 14h almost half of the complete length of meiotic division in *Arabidopsis thaliana*.

(i) Metaphase I chromosomes are fully condensed and can be seen as five bivalents, each comprising of four sister chromatids. Opposing microtubule-pulling forces confer their alignment at the cell equator. In difference to mitosis, sister chromatid centromeres are monopolar oriented to the same direction and attached to microtubules, emanating from the same spindle pole. Pulling forces are compensated by chiasmata, which themselves are stabilized by distal cohesin molecules, located at the chromosome arms.

(k+l) Anaphase I is initiated by cleavage of the meiosis-specific kleisin subunit REC8 on chromosome arms. Subsequently, paired homologous chromosomes are separated to opposing cell poles instead of sister chromatids. Centromeric cohesin is protected from cleavage through phosphatase PP2A which is recruited by centromeric localized SGO1 as discussed in mitotic cell division.

Figure 7 | Spreadings of DAPI-stained Meiotic Division Stages (continued). (m) Events past anaphase I differ in several classes of eukaryotes, by means of cell wall formation and reassembly of the nuclear lamina in telophase I. Five chromosomes decondense and form a cluster at each pole. In *Arabidopsis thaliana* neither nuclear lamina reconstitution, nor cell wall formation is taking place. Hence, interkinesis is very short in comparison to mammalian meiotic cell division. Cytologically, Interkinesis is characterized by partial chromosome decondensation. Moreover preprophase band formation is visible.

(p+q) The second meiotic cell division is cytologically similar to mitotic cell division. In metaphase II two groups of recombined chimeric sister chromatids align separately at two division pllanes at the cell equator, mediated by opposite kinetochore orientation and bipolar spindle attachment (panel n). Anaphase II is triggered by Separase mediated centromeric REC8 cleavage, followed by chromosome segregation. Segregated sister chromatids form four clusters of new chromosomes (panel o). Finally, telophase II is completed by chromosome decondensation, nuclear lamina and cell wall formation, resulting in four haploid gamete-precursors.

2.5.5. Final Stages of Meiotic Division

During metaphase bivalents align at the cell equator, driven by opposing pulling forces, which are mediated by the cellular spindle apparatus. In difference to mitosis, kinetochores of both sister chromatids are oriented to the same direction and monopolar attached to microtubules originating from the same spindle pole. The pulling force necessary for stabilizing the microtubule attachments is generated by chiasmata, which are stabilized by distal cohesin molecules.

Cleavage of chromosome arm cohesin leads to the resolution of chiasmata and subsequent separation of now chimeric homologous chromosomes, which have exchanged genetic information through CO-resolution of the formed HJs. Centromeric cohesin is protected from Separase cleavage similar to mitosis by constant Rec8 dephosphorylation due to Sgo-PP2A complex formation, leading to separation of recombined parental chromosomes in anaphase I (Nasmyth and Haering, 2005; Watanabe, 2005). Meiotic cohesin localizes not only to pericentromeric regions but also to the core centromere, joining both kinetochore domains at meiosis I (Watanabe, 2004). Mutations in Rec8 homologs in fission yeast as well as in *Arabidopsis* lead to an ‘equational’ division at meiosis I and suggest a conserved mechanism in higher eukaryotes (Chelysheva *et al*., 2005). In budding yeast, a different set of proteins, called monopolins, is required for mono-orientation (Petronczki *et al*., 2006).

In some organisms the first meiotic division is completed by the formation of a new cell wall. The second meiotic division is mechanistically similar to mitosis. Due to preserved sister chromatid cohesion at centromeres, chimeric homologs align through bipolar microtubule attachment to now opposite oriented kinetochores. Cleavage of centromeric cohesin, segregation of chimeric sister chromatids and cell wall formation give finally rise to four haploid meiosis products called spores (reviewed in Orr-Weaver, 1999; Lee and Orr-Weaver, 2001; Ishiguro and Watanabe, 2007).

2.6. Hotspots of Meiotic Recombination

Genetic distances are measured by the frequence of crossing over between linked markers. Meiotic recombination occurs preferentially at certain genomic regions, which are referred to as hotspots of recombination, while other regions display almost no genetic recombination and are therefore called coldspots. For all organisms examined, including the yeast *Saccharomyces cerevisiae, Arabidopsis thaliana, Drosophila melanogaster, Mus musculus*, and man, meiotic recombination rates (expressed as cM/Mb) vary by almost two orders of magnitude (10-100-fold) along chromosomes (Pecina *et al*., 2002).

As meiotic recombination is important for generating genetic diversity and ensuring faithful chromosome segregation during meiosis, meiotic hotspots have been extensively studied and mapped by biochemical approaches in yeast. Since synchronized meiosis can be induced (Gerton *et al*.,2000), hotspots of meiotic recombination were characterized in plants, mice and humans as well. The factors that determine hot and cold regions of meiotic recombination are yet poorly understood.

Within yeast hotspots, DSBs occur locally in 50-250 bp sequence regions without obvious sequence similarity, mostly in nucleosome–free intergenic regions, which often bear transcription factor (TF) binding sites. Hotspot activity was classified according to dependence on the transcriptional status (Petes, 2001). α hotspot activity was found to be dependent on TF binding but not on transcriptional activity. Thereby TF binding is recruiting chromatin remodelling complexes like histone acetyltransferases (HATs) which render chromatin accessible by changing the nucleosome compaction through histone tail modification. Another class, β hotspots, are not dependent on transcriptional status with regard to their activity. In contrast to α hotspots they are harboring nucleosome excluding sequences, which stimulate both transcription and recombination (Iyer and Struhl, 1995; Kirkpatrick *et al*., 1999). Finally, γ hotspots might contain CpG islands, which are targeted by CpG-binding proteins that subsequently recruit again HAT, modifying the histone status.

Commonly, hotspots in yeast correlate with regions of high GC content and are located in regions with open chromatin structure (as expressed through DNaseI or micrococcal nuclease (MNase) hypersensitivity). Large scale analyses show that DSBs occur preferentially in chromatin loops, clustering in 50-100 kb hot domains while few DSBs occur in rather cold telomeric or centromeric regions. Higher-order chromatid structures seem to be important in comparison to local chromatin compaction since cold domains were found to contain open chromatin as well. Neighbouring hotspots were found to interact, and reduce activity of one another. It should be noted that some features of DSB distribution might bear a certain amount of incertitude, since those have been revealed using *rad50S* or *sae2*Δ mutants, accumulating unprocessed DSBs but showing reduction in DSB formation at particular regions (Pecina *et al*., 2002; Fukuda *et al*., 2008)

On a global scale entire chromosomes can be divided into large hot and cold domains concerning DSB formation activity. The molecular basis of these findings is yet not identified. Chromosomal structure might play a role over local determinants previously discussed (Borde *et al*., 1999). Trans-acting factors have a considerable effect on DSB induction. Several genes are essential for DSB formation, including *SPO11*, *MEI4*, *MER2*/*REC107*, *MRE2*/*NAM8*, *MRE11*, *RAD50*, *REC102*, *REC103*/*SKI8*, *REC104*, *REC114*, and *XRS2* as null mutants are recombination-defective during meiosis (Keeney, 2001; reviewed in Nishant and Rao, 2006). Studies in *Arabidopsis* have likewise demonstrated that the distribution of meiotic COs along chromosomes is non-random, displaying large differences in recombination frequencies (Drouaud *et al*., 2006; Singer *et al*., 2006; Kim *et al*., 2007).

Detailed mapping of recombinational hotspots has been conducted for *Arabidopsis* chromosome 4 (Drouaud *et al*., 2006), thereby showing no centromere-to-telomere gradient of recombination as proposed in other plants (reviewed in Mezard, 2006). Possibly recombination between highly repeated sequences (*e.g*. telomeres) is repressed to protect the genome against global rearrangements. Along chromosome 4 variations in CO rate ranging from 0 to >100 cM/Mb compared to average 4.6 cM/Mb are observed, clustering within intervals of a few kilobases. Fragments of less than 5 kb in size thereby display recombination rates of at least 5-fold above average. Specifically, hotspots of recombination are not corellated with the distribution of genes, pseudogenes, transposable elements or dispersed repeats (Drouaud *et al*., 2006).

Analysis of highly variable genome-wide patterns of linkage disequilibrium (LD) (the nonrandom association of alleles at different loci) likewise reveals a clear evidence for hotspots of recombination (Kim *et al*., 2006). In this study hotspots are found preferentially in intergenic regions (58 % vs. 44 % in genic regions). 260 hotspots have been identified, being typically 1-2 kb long and displaying up to 200x times higher recombination than the average background.

Linkage-mapping analysis of different *Arabidopsis thaliana* accessions has been able to identify non-uniform distribution of recombination, single feature polymorphisms (SFPs) and marker segregation rates (Singer *et al*., 2007). In detail, SFP distribution is found to display higher polymorphisms frequencies in pericentromeric regions and gene clusters. Only 12 % of recombination breakpoints map to genic regions. Genome-wide recombination rates display variation from 0.3 cM/Mb to 251 cM/Mb. Lowest recombination rates are found at centromeres and the chromosome 4 heterochromatin knob, as expected. High recombination rates can be found at localized genomic regions, at proximal telomeres of chromosomes 2, 3, 4 and at the distal end of chromosome 5.

2.7. Generation of Artificial Hotspots of Recombination

Considerable efforts have been put into the analysis of hotspots of meiotic recombination over the past years, gaining knowledge about the molecular features that define recombinational hotspots. The generation of artificial hotspots of recombination is beneficial to both basic research and applied sience. In basic research, the creation of artificial hotspots of recombination will allow to manipulate the distribution of DSBs over the chromosome. Thereby, further insight on CO regulation mechanisms will be obtained. In applied science, the generation of ectopic recombination will allow to stimulate HR dependend DNA repair. As a consequence gene conversion events might occur, thereby altering the allelic composition of the respective genome. Ectopic recombination induction between linked markers, might facilitate their segregation and the generation of novel recombinants. Thereby valuable tools for use in agriculture will be obtained.

Pioneering work in generating artificial hotspots of recombination was initially conducted in *Saccharomyces cerevisiae* to analyse control of frequency and distribution of meiotic recombination hotspots. Generation of a fusion protein comprising of Spo11 bearing the Gal4 DNA binding domain (*Gal4BD-Spo11*) rescued *spo11*Δ spore viability and generated DSBs. WT-like DSB induction was observed as well as strong DSB formation near Gal4 binding sites. Promisingly, *Gal4BD-Spo11* was able to create a recombinational hotspot at *GAL2*, a naturally DSB-cold locus, showing that the targeting of Spo11 to a specific site is sufficient to stimulate meiotic recombination (10-fold increase) that is under normal physiological control (Pecina *et al*., 2002).

When examining genome-wide binding and cleavage properties of *Gal4BD-Spo11*, only a subset of its binding sites was found to be cut, indicating that mere association of Spo11 with chromatin is not sufficient for DSB formation. In addition, *Gal4BD-Spo11* introduced DBSs inhibit surrounding DSB formation over distances up to 60 kb, keeping constant the number of DSBs per chromosomal region. These results demonstrate that targeting of Spo11 to new chromosomal locations leads to both local stimulation and genome-wide redistribution of recombination initiation and that some chromosomal regions (the centromeres) are inherently cold regardless of the presence of Spo11 (Robine *et al*., 2007).

The initial strategy was extended by introducing ectopic Gal4 target sites in form of four upstream activation sequences (4xUAS) (Pecina *et al*., 2002) or VDE-recognition sequences (VRSs) into distinct loci within the budding yeast genome. In this strategy an endogenous intein-encoded nuclease, VDE (also called PI-*Sce*I), which is a member of the homing endonuclease protein family was alternatively used to generate meiosis-specific DSBs at VRS sites in a Spo11-independent manner (reviewed in Fukuda *et al*., 2003).

Integration of ectopic UAS sites led to formation of flanking open chromatin structures, thereby elevating Spo11 mediated DSBs formation at the UAS site even in absence of *Gal4BD-Spo11* proteins. *Gal4BD-Spo11* was able to cleave UAS target sequences inserted in hot domains but rarely in cold domains. These data raise the possibility that two neighboring open chromatin sites may compete for the DSB formation machinery, leading to reduced activation at both sites.

Self-association of differently tagged Spo11 molecules occurred at UAS in a hot domain but not in a cold domain, raising the possibility that Spo11 remains in an inactive intermediate state in cold domains. PI-*Sce*I efficiently cleaved VRS sites in either context, suggesting that a cold domain is not a region of inaccessible or uncleavable chromosome structure (Fukuda *et al*., 2008).

In detail, integration of ectopic UAS and VRS sites was performed at various hotspots (*YCR048W*, *CYS3*, *GAT1*) to detect competitive interaction among hotspots, and yielded two types of effects. At *YCR048W* and *CYS3* regions, UAS integration and *Gal4BD-SPO11* expression caused the formation of an additional artificial hotspot. UAS insertion caused elevated meiotic DSBs at the insertion site and reduced natural hotspot activity, keeping the DSB number nearly constant within a given interval. This effect was observed in a Spo11 WT strain, but stronger in *Gal4BD-SPO11* strains. These data are consitent with a model of competition for DSB induction around hotspots, indicating that natural hotspot repression is higher when artificial DSB induction is stonger at a given site (Fukuda *et al*., 2008).

UAS integration near the *GAT1* locus likewise reduced natural hotspot. In contrast to both previously discussed hotspot regions, no artificial DSB induction was detectable at the UAS site (in a WT Spo11 context, while hotspot activity was somewhat higher in a strain expressing *Gal4BD-Spo11*). Insertion of the UAS site might provide a potential site for meiotic DSB induction. During meiosis, competition between the hotspot and the UAS site is taking place and resulting in a lack of sufficient DSB induction at either site. Forced recruitment of the DSB formation machinery to the UAS may enhance the capacity to form DSBs at this region and thus overcome the inhibitory effects of the UAS insertion. Hotspot activity gradually increased as the UAS was inserted further from the hotspot, whereas DSB formation at the inserted UAS remained at lower than detectable levels (Fukuda *et al*., 2008).

Insertion of VRS at the same site in a PI-*Sce*I deficient strain neither repressed DSB formation at the *GAT1* hotspot nor caused DSBs at the insertion site, while a reduction in hotspot activity was observed in a PI-*Sce*I proficient strain, when VDE-mediated DSBs were introduced proximally over regions of about 20 kb in length. Taken together, the VRS insertion itself does not affect hotspot activities like the UAS insertion, indicating that the observed reductions are directly due to VDE-mediated DSBs. Lower level of hotspot activity near the UAS and VRS integration sites is strongly suggested to be due to competitive interactions among DSB sites rather than due to artificial sequence interruption (Fukuda *et al*., 2008).

In *Schizosaccharomyces pombe*, the natural hotspot *mbs1* was modified to create a system for generating a single meiotic DSB, located at the *mbs1* region to measure crossover induction associated with gene conversion. Thereby, an exact replacement of the *rec12* ORF by that of the homing restriction endonuclease I-*Sce*I was engineered, putting I-*Sce*I expression under meiosis-specific physiological control. Moreover, an 18 bp target site for I-*Sce*I was introduced at the *mbs1* region. Thereby, site specific DSB induction could be achieved, leading to an 4 to 7-fold elevation of CO formation within a 26 kb or 243 kb window, respectively (Cromie *et al*., 2005).

2.8. Polydactyl Zinc-Finger Proteins, Meiosis-specific Nucleases

During recent years, zinc-finger protein (ZFP) DNA binding motifs received increasing attention and were involved in gene targeting strategies. ZFPs play an important role in a variety of cellular functions including transcriptional regulation, DNA and RNA binding, regulation of apoptosis, and protein-protein interactions. ZFPs can be classified in to serveral subtypes (C_2H_2, C_2C_2, C_2HC, $C_2C_2C_2C_2$, and $C_2HCC_2C_2$) depending on the number and order of Cysteine and Histidine residues within the motif (Klug and Schwabe, 1995; Mackay and Crossley, 1998). The C_2H_2-ZF motif was first discovered in the *Xenopus* oocyte transcription factor TFIIIA (Miller *et al*., 1985). At present date it is one of the best studied ZFP among eukaryotes (Laity *et al*., 2001). Early studies suggested an association with 5S rRNA (Picard and Wegnez, 1979), while later on the protein was suggested to display DNA binding activities and rather regulate the expression of the 5S rRNA gene (Pelham and Brown, 1980).

C_2H_2-type transcription factor ZFPs are often referred to as the classical zinc-finger (ZF), comprising in general of several zinc-finger domains that resemble an extensively studied DNA-binding motif (Lee, *et al*., 1989), which was crystallized successfully for the murine TF Zif268. The ZFs bind to the major groove of B-DNA and wrap way around the double helix. Each ZF domain is consisting of about only 30 amino acids, including two conserved Cys and two conserved His residues, which are tetrahydrally bound to a single zinc ion.

The C_2H_2-motif is representing a $\beta\beta\alpha$-fold, of two antiparallel β-sheets and an α-helix (Wolfe *et al*., 2000), wherein the chelation of the zinc ion is stabilizing the domains and contributing to domain folding (Wolfe *et al*., 2000; Laity, *et al*., 2001). Within this structure several conserved hydrophobic amino acids (commonly phenylalanine; F and leucine; L) are found to be essential for DNA binding activity, while amino acids within the α-helix are conferring DNA binding specificity. Each finger thereby contacts a three base pair subsite, conferring sequence specificity to a DNA stretch of 9bp in total (Figure 8; Pavletich *et al*., 1991; Pabo *et al*., 2001).

In-silico analysis within the *Arabidopsis* genome revealed a large number of C_2H_2-ZFPs, being plant specific and not conserved within other eukaryotes (Englbrecht *et al*., 2004). Two main structural features of plant ZFPs make them different from other eukaryotes. In plants ZF domains are separated by long spacers that vary in length and sequence from protein to protein (Sakamoto *et al*., 2004), while in animals a short spacer (six to eight amino acids, often TGEKP) is separating the domains. Moreover, most of the plant ZFPs bear a common QALGGH motif within the ZF α-helix, while animal and yeast lack this motif (Takatsuji, 1999; reviewed in Ciftci-Yilmaz *et al*., 2008).

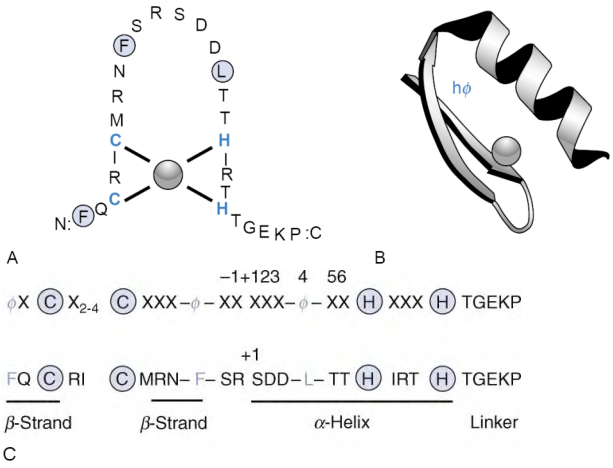

Figure 8 | ZF Sequence Conservation and 3D Structure of Zif268. The ZF domain fold is stabilized by chelation of a zinc ion by each two conserved Cys and His residues (marked in blue), respectively (panels A and B). Interaction with the major groove of B-DNA is mediated by conserved hydrophobic amino acid residues (blue circles), localized within the β-sheet and α-helix (panel A and C). Detailed analysis has led to the identification of amino acid residues that confer ZFP target site specificity, namely positions -1, 2, 3 and 6 (+1 refers to the first amino acid within the α-helix) within the helix domain. Individual ZF-domains are separated by a short linker, TGEKP in Zif268 (panel C).

The modular mode of interaction was investigated by phage display (Smith, 1985) by employing phage display libraries of the Zif268 DNA-binding domain, randomly altered in one of the three ZF-domains, and screening with different Zif268-like binding sites where the corresponding trinucleotide was altered to a given sequence. In short, only a subset of available triplets resulted in the selection of sequence-specific ZFs.

In more detail ZF phage selections were successful only when the 5' base of the triplet subsite was fixed (to G or T in case of Zif268), suggesting that individual ZF derivates are restricted to specifying a small repertoire of triplet sequences in the form of GNN and TNN (as well as ANN and CNN). ZF amino acid residues -1, 2, 3 and 6 were found to interact with 3 bp subsites and to specifiy overlapping 4 bp subsites.

This model is further supported by X-ray crystal structures of Zif268 (Elrod-Erickson *et al*., 1996, 1998), indicating that specificity for the base pair at the boundary between two DNA subsites arises from synergy of binding by amino acids (AA) from two adjacent zinc fingers, called target site overlap (TSO; *i.e.* recognition of the 5' position of a triplet is accomplished by contacts of AA residues +6 of one ZF and cross-strand interaction to the complementary base from position +2 of the following ZF; Figure 9). Specifically, TSO is limiting the number of GNN, ANN, CNN and TNN triplets (where N is either G, A, C or T) as the AA residue at position +2 is incompatible with cross-strand binding of certain nucleotides (Isalan *et al*., 1997; reviewed in Isalan *et al*., 1998; Papworth *et al*., 2006).

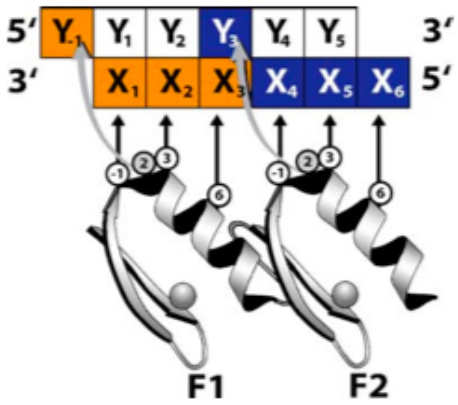

Figure 9 | PZF DNA Recognition Model. Adjacent ZFs (F1 and F2) bind within the major groove of the target DNA and recognize a 7 bp long binding site. Protein-DNA interaction is mediated by AA residues -1, 2, 3 and 6, respectively (AA positions involved in contacting DNA are circled and contacted bases are depicted as squares coloured orange for F1 and blue for F2).
Contacts to the primary DNA strand (positions X_1 to X_6) are made by AAs in positions −1, 3 and 6 (interactions are marked as straight black arrows), while the complementary strand of DNA (positions Y_{-1} to Y_5) is contacted by AA in position 2 (gray circle).
This cross-strand interaction is responsible for TSO between the F1 (orange) and F2 (blue) binding sites. Note that zinc fingers bind anti-parallel to 5′–3′ orientation of the primary DNA strand.

(Papworth *et al*., 2006)

As ZFP domains display a highly modular assembly, the C_2H_2-ZFP Zif 268 was used as a scaffold for designing ZFPs with novel sequence specificities. By mutating and replacing single ZF domains, different DNA sequences could be recognized. Phage Display techniques allowed for the analysis of a large number of recognition triplets, while several groups were using different approaches of sequential selection by randomization of single ZF domains within Zif268 (Greisman and Pabo, 1997), the selection of individual fingers (Segal *et al*., 1999; Segal and Barbas, 2000) and a bipartite library approach (Isalan *et al*., 1998, 2001). Moreover, other selection and library-screening techniques aside from phage display were developed to select ZFPs of desired DNA binding specificities (Cheng *et al*., 1997; Joung *et al*., 2000; Hurt *et al*., 2003; Hughes *et al*., 2005). Collected DNA binding data suggested that certain AA within the helical contact positions exhibited preferences for certain DNA bases, and led to the creation of a „recognition code"

With the help of growing open-source data bases, ZFPs are able to be constructed from scratch by mixing and matching modules from various archives (Mandell *et al*., 2006; Maeder *et al*., 2008; Fu *et al*., 2008).

To achieve a high specificity of ZFP target site binding within a larger genome, longer arrays of ZFPs (i.e. 6x ZF) have to be constructed. By the extended length of the ZFP binding problems arise, as the periocidicity of the ZFP modules does not match exactly the periocidicity of DNA. Canonical TGEKP linkers can put an excessive mechanical stress on the complex and result in decreased affinity of the ZFP. Slightly longer linkers in general, as well as three sets of 2x ZF or two sets of 3x ZF two fingers joined by extended linkers have been sucessfully used already (reviewed in Papworth *et al*., 2006). At present date, several applications of PZF domains involved in DNA binding in living cells has been described in literature (reviewed in Beerli and Barbas, 2002; Blancafort *et al*., 2003; Papworth *et al*., 2006).

An in particular interesting application employs the strategy of fusing a PZF domain to the catalytical non-specific cleavage domain of the prokaryotic type IIS restriction endonuclease *Fok*I, thereby successfully creating a site-directed DNA endonuclease (Kim *et al*., 1996). As the catalytical *FokI* domain only induces single-stranded DNA breaks, two molecules have to be directed to the same target, by fusion to PZFs targeting 2x 9 bp DNA stretches that margin the DNA cleavage site (Mani *et al*., 2005). Only when the monomers are in close proximity, a DNA DSB is successfully introduced. As DNA binding is needed to activate the nuclease, a highly 18 bp site-specific restriction enzyme is created.

This artificial fusion protein is capable of creating site-specific DSBs at desired genomic locations and will be referred to as zinc finger nuclease (ZFN) in future discussion. With the construction of ZFNs directed genome alterations are becoming possible. As low HR rates between ectopic and genomic DNA in plant cells suggested a rather NHEJ-based default repair pathway of DSBs in somatic cells, the strategy of ZFN-mediated DSB induction was primarily used for site-directed mutagenesis (Lloyd *et al*., 2005). Within this strategy, the use of site-specific DSB induction and subsequent repair through the error-prone NHEJ pathway, was resulting in an altered target gene sequence (Figure 10; Tzfira and White, 2005).

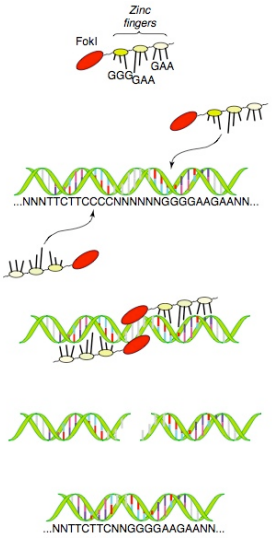

Figure 10 | ZFNs as a Tool for Site-directed Mutagenesis. Zinc finger nucleases are comprising of non-specific, catalytical *Fok*I nuclease domains fused to polydactyl zinc-finger DNA-binding motifs. ZF modules together confer high DNA binding specificity and target the protein to a 9 bp recognition sequence.

Two molecules of FokI are needed to introduce a DSB, and are targeted by a set of two different polydactyl zinc-finger proteins (PZF). After DSB induction, NHEJ-mediated DNA repair generates small insertion or deletion mutants within the targeted gene.

(Tzfira and White, 2005)

It could be shown that ZFNs are capable of generating mutations at the targeted locus with high frequency (0.2 mutations per target; Lloyd *et al*., 2005). However, other studies have used this strategy successfully along the course of HR mediated gene correction (Urnov *et al*., 2005), as well as in HR mediated integration of an ectopic recombination template in plants (10 % HR events per target; Wright *et al*., 2005). As induced HR repair at the DSB site is considerably higher than spontaneous HR-mediated integration elsewhere in the genome, these studies clearly display that the generation of desired DSBs is the rate-limiting step along HR-mediated gene modification. Since recognition specificities of PZFs can be easily manipulated, ZFN-based technologies are thereby gaining importance as key players in targeted mutagenesis as well as in gene correction and gene replacement in a wide range of organisms from flies to man (reviewed in Durai *et al*., 2005; Tzfira and White, 2005; Papworth *et al*., 2006; Wu *et al*., 2007).

The major drawback of this strategy, the low ratio of locus-specific HR-mediated integration to NHEJ-mediated random insertion requires for the screening of high numbers of calli or seeds to detect favorable site-specific recombination events. Moreover, eventual HR events are taking place in somatic tissue. If seedlings have been subjected to site-directed HR induction, then a high number will have to be screened to identify transformants that have successfully undergone HR mediated genome alteration within gametophyte precursors. In addition the progeny of such a plant has to be screened again to identify modified plants after mendelian segregation of the genetic alteration. In case that protoplasts were used for induction of HR, callus regeneration and subsequent steps of callus differentiation have to be conducted to obtain heterozygous transgenic plantlets that have to be propagated further to obtain transgenic progeny (described in detail in Wright *et al*., 2005).

An alternative strategy of induction of site-specific HR involves the use of meiosis-specific nucleases (section 2.7). Initially this basic research strategy was used to create artificial hotspots of recombination. Targeted DSB formation within known hotspots and coldspots was used to gain basic insight into hotspot definition and formation as well as into the phenomenon of crossover interference, the spatial inhibition of homologous recombination within a certain distance around the artificially introduced hotspot of recombination. Several studies were successfully targeting a fusion protein of Spo11 with a Gal4 DNA-binding domain (*Gal4BD-Spo11*) to distinct genomic loci, thereby stimulating DSB induction within those genomic regions.

This strategy can be extended to create a meiosis-specific nuclease by fusing *Spo11* to a locus-specific PZF protein. Both *Gal4BD-Spo11* (Pecina *et al*., 2002, Fukuda *et al*., 2008) and *Spo11-PZF* constructs (*QQR-Spo11*; Borde *et al*., 2009) have been successfully enhancing DSB formation at certain loci. As during meiosis either ZMM protein and Mus81/Eme1 mediated HR are the major DSB repair pathway besides SDSA (section 2.5.3), artificially introduced DSBs might be repaired by HR with considerable efficiency, resulting in successful recombination of flanking genetic markers or transgene integration in the presence of an exogenous, ectopic recombination substrate. Together with high-throughput screening methods available in plants, which are addressing HR based on pollen-specific fluorescent marker exchange (Francis *et al*., 2007), this strategy has the potential to become the state-of-the-art in induction of targeted locus-specific recombination events.

2.9. Aims and Objectives

Meiotic DSB formation is essential to ensure genetic diversity and faithful chromosome segregation. Recombination hotspots are well characterized in budding yeast. In plants however, knowledge about these chromosomal regions is still incomplete with respect to distribution and interference with one another. The conserved protein SPO11 plays a central role in both DSB induction and localization within hotspots of meiotic recombination. Correspondingly, the protein is involved in all main objectives of this project.

The main project of this thesis is directed towards generation of meiosis-specific site directed nucleases. The creation of a meiosis-specific nuclease is beneficial both to basic research as well as to applied agricultural science. In basic research, the induction of site-specific DSBs in a meiotic context allows for the analysis of CO control mechanisms in different mutant backgrounds as well as for the recovery of novel recombinants in the course of genetic crosses. In detail, an enhanced level of site-directed DSB formation leads to stimulation of HR events at the target locus. Thereby, the segregation of normally closely linked markers can occur. Inversely, this strategy can be used to successfully combine mutant alleles at will. If their genetic distance is low, it is extremely labor intensive to create certain allelic combinations by simple crossing of single mutants (*e.g*. Mourad *et al*., 1994). The latter strategy can be applied to the field of plant breeding as well, thereby facilitating the combination of genetic markers, and the combination of desired traits.

Studies in yeast have been successful to fuse Spo11 to Gal4 and PZF DNA binding domains to induce HR in a meiotic context. Our strategy involved the generation of a series of different *At*SPO11-PZF fusion proteins. Generated *At*SPO11-PZF fusion proteins likewise may resemble site-specific nucleases that are introducing DSBs in a meiotic context. So far this strategy has been successfully implemented in budding yeast. *At*SPO11-PZF fusion proteins bearing an additional 18x *c-Myc* epitope were designed to allow immunochemical protein manipulation.

The following main objectives were anticipated to be addressed within this study:

1) A series of different *At*SPO11-PZF fusion proteins should be designed. *At*SPO11-1 was chosen initially for *At*SPO11-1-PZF fusion protein generation, sparing *At*SPO11-2-PZF construction for future experiments.

2) Constructed *At*SPO11-1-PZF and 18x Myc tagged derivatives should be analyzed for their ability to complement endogenous *At*SPO11-1 protein function *in-planta*.

3) *At*SPO11-1-PZF expression should be addressed either *in-vivo* or *in-planta*.

4) Constructed *At*SPO11-1-PZF and 18x Myc tagged derivatives should be analyzed for DNA binding activity.

*5) Constructed At*SPO11-1-PZF and 18x Myc tagged derivatives should be analyzed for locus-specific HR stimulation activity.

With the successful verification of *At*SPO11-PZF locus-specific nuclease activity, a tool for locus-specific DSB induction will be generated. As a consequence, generated *At*SPO11-PZF fusion proteins will induce DSBs at a chosen locus within the *Arabidopsis* genome, thereby successfully generating an artificial hotspot of recombination. After this initial proof-of-principle, the *CSR1*-specific PZF DNA-binding will be substituted for any target-specific PZF domain and will be utilized in basic research, adressing hotspot distribution and interference.

3. Results

3.1. General *At*SPO11-1 Fusion Protein Construction Strategy

Though *At*SPO11-1 and *At*SPO11-2 were recently identified as the plant key players in meiotic DNA DSB formation, their mode of action remains elusive (Grelon *et al*., 2001; Hartung and Puchta, 2000, 2001; Stacey *et al*., 2006). The basic mechanistic mode of DSB induction seems to be conserved in all eukaryotic kingdoms, however the regulation of this initial step of meiotic recombination is different in yeast and higher eukaryotes concerning essential proteins and involved protein complexes. A potential interaction of *At*SPO11-1 and *At*SPO11-2 remains to be confirmed, and the composition of DSB inducing complexes in higher eukaryotes as well remains to be determined.

The creation of differentially tagged *At*SPO11-1 and *At*SPO11-2 fusion proteins and subsequent Co-IP experiments will give insight into *At*SPO11 multimer complex composition and allow for the identification of interaction-partners.

Previous to this thesis, strategies of *At*SPO11-1 fusion protein construction were assessed. A common technique within the plant field, the creation of cDNA constructs in order to complement genomic mutations of the gene of interest (*e.g*. described in Durrant *et al*., 2007) was found to be non-successful, as an *Atspo11-1* mutation could not be complemented by an *AtSPO11-1* cDNA construct (Mathilde Grelon and Christine Mezard, Institut Jean-Pierre Bourgin, INRA de Versailles, France; Peter Schlögelhofer, MFPL, Vienna, Austria; personal communication).

Analysis of the *AtSPO11-1* gene has revealed, that the gene harbours an intron in the 3' untranslated region (UTR), which is not always spliced out. In addition, 3' RACE experiments revealed three polyadenylation sites (poly(A) sites), one located within the 3' UTR intron and two distal to the intron. Alternatively spliced cDNAs could be detected in somatic and generative tissue (Hartung and Puchta, 2000).

These findings establish the possibility that *At*SPO11-1 stability might be differently regulated in somatic and generative tissue by alternative splicing and subsequent rapid mRNA decay of premature stop codon-comprising mRNA molecules along the course of the nonsense-mediated decay (NMD) pathway (Gutierrez *et al*., 1999). To circumvent this possibility, it was decided to clone the whole genomic locus of the *AtSPO11-1* gene, including 5' and 3' UTR regions, harbouring putative promoter and potential regulatory downstream sequences (Figure 11 for further details; detailed description in Krsicka, 2007).

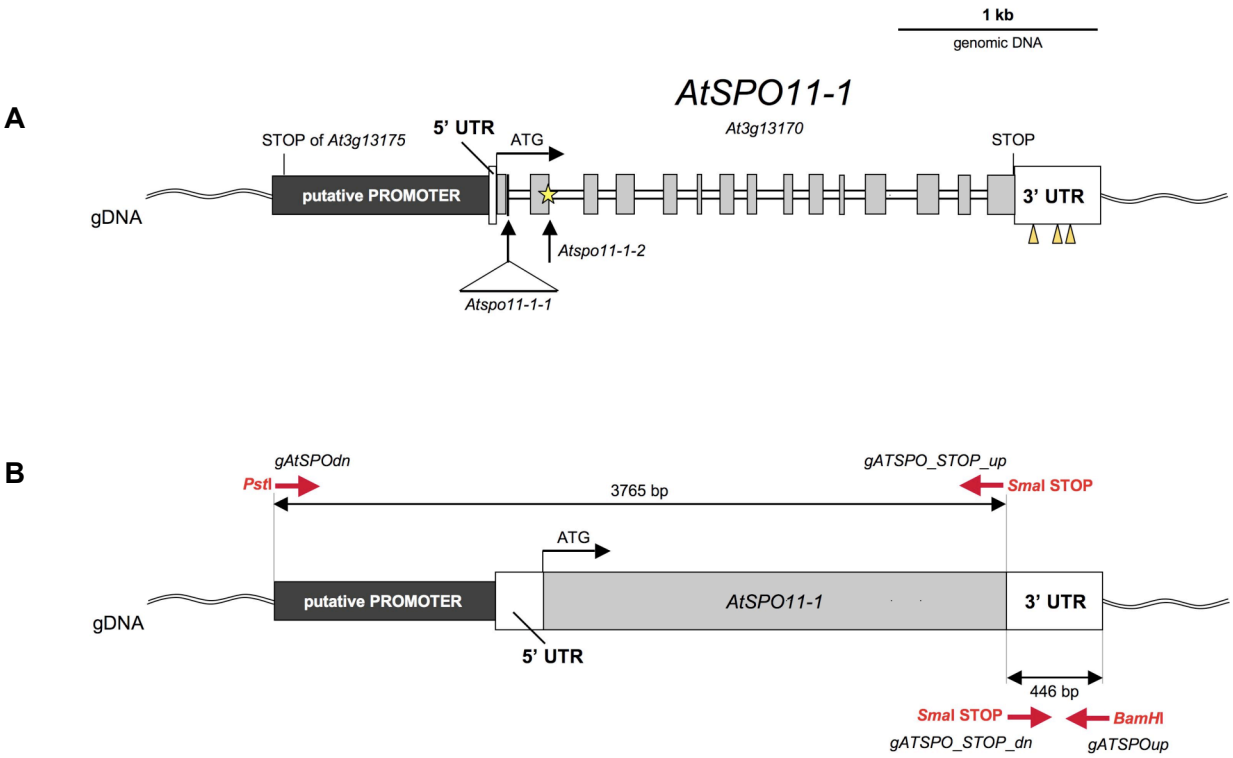

Figure 11 | *AtSPO11-1* Genomic Locus Cloning Details. (A) Schematic of the genomic locus of *AtSPO11-1*. Exons are depicted as filled boxes (light grey) and introns as open lines. Positions of *AtSPO11-1* mutant alleles are depicted as black arrows. The *Atspo11-1-1* allele is a T-DNA insertion mutant, while Atspo11-1-2 is a point mutation introduced by EMS mutagenesis, creating an artificial CAPS marker (indicated by a yellow star). Three poly(A) sites within the 3' UTR (Hartung and Puchta, 2000) are indicated as yellow triangles.

(B) Schematic representation of cloned *At*SPO11-1 wild-type like transgene. Previous to this thesis the whole genomic region was cloned by PCR amplifition of two separate fragments (bordered by vertical lines). Oligonucleotide primers were designed to amplify the first fragment from the stop codon of the upstream gene (At3g13175), including the putative promoter (dark grey), 5' UTR, and the full-length gene from start codon (ATG) to the last nucleotide upstream of the stop codon (STOP). Primers *gATSPOdn* and *gATSPO_STOP_up* were designed to introduce artificial restriction endonuclease (RE) sites *Pst*I and *BamH*I, allowing downstream cloning of the amplified genomic region (indicated in red). The second fragment was amplified from the stop codon (STOP), artificially introducing a *Sma*I RE site in frame with and right upstream of the stop codon, down to the start codon of the downstream gene (At3g13160), using primers *gATSPO_STOP_dn* and *gATSPOup*. The *Sma*I RE site in frame with the stop codon of *At*SPO11-1 allows for the introduction of protein tags at the C-terminus of *At*SPO11-1 and thereby for the creation of artificial fusion proteins.

This strategy ensured that the *AtSPO11-1* gene is expressed under the control of its endogenous regulatory sequences. Thereby transgene expression occurs under physiological control. Moreover, the generation of Spo11 fusion proteins was already successfully accomplished in different studies in yeast (*Gal4BD-Spo11*, Pecina *et al.*, 2002; *QQR-Spo11*, Borde *et al.*, 2009).

Cloning and tagging of *AtSPO11-1* was conducted previous to this thesis (Krsicka, 2007). To this end, the *AtSPO11-1* genomic locus was amplified from *Arabidopsis thaliana* ecotype columbia (Col-0) genomic DNA (gDNA) in form of two fragments. The oligonucleotide primers used for PCR amplification of the gDNA locus were designed to harbour artificial restriction endonuclease (RE) sites at their 5' termini (Fragment (1) *Pst*I upstream, *Sma*I/*BamH*I downstream; Fragment (2) *Sma*I upstream, *BamH*I downstream).

Both fragments were amplified using a high fidelity, proofreading DNA Polymerase. PCR amplicons were precipitated, resolved and subjected to a single *Taq* DNA polymerase mediated incubation step, resulting in addition of a single adenosine residues at the 3' DNA termini. Processed PCR fragments were then introduced into a TA cloning compatible vector (*pCR2.1-TOPO*). After verification of the DNA sequences by cycle sequencing, Fragment (1) was cloned as a *Pst*I/*BamH*I fragment into the multiple cloning site (MCS) of the plant binary vector *pCB302* (Xiang *et al*., 1999), released from its *pCR2.1-TOPO* vector backbone after RE digest. Fragment (2) was cloned similarly into pCB302.Fragment (1) as a *Sma*I/*BamH*I fragment.

The resulting construct was termed *pCB302.AtSPO11-1* and harbours the whole *AtSPO11-1* genomic locus, including upstream putative promoter sequences, 5' UTR as well as the 3' UTR with potential downstream regulatory sequences. As discussed previously, the construct harbours a *Sma*I RE site right upstream of the endogenous stop codon. Introduction of the *Sma*I site *CCCGGG* led to the addition of the two amino acids, proline and glycine, at the C-terminus of *At*SPO11-1. The *Sma*I site allows any protein tag of interest to be fused in-frame to the *At*SPO11 C-terminus. Furthermore in a separate construct the 735 bp coding sequence of an 18x *c-Myc* epitope (18xMyc) was introduced at the *Sma*I site of *pCB302.AtSPO11-1* as blunt-ended *Sma*I/*EcoR*V fragment, released from *pCR2.1-TOPO.18xMyc* after RE digest, giving rise to the construct *pCB302.AtSPO11-1.18xMyc*.

Both constructs *pCB302.AtSPO11-1* and *pCB302.AtSPO11-1.18xMyc* harbour a plant selectable marker conferring phosphinotricin herbicide resistance (BASTA®) and the 4211 bp *AtSPO11*-transgene under endogenous control, either in a wild type-like situation in the first construct, or in a tagged version in the latter construct, representing the starting point material for this thesis (Figure 12; see supplementary data for detailed sequence information).

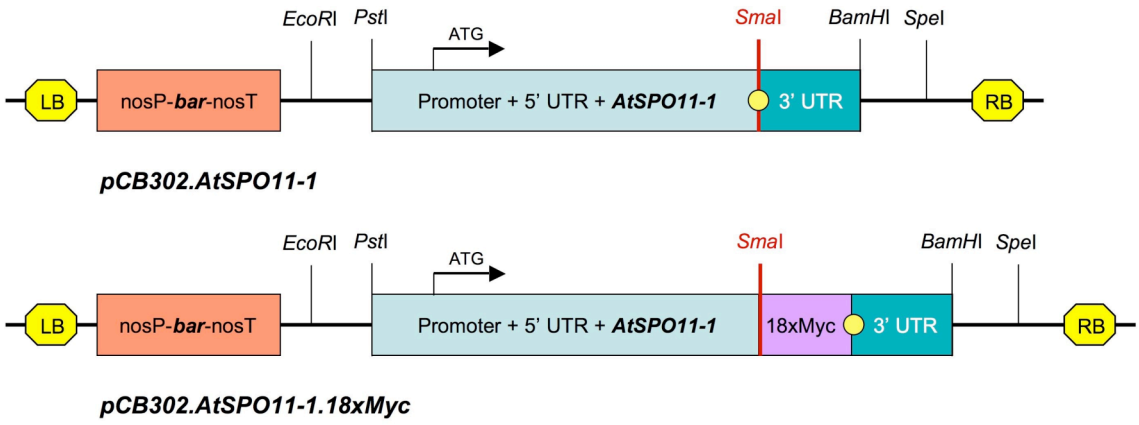

(Vector maps are not drawn to scale, see supplementary data for detailed sequence information)

Figure 12 | Initial *AtSPO11-1* Construct Details. Properties of the generated constructs *pCB302.AtSPO11-1* and *pCB302.AtSPO11-1.18xMyc*. Both constructs were generated within the plant binary vector pCB302 backbone. Left border and tight border (LB and RB, respectively) sequences allow random T-DNA integration into the plant genome during *Agrobacterium* mediated *in-planta* transformation. The *Streptomyces hygroscopicus bar* gene under control of the nopaline synthase promoter and terminator (nosP / nosT) serves as plant selectable marker, conferring BASTA resistance. The cloned 4211 bp *AtSPO11-1* genomic region (light and dark blue), an artificial 18x *c-Myc* epitope (purple) and the artificial *Sma*I RE site (*Sma*I, red), followed by the stop codon (yellow circle) are marked.

3.2. Generation of *At*SPO11-1-PZF Fusion Proteins

3.2.1. Design and Construction of PZF DNA Binding Motifs

PZF design rules and protocols for ZFN assembly have been reviewed in various reports (*e.g.* Carrol *et al.*, 2006; Mani *et al.*, 2005, Wright *et al.*, 2006). Moreover, tools and vectors for the design and assembly of novel ZFNs are available from different Labs and consortiums (Barbas Lab, www.zincfingertools.org; Zinc Finger Consortium, www.zincfingers.org; ZiFiT, Zinc Finger Targeter, http://bindr.gdcb.iastate.edu/ZiFiT/). Even though ZFNs can be designed to target most genomic sequences, failures in targeting experiments may occur (Ramirez *et al.*, 2008), emphasizing the need for target site binding activity assays *in-vitro* as well as *in-vivo* (*in-planta*). For this purpose the Tzfira group designed a series of different vector systems, which allow an easy assembly and transfer of ZFN coding sequence (CDS) between bacterial and plant expression vectors, as well as digestion assays for the functional analysis of newly designed ZFNs (reviewed in Tovkach *et al.*, 2008).

Previous studies in yeast had shown that locus-specific DNA DSB induction was mediated by *GAL4BD-SPO11* constructs, and that levels of HR were artificially elevated at these loci (Pecina *et al.*, 2002, Fukuda *et al.*, 2008). At the beginning of this thesis *At*SPO11-1-GAL4BD fusion proteins and 5xUAS site bearing plant lines were successfully generated, but not assessed concerning stimulation of locus-specific HR (Bernd Edlinger, MFPL, University of Vienna, Austria; personal communication; Krsicka, 2007).

The *At*SPO11-1-PZF strategy was anticipated to induce DNA DSBs in a site-specific manner, resulting ultimatively in the exchange of flanking markers due to HR-mediated DSB repair. A putative target locus had to be chosen to screen to screen for site-specific recombination events *in-vivo.* Therefore, the careful selection of the target locus was an important factor during generation of an *At*SPO11-1-PZF fusion protein.

The endogenous *Arabidopsis CSR1* locus was chosen as target for PZF constructs because of its unique characteristics that allow detection and screening of HR events (discussed in section 3.5 in further detail). The *CSR1* locus encodes an enzyme called acetolactate synthase (ALS), which is involved in branched amino acid metabolism. Two EMS-mutagenesis derived alleles, *csr1-1* and *csr1-2*, both point mutations, are spaced 1369 bp apart and confer resistance to different herbizide classes. Test crosses between *csr1-1* and *csr1-2* indicated very low intragenic recombination rates of 0.008 cM, corresponding to four recombination events in 100.000 crosses (Mourad *et al*., 1994), and will allow the detection of elevated recombination events after *At*SPO11-PZF induced DSB formation.

At the beginning of this study, standardized protocols for design and construction of ZFNs were readily available (Mani *et al*., 2005; Carroll *et al*., 2006; Wright *et al*., 2006), all of them discussing the construction of *Fok*I-3x ZF fusion proteins, targeting two 9 bp target sites, spaced apart by 6-8 nt (section 2.8, Figure 10). As *Fok*I induces DNA cleavage only as a dimer, this strategy gave rise to 18 bp site-specific nucleases that thereby can target virtually any locus within a given higher eukaryotic genome with high specificity. As the direct mode of *At*SPO11-mediated DSB formation remains to be elucidated, this strategy was not directly applicable to generation of an *At*SPO11-PZF fusion protein. Therefore, we decided to design and construct *At*SPO11-PZF fusion proteins that obtain enhanced target specificity by a single PZF DNA binding domain and not by dimerization of two directed ZFN molecules.

To get insight into the ratio of PZF-mediated target sequence length and potential binding site occurence within the Arabidopsis genome, a series of 3xZF and 4xZF PZF proteins were designed *in-silico* and subjected to a computational binding site prediction analysis. Initial *de-novo* PZF design was performed together with our external collaborator (Tsvi Tzfira, Department of Molecular, Cellular and Developmental Biology, University of Michigan, Ann Arbor, MI, USA). A series of previously constructed 3xZF constructs, termed *ZFN2* and *ZFN4*, were used to estimate the number of 9 bp target sites within the genome. Two independent 4xZF PZF constructs, termed *ZF-G* and *ZF-F,* were newly designed to specifically target the endogenous *CSR1* locus of *Arabidopsis thaliana*. Target site sequences were converted into ZF protein AA sequences with the help of the Barbas Lab online resource ZF Tools v.3.0 (www.zincfingertools.org).

Binding prediction analyses were performed with the help of the bioinformatics unit of the IMP Research Institute of Molecular Pathology (Novatchkova, IMP - Research Institute of Molecular Pathology, Vienna, Austria).

Table 1 | Initial Zinc Finger Designs and Binding Site Numbers within the *Arabidopsis* Genome.

Target Site	Site Sequence	Triplet Subsites	Contact Residues and DNA CDS (reverse translated)	ZF Binding Sites Chr. I; II; III; IV; V
ZFN2	GTG GCC GCT	RH1 GCT	**Q** S S **D** L T **R** CAG TCT TCT GAT CTT ACT CGT	31; 15; 38; 19; 30
		RH2 GCC	**D** R S **D** L T **R** GAT CGT TCT GAT CTT ACT CGT	
		RH3 GTG	**R** S D **A** L T **R** CGT TCT GAT GCT CTT ACT CGT	
ZFN4	ATG GAT GCA	RH1 GCA	**Q** S G **D** L R **R** CAG TCT GGA GAT TTG CGT CGT	NA
		RH2 GAT	**T** S G **N** L V **R** ACT TCT GGA AAT TTG GTT CGT	
		RH3 ATG	**R** R D **E** L N **V** CGT CGT GAT GAA TTG AAT GTT	
ZF-G	GGT ACA GAT GCG	RH1 GCG	**R** S D **D** L V **R** CGT TCT GAT GAT CTT GTT CGT	1; 0; 2; 0; 3
		RH2 GAT	**T** S G **N** L V **R** ACT TCT GGA AAT TTG GTT CGT	
		RH3 ACA	**S** P A **D** L T **R** AGC CCG GCG GAT CTG ACC CGC	
		RH4 GGT	**T** S G **H** L V **R** ACT TCT GGA CAT CTT GTT CGT	
ZF-F	GGT CCT GGT GTA	RH1 GTA	**Q** S S **S** L V **R** CAG TCT TCT TCT CTT GTT CGT	1; 1; 1; 1; 1
		RH2 GGT	**T** S G **H** L V **R** ACT TCT GGA CAT CTT GTT CGT	
		RH3 CCT	**T** K N **S** L T **E** ACT AAA AAC TCT CTT ACC GAA	
		RH4 GGT	**T** S G **H** L V **R** ACT TCT GGA CAT CTT GTT CGT	

ZFN2 and ZFN4 were designed previously and serve to estimate 3xZF target site numbers within the *Arabidopsis* genome. ZFN-G and ZFN-F were designed to target different single 9 bp sites (ZFN-G, 625-636 bp; ZFN-F, 1911-1922 bp) within the endogenous *Arabidopsis CSR1* locus (AT3G48560). Contact residues -1, 3 and 6 within recognition helices (RH) confer triplet subsite binding specificity and are depicted in bold.

Computational analysis of target site occurrence within the Arabidopsis genome revealed, that 3xZF PZF proteins target numerous perfect-matched loci, ranging from 15 to 38 per chromosome. Those values are even higher if a single ‘wobble base’ is considered in 3xZF target site pairing. Therefore they are not suited for the directed induction of site-specific DSBs, as high numbers of off-target cleavage might occur. 4xZF PZFs are targeted to few or single perfect-matched loci, ranging from zero to three target sites per chromosome, respectively.

Both 3xZF constructs were found to target between 15 to 38 sites per *Arabidopsis* chromosome and are therefore not suited to confer specificity to a single target locus. The 4xZF constructs *ZF-G* and *ZF-F* were found to display a lower number of target sites. *ZF-G* was predicted to bind five ectopic target sites, located on chromosomes I, III and V. *ZF-F* was predicted to bind once within every chromosome I to V, thereby binding four ectopic target sites (Table 1). Both 4xZF designs were chosen for the construction of *At*SPO11-1-PZF fusion proteins.

PZF protein construction was performed by our collaborator according to a modified standardized protocol (Mani *et al*., 2005). In brief a modular assembly strategy was used in contrast to the modification of preexisting PZFs (*e.g*. Zif268). For this purpose, the well-defined human transcription factor SP1 ZF motif was divided into invariant consensus framework backbone sequences and variable specificity-determining α-helical domains. For each of those domains, overlapping oligonucleotides, encoding the according AA sequence were generated. Three invariant backbone oligos (BBO1 to BBO3) and three specificity determining oligos (SDO1 to SDO3), designed to encode the appropriate contact residues at helix positions -1 to +6, were linked to generate a construct, encoding a PZF AA sequence that recognizes a specific 9 bp target site. Moreover, BBOs and SDOs were designed to carry RE sites at the begin and end of a complete BBO-SDO complex, allowing lateron the replacement of single fingers, as well as the addition of other ZF modules to generate enhanced target site specificity (Figure 13; described in detail in Mani *et al*., 2005).

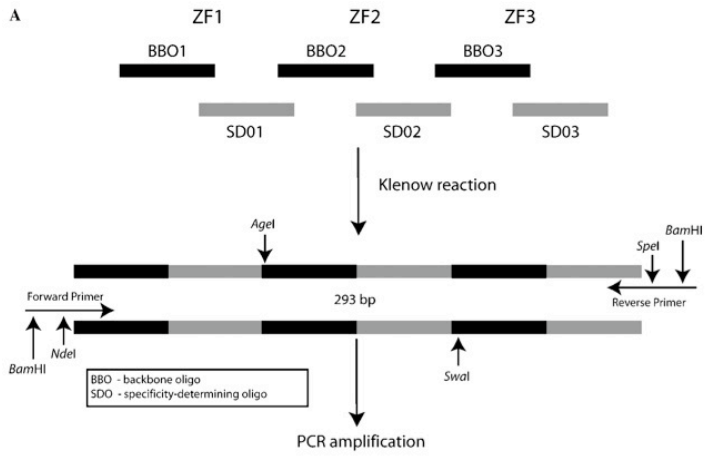

Figure 13 | PCR-mediated PZF Synthesis. Invariant backbone oligonucleotides (BBO) and variable specificity determining oligos (SDO) were designed to share sequence identity at their overlapping 5' and 3' termini. After initial annealing, gaps are filled up by a Klenow fragment-mediated extension reaction. A final PCR mediated amplification reaction is performed, using RE site flanked oligonucleotide primers that allow downstream cloning of the constructed PZF sequence.

In contrast to the scheme, oligonuleotides harbouring RE sites *Xho*I and *Spe*I were used within *ZFN2*, *ZFN4*, *ZF-G* and *ZF-F* construction.

(Mani et al., 2005)

BBOs and SDOs were annealed and the gaps filled up by Klenow reaction. The assembled PZF sequences were subjected to a PCR amplification, using *Xho*I and *Spe*I RE site flanked oligonucleotide primers, and ligated into a *Xho*I/*Spe*I-cleaved *pSAT4.35S.NLSFokI* vector, thereby linking the PZF sequence to the N-terminus of a catalytical *Fok*I cleavage domain. The construction of *pSAT4.35SP.NLSFokI* allows the assembly of a PZF-*Fok*I fusion construct in a plant expression vector in a single cloning step.

In addition, the constitutive 35S promoter can be easily replaced as an *Age*I/*Nco*I fragment, and the whole plant expression cassette can be mounted onto *pRCS* based *A.tumefaciens* binary vectors (reviewed in Tzfira *et al*., 2005).

To allow the expression of PZF-*Fok*I fusion proteins in *E.coli* cells, constructs were mobilized as *Nco*I/*BamH*I fragments and cloned into the bacterial expression vector *pET28.XH* (Figure 14; described in detail in Tovkach *et al*., 2008) finally giving rise to constructs termed *pET28.CSR1-ZFN-G* and *pET28.CSR1-ZFN-F*, respectively (see supplementary data for detailed sequence information).

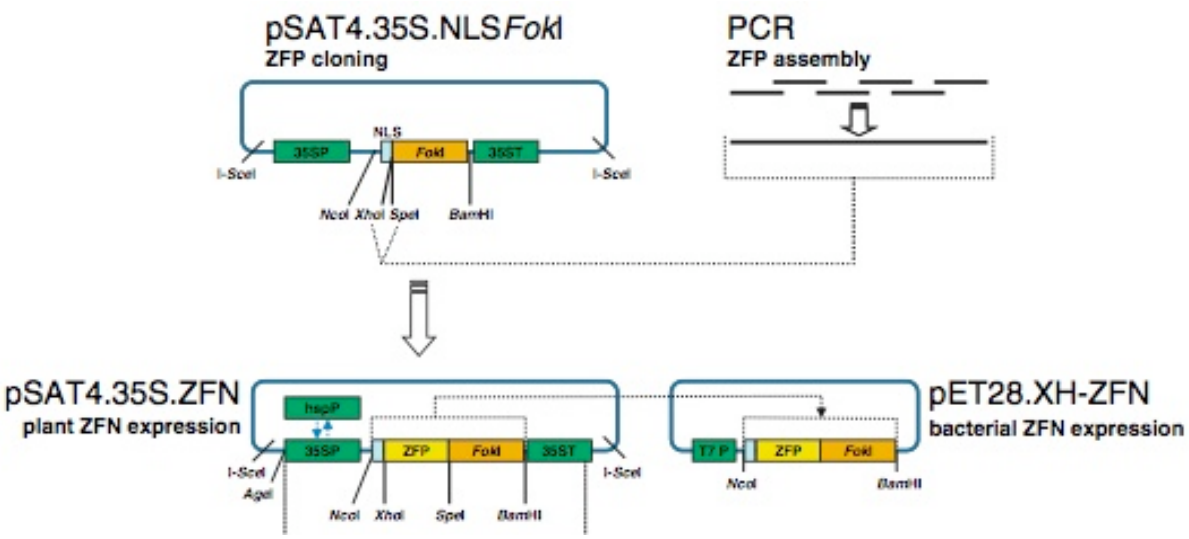

(adapted from Tovkach *et al*., 2008)

Figure 14 | PZF Assembly and Subcloning. After synthesis of the PZF encoding molecule (ZFP) by subsequent Klenow/PCR reaction, the PZF is cloned in-frame into *pSAT4.35S.NLSFokI*, as *Xho*I/*Spe*I fragment, thereby creating a construct pSAT4.35S.ZFN. This construct encodes a fusion protein under the constitutive 35S plant promoter (35SP), where the PZF is fused to the N-terminus of a catalytical *Fok*I cleavage domain.

To obtain a test system for *in-vitro* DNA cleavage activity, the whole ZFP-*Fok*I construct is subcloned into the bacterial expression vector *pET28.XH* as *Nco*I/*BamH*I fragment, resulting in the construction of *pET28.XH-ZFN*.

3.2.2. *In-vitro* Analysis of 4xZF DNA Binding Activity

PZF DNA binding activity was addressed by the detection of PZF-*Fok*I mediated plasmid-embedded PZF target site cleavage. For this purpose two complementary oligonucleotide primers were designed, which code for the *ZF-F* and *ZF-G* target sites in opposite direction. Both sites are separated by a 6 nt long spacer, bearing a *Sac*I RE site. The oligonucleotides were annealed and cloned as *Nco*I/*Pst*I fragment into the vector *pSAT6-MCS* (Tzfira *et al*., 2005), giving rise to constructs termed *pSAT6.CSR1-ZFN-F-TS* and *pSAT6.CSR1-ZFN-G-TS*.

Constructs *pET28.CSR1-ZFN-G* and *pET28.CSR1-ZFN-F* were transformed separately into BL21 *E.coli* cells, and the crude bacterial lysate was used after overexpression of the PZF-*Fok*I fusion proteins for analysis of in-vitro target site DNA ceavage activity. Target site bearing plasmids *pSAT6.CSR1-ZFN-F-TS* and *pSAT6.CSR1-ZFN-G-TS* were subjected to several parallel biochemical assays.

Plasmids were subjected to *Age*I and *Age*I/*Sac*I RE digests, linearizing the 4488 bp target site plasmids, or releasing a 953 bp vector fragment, respectively. To address target site cleavage ability both PZF-*Fok*I fusion proteins were used in combination with *Age*I. *Age*I/*Sac*I and *Age*I/ZFN digestion patterns were similar and dependend on the ammount of ZFN within the reaction mixture. These results indicated that both 4xZF constructs *ZF-F* and ZF-G could cleave their corresponding target sites in an *in-vitro* context (Figure 15; described in detail in Tovkach *et al.*, 2008).

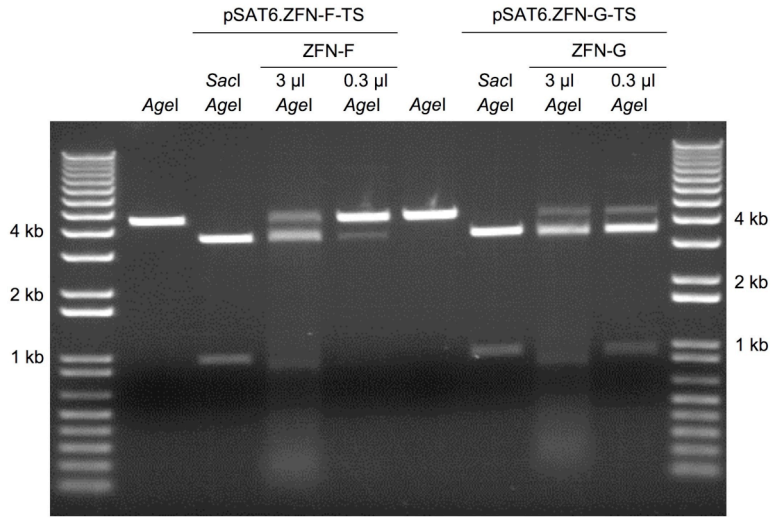

Figure 15 | 4x ZF in-vitro DNA Binding Activity Assay. Target site harbouring plasmids were subjected to *Age*I and *Age*I/*Sac*I restriction endonuclease digests, resulting in linearization of the 4488 bp plasmid or release of a 953 bp fragment.

As the *Sac*I RE site resembles the 6 nt spacer between the two opposite oriented 4xZF target sites, the proper localization of a *Fok*I dimer at the spacer region is anticipated in giving rise to a similar digestion pattern.

Both constructs *ZF-F-Fok*I and *ZF-G-Fok*I are able to generate the similar 3535 bp / 953 bp band pattern as seen in the *Age*I/*Sac*I double digest, indicative of successful target site-specific DNA cleavage *in-vitro*.

(Courtesy of Andriy Tovkach)

3.2.3. Fusion of *At*SPO11-1 with 4xZF DNA Binding Motifs

Successful design of two independent 4x ZF constructs *ZF-G* and *ZF-F*, both targeting the endogenous *CSR1* locus of *Arabidopsis* was addressed at computational level as well as *in-vitro*. Initial analyses showed that both designed PZF modules target not more than one or two distinct loci per chromosome. Moreover both constructs were found to confer site-specific DNA cleavage activity *in-vitro* in the context of a PZF-*Fok*I fusion protein. These findings qualified both constructs *ZF-F* and *ZF-G* for further use in generation of an *At*SPO11-PZF fusion protein.

The C-terminal *Sma*I RE site of construct *pCB302.AtSPO11-1* (Krsicka, 2007) was selected as insertion site of the 4ZF constructs. Oligonucleotide primers were designed to amplify *ZF-F* and *ZF-G* coding regions, spanning domains BBO1 to SDO4 from templates *pET28.CSR1-ZFN-F* and *pET28.CSR1-ZFN-F*, respectively, avoiding amplification of the NLS sequence. Downstream primer *4xZFN FW1* was designed to introduce an N-terminal *Sma*I RE site, followed by an *Arabidopsis* codon-usage optimized 1x Ala, 3x Gly linker (see supplementary data for detailed sequence information), while upstream primer *4xZFN REV1* introduced a C-terminal *EcoR*V RE site within *ZF-F* and *ZF-G* encoded proteins.

336 bp *ZF-F* and *ZF-G* encoding fragments were amplified using the high fidelity *Ex Taq* DNA Polymerase (TaKaRa Bio Inc.). Processed 368 bp PCR amplicons were ligated into a TA cloning compatible vector (*pCR2.1-TA*, Invitrogen) giving rise to constructs *pCR2.1-TA.CSR1-ZFP-F* and *pCR2.1-TA.CSR1-ZFP-G*, respectively (see supplementary data for detailed sequence information). Cloned *ZF-F* and *ZF-G* sequences were further verified by cycle sequencing, using primers *M13 forward (-20)* and *M13 reverse*. Fragments *ZF-F* and *ZF-G* were subjected to a RE double-digest and released as 354 bp *Sma*I/*EcoR*V fragments from their respective vectors *pCR2.1-TA.CSR1-ZFP-F* and *pCR2.1-TA.CSR1-ZFP-G. ZF-F* and *ZF-G* fragments were ligated into *Sma*I digested, linearized 9262 bp *pCB302.AtSPO11-1* vector. Transformants harbouring the 4xZF constructs in appropriate orientation were identified by „Colony-PCR“ using oligonucleotide primer pairs *4xZFN REV1* and *SpoSeq5dn*. Verified constructs were termed *pCB302.AtSPO11-1.CSR1-ZFP-F* and *pCB302.AtSPO11-1.CSR1-ZFP-G*, respectively (see supplementary data for detailed sequence information). Cloned *ZF-F* and *ZF-G* sequences were again verified by cycle sequencing using primers *4xZFN FW1*, *4xZFN REV1* and *Spo11Seq5dn.* Verified constructs were further transformed into an *Agrobacterium* GV3101 strain. Both generated constructs *pCB302.AtSPO11-1.CSR1-ZFP-F* and *pCB302.AtSPO11-1.CSR1-ZFP-G* harbour the whole *At*SPO11-1 genomic locus and regulatory sequences (section 3.1) as well as different 354 bp coding sequences of *CSR1* locus-specific *4x ZF-F* and *4x ZF-G* DNA binding motifs (Figure 16).

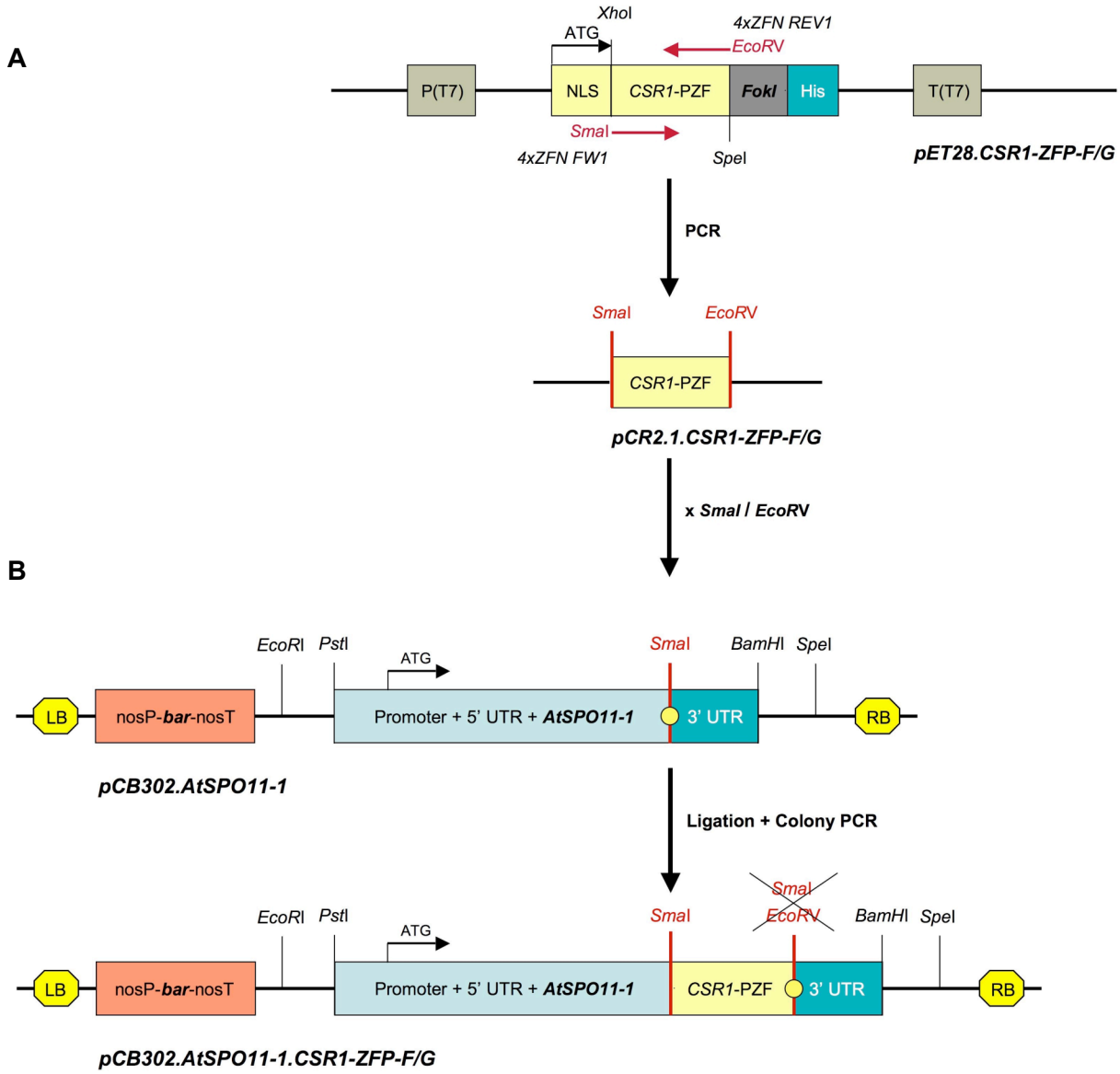

(Vector maps are not drawn to scale, see supplementary data for detailed sequence information)

Figure 16 | *At*SPO11-1-*CSR1*-ZFP Construction Scheme. (A) The coding regions of *CSR1* locus-specific *ZF-F* and *ZF-G* DNA binding proteins (*CSR1*-PZF) were PCR amplified using primers 4xZFN FW1 and 4xZFN REV1, thereby introducing flanking RE sites *Sma*I N-terminal and *Eco*RV C-terminal (with regard to *CSR1*-PZF protein orientation). The PCR amplicons were introduced into vector pCR2.1-TA, giving rise to constructs *pCR2.1.CSR1-ZFP-F* and *pCR2.1.CSR1-ZFP-G*, respectively.

(B) After sequence verification *ZF-F* and *ZF-G* encoding sequences were mobilized as blunt-ended *Sma*I/*Eco*RV fragments after RE double-digest, and ligated into a *Sma*I linearized *pCB302.AtSPO11-1* construct. The cloned 354 bp *ZF-F* or *ZF-G* encoding regions (*CSR1*-PZF, yellow) are in-frame with regard to the *At*SPO11-1 genomic context. Resulting constructs were designated *pCB302.AtSPO11-1.CSR1-ZFP-F* and *pCB302.AtSPO11-1.CSR1-ZFP-F* and resemble putative site-directed AtSPO11-PZF fusion proteins.

3.2.4. Fusion of *At*SPO11-1-*CSR1*-ZFP Constructs with *c-Myc* Protein Tags

Completing successful confirmation of PZF-*Fok*I fusion protein mediated site-specific DNA cleavage activity *in-vitro*, *AtSPO11-CSR1-ZF* constructs have to be subsequently tested for their *in-vivo* activity as well. We decided to address *AtSPO11-CSR1-ZF* mediated DNA binding and cleavage activity separately. As Spo11-DNA and *At*SPO11-DNA recombination intermediates were enriched in an *Atcom1-1*$^{-/-}$ mutant backgorund (Keeney *et al*., 1997; Uanschou *et al*., 2007), ChIP of *At*SPO11-CSR1-ZF should therefore allow to address DNA binding activity in common, while target site specificity can be confirmed by successful amplification of target site-flanking DNA regions (discussed in sections 3.5, 4.4.3 and 4.4.4 in further detail).

Prior to this thesis, various strategies for biochemical *At*SPO11-1 detection were addressed. An *AtSPO11-1* antibody (Courtesy of Chris Franklin, School of Biosciences, University of Birmingham, United Kingdom) was available but failed in *At*SPO11-1 IP experiments (Peter Schlögelhofer, MFPL, Vienna, Austria; personal communication). The composition of the DSB inducing complex in higher eukaryotes is still unsolved. Therefore the possibility, that *At*SPO11-1 and *At*SPO11-2 induce DSBs, embeded within a multiprotein complex, still remains.

It might be possible that accessory proteins hinder the immunological detection of *At*SPO11-1 by masking the immunogenic epitopes (Ondrej Krsicka, former MFPL, Vienna, Austria; personal communication). As an alternative strategy, an 18x *c-Myc* epitope was introduced at the transgenic *At*SPO11-1 C-terminus, giving rise to the construct *pCB302.AtSPO11-1.18xMyc* (section 3.1) and successfully used in immunobiochemical transgene detection (Krsicka, 2007).

To enable future ChIP experiments of generated *At*SPO11-CSR1-ZF constructs, it was decided to generate 18x *c-Myc* epitope tagged variants As no experience regarding a possible interaction of the 18x *c-Myc* epitope and the CSR1-ZF DNA bining domain was available, different versions of fusion proteins were designed by. Thereby the 18x *c-Myc* epitope was introduced either at the N-terminus or at the C-terminus of the *CSR1*-ZF domain. As only the in-frame *SmaI* RE site in front of the *At*SPO11-1 stop codon can be used for generation of AtSPO11-1 fusion proteins two different design strategies were applied. A *Sma*I/*EcoR*V fragment of *ZF-F* and *ZF-G*, respectively was introduced into *pCB302.AtSPO11-1.18xMyc*, giving rise to *At*SPO11-1-CSR1-ZF-18xMyc configuration. Alternatively, a *Sma*I/*EcoR*V fragment of the 18x *c-Myc* epitope was introduced into previously generated constructs *pCB302.AtSPO11-1.CSR1-ZFP-F* and *pCB302.AtSPO11-1.CSR1-ZFP-G*, respectively, giving rise to *At*SPO11-1-18xMyc-CSR1-ZF (Figure 17; see supplementary data for detailed sequence information).

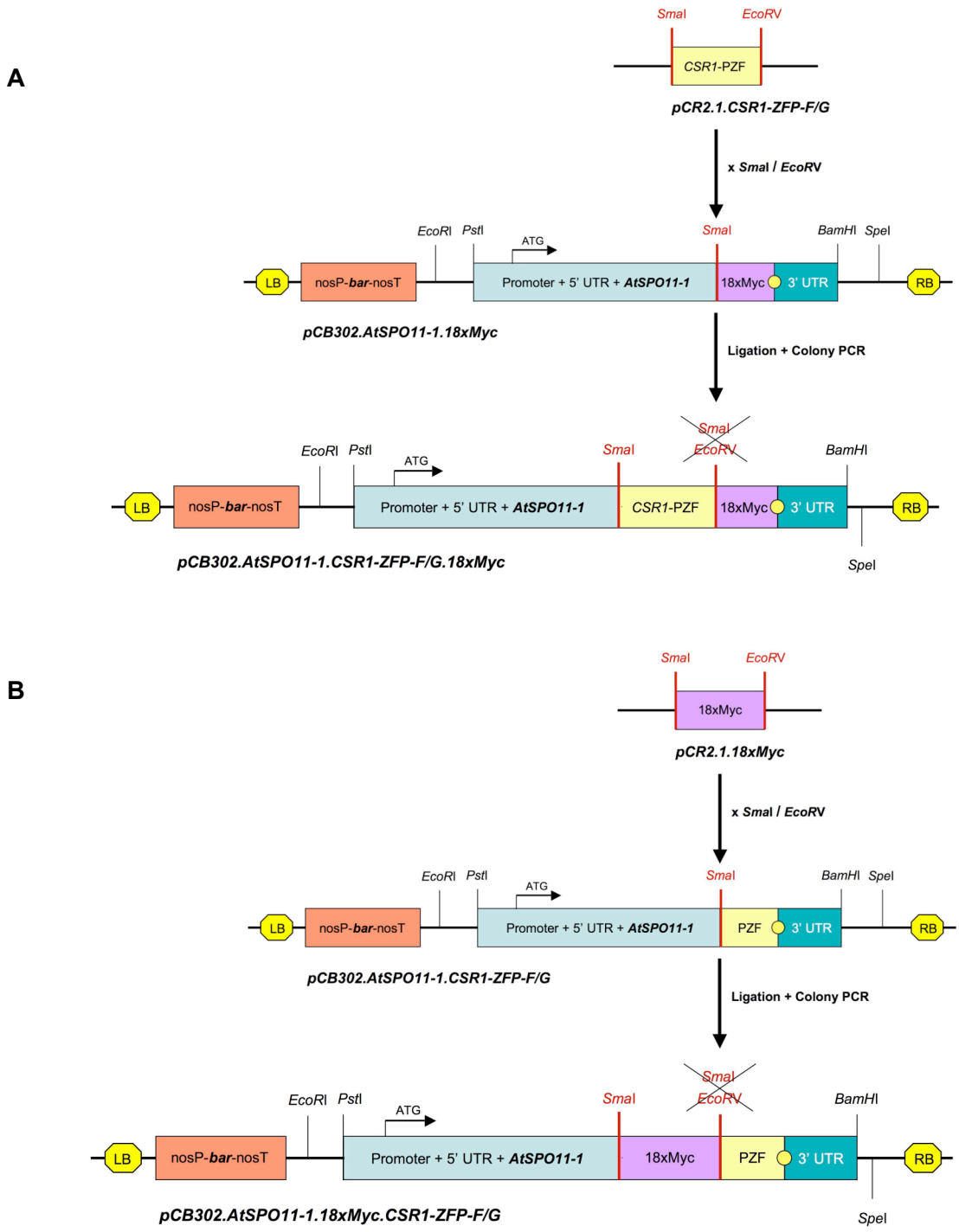

(Vector maps are not drawn to scale, see supplementary data for detailed sequence information)

Figure 17 | Generation of *18x c-Myc* Epitope-tagged *At*SPO11-1-*CSR1*-ZFP Constructs. During generation of *18xMyc* tagged *At*SPO11-1.CSR1-ZFP constructs two parallel strategies were used, allowing the introduction of the *18xMyc* tag at the *CSR1*-ZFP N-terminus and C-terminus, respectively.

(A) *ZF-F* and *ZF-G* encoding sequences were mobilized as blunt-ended *Sma*I/*EcoR*V fragments after RE double-digest, and ligated into a *Sma*I linearized *pCB302.AtSPO11-1.18xMyc* construct. *At*SPO11-1 (light blue), *CSR1*-PZF (yellow) and 18xMyc (purple) encoding regions are in-frame with regard to the *At*SPO11-1 genomic context. Resulting constructs contain a distal 18xMyc epitope and were designated *pCB302.AtSPO11-1.CSR1-ZFP-F.18xMyc* and *pCB302.AtSPO11-1.CSR1-ZFP-G.18xMyc.*

(B) In parallel, the 18xMyc encoding sequence was likewise mobilized as blunt-ended *Sma*I/*EcoR*V fragment from *pCR2.1.18xMyc* and ligated into a *Sma*I linearized *pCB302.AtSPO11-1.CSR1-ZFP-F* and *pCB302.AtSPO11-1.CSR1-ZFP-G*, harbouring the 18xMyc epitope in a more proximal position. Resulting constructs were designated *pCB302.AtSPO11-1.18xMyc.CSR1-ZFP-F* and *pCB302.AtSPO11-1.18xMyc.CSR1-ZFP-G.*

In detail, Fragments *ZF-F* and *ZF-G* were subjected to a RE double-digest and released as 354 bp *Sma*I/*EcoR*V fragments from their respective vectors *pCR2.1-TA.CSR1-ZFP-F* and *pCR2.1-TA.CSR1-ZFP-G.* Processed blunt-ended *ZF-F* and *ZF-G* fragments were ligated into *Sma*I digested, linearized 9997 bp *pCB302.AtSPO11-1.18xMyc* vector. In parallel, the 18x *c-Myc* Epitope encoding region was subjected to a RE double-digest and released as 735 bp *Sma*I/*EcoR*V fragment from the respective vector *pCR2.1-TOPO.18xMyc.* The processed blunt-ended 18xMyc fragment was ligated into *Sma*I digested, linearized 9997 bp *pCB302.AtSPO11-1.CSR1-ZFP-F and pCB302.AtSPO11-1.CSR1-ZFP-G* vectors, respectively. Transformants harbouring the 4xZF constructs in appropriate orientation were identified by colony PCR using oligonucleotide primer pairs *4xZFN REV1* and *SpoSeq5dn*, and clones bearing the 18xMyc epitope using oligonucleotide primer pairs *c-myc_new_dn* and *4xZFN REV1*.

Verified constructs were termed *pCB302.AtSPO11-1.CSR1-ZFP-F.18xMyc and pCB302.AtSPO11-1.18xMyc.CSR1-ZFP-F*, respectively (constructs bearing *ZF-G* were termed likewise, including the designation ZFP-G). *At*SPO11-1-CSR1-ZF-18xMyc derivatives, bearing cloned *ZF-F* and *ZF-G* sequences were again verified by cycle sequencing using primers *4xZFN FW1, 4xZFN REV1* and *Spo11Seq5dn.* After sequence verification constructs *pCB302.AtSPO11-1.CSR1-ZFP-F.18xMyc and pCB302.AtSPO11-1.CSR1-ZFP-G.18xMyc* were transformed into an *Agrobacterium* GV3101 strain. Both constructs *pCB302.AtSPO11-1.18xMyc.CSR1-ZFP-F* and *pCB302.AtSPO11-1.18xMyc.CSR1-ZFP-G* were stored and further processed after completion of this study.

3.3. Complementation Analysis of *At*SPO11-1-PZF Variants

Both *Arabidopsis* Spo11 homologues *At*SPO11-1 and *At*SPO11-2, have been found to be required for meiotic recombination initiation (Grelon *et al*., 2001; Hartung and Puchta, 2000, 2001; Stacey *et al*., 2006) as each single mutant displayed a typical severe asynaptic meiotic phenotype, as well as significantly reduced seed production (Grelon *et al*., 2001; Stacey *et al*., 2006). As it has been shown that genomic constructs of *AtSPO11-1* and *AtSPO11-2* successfully complemented the respective *Atspo11-1* and *Atspo11-2* mutant phenotypes (Hartung *et al*., 2007; Krsicka, 2007). Complementation analysis of *At*SPO11-1-CSR1-ZF derivates should therefore evaluate the functionality of the generated fusion protein constructs.

Different studies described and characterized mutant alleles for both *A*tSPO11-1 (Grelon *et al*., 2001; Stacey *et al*., 2006) and *At*SPO11-2 (Stacey *et al*., 2006; Hartung *et al*., 2007). Three mutant *Atspo11-1* alleles are available. A Versailles collection T-DNA insertion mutant (Bechtold *et al*., 1993) within the Wassilewskija (Ws) ecotype was termed *Atspo11-1-1* and was found to yield residual chiasmata formation (7 % of WT) and recombination frequency (10 % of WT). An EMS mutagenesis-derived allele termed *Atspo11-1-2* was generated within the col-0 ecotype, and found to be a true null-allele (Grelon *et al*., 2001). Moreover a SALK Institute (Alonso and Stepanova, 2003) T-DNA insertion allele (SALK_146172) Atspo11-1-3 (Stacey *et al*., 2006) is available.

In case of *At*SPO11-2, three different meiosis-specificmutant alleles have been previously described, namely the The RIKEN (Ds) transposon (Kuromori *et al*., 2004) mutant (Ds11-6598-1) *Atspo11-2-1*, and Syngenta T-DNA insertion library (Sessions *et al*., 2002) mutant (SAIL_551_F05) *Atspo11-2-2* (both described in Stacey *et al*., 2006) as well as GABI collection (Rosso *et al*., 2003) insertion mutant (GABI-Kat 749C12) *Atspo11-2-3* (Hartung *et al*., 2007).

Figure 18 | *Atspo11-1* Mutant Phenotype. Comparison of adult wild-type ecotype Columbia (Col-0) and *Atspo11-1-2* plants clearly shows the mutant-associated low-fertility phenotype expressed by reduced silique size. In the right panel the *Atspo11-1-2* mutant fertility phenotype is indicated, being identical *Atspo11-1-1* and *Atspo11-1-3* alleles (Stacey *et al*., 2006; Hartung *et al*., 2007; personal observation).

While *Atspo11-1* mutant plants exhibit an overall morphology similar to WT, seed production is significantly reduced in both *Atspo11-1-1* and *Atspo11-1-2* alleles (average 2 seeds / silique compared to 45+/- 5 for WT plants) as well as seed abortion (32%) (Grelon *et al*., 2001).

Generally, single mutants *Atspo11-1-1*, *Atspo11-2-1* and *Atspo11-2-2* were found to confer a similar mutant low-fertility phenotype, (Grelon *et al*., 2001; Stacey *et al*., 2006; Figure 18 for further details), as well as *Atspo11-1-3; Atspo11-2-3* homozygous double mutants (Hartung *et al*., 2007). For complemetation analysis of present and future *At*SPO11-PZF derivates, mutant alleles *Atspo11-1-2* and *Atspo11-2-3* were chosen.

Characterization of available *Atspo11-1-1* and *Atspo11-1-2* mutant alleles has shown that homozygous mutant plants display a severe meiotic defect, resulting in significantly lowered seed formation and viability (Grelon *et al*., 2001). Homozygous mutant *Atspo11-1-1* and *Atspo11-1-2* plants derived from selfing display low seed formation (average 2 seeds/silique) and seed viability (average 33 % abnormal seeds). Reciprocal crosses of homozygous *Atspo11-1-1* and wild-type ecotype Wassilewskija (Ws) plants result in 3.2 seeds/silique and 0.2 % seed abortion in case of female mutant plants and 10.1 seeds/silique and 33 % seed abortion in case of male mutant plants as crossing partners.

Heterozygous mutant *Atspo11-1* plants, however, are morphologically indistinguishable from WT plants, regarding seed production fertility and meiotic progression. *Atspo11-1* alleles can be classified as recessive mutations as half of the *AtSPO11-1* gene dosage is sufficient for WT-like plant development (Grelon *et al*., 2001; Stacey *et al*., 2006; Hartung *et al*., 2007). For this reason, *Atspo11-1* mutations are propagated in a heterozygous state to maintain WT-like fertility levels. Analogously, heterozygous *Atspo11-1-2* plants were used for *Agrobacterium*-mediated transformation.

Constructs *pCB302.AtSPO11-1.CSR1-ZFP-F* and *pCB302.AtSPO11-1.CSR1-ZFP-F.18xMyc* were initially used to transform a population, representing the offspring of a heterozygous *Atspo11-1-2* plant according to a modified floral dip method (Clough and Bent, 1998). As *Agrobacterium*-mediated transformation efficiency is considerably low, successfully transformed T_0 progeny was selected for BASTA resistance. For each transformed construct, 96 individual, BASTA resistant transformants were selected.

As the offspring of an *Atspo11-1-2* heterozygous plant was used for *Agrobacterium* mediated transformation, segregation of the *Atspo11-1-2* allele was taking place in the subsequent generation. Thereby *AtSPO11-1* plants, *Atspo11-1-2* heterozygous and homozygous plants were transformed with *AtSPO11-PZF* constructs. To address the ability of generated *At*SPO11-1-CSR1-ZF derivates to complement homozygous *Atspo11-1-2* mutations, the endogenous *AtSPO11-1-2* genotype had to be determined for two reasons.

First, A*tspo11-2* heterozygous and homozygous plants would display different ratios of sterile plants upon transgene non-complementation in the next generation of 25 % and 100 %, respectively (described below in further detail). Second, homozygous *Atspo11-1-2* mutant plants had to be identified to confirm successful *AtSPO11-1-CSR1-ZF* transgene complementation and to obtain plant lines that do no longer segregate the mutant genotype, allowing the generation of non-segregating *Atspo11-1-2*$^{-/-}$*; AtSPO11-1-CSR-ZF*$^{+/+}$ plant lines.

PCR-mediated *Atspo11-1-2* genotype determination was performed, utilizing a CAPS marker within the *Atspo11-1-2* EMS-allele in form of a newly formed *Vsp*I RE site. The *Atspo11-1-2* genotype was assessed after *Vsp*I RE digestion of the oligonucleotide primer *spo11-1-2-MG52* and *spo11-1-2-MG96* generated PCR amplicon, resulting in a full-length PCR product conferred by the *AtSPO11-1* WT allele, and a *Vsp*I cleaved amplicon derived from mutant allele amplification. As both oligonucletotide primers did bind within the cloned genomic region used for *At*SPO11-1-CSR1-ZF transgene construction, a WT band was always observed, generated by PCR amplification from the integrated transgene, regardless of the *Atspo11-1-2* genotype. Therefore only the presence of the mutant *Atspo11-1-2* allele could be addressed, but not the allelic situation at the *Atspo11-1-2* locus, leaving heterozygous and homozygous mutant *Atspo11-1-2* alleles virtually indistinguishable. However, heterozygous and homozygous mutant alleles could be identified after propagation of mutant lines by selfing. An *Atspo11-1-2* heterozygous allele would segregate in the subsequent generation, giving rise to 25 % *AtSPO11-1* WT plants. Those can be identified through PCR-mediated genotype determination due to lack of the CAPS marker. In contrast, an *Atspo11-1-2* homozygous allele would no longer segregate, giving rise to 100 % *Atspo11-1-2* homozygous progeny. As a consequence a CAPS marker-specific fragment pattern would be detected in all analyzed samples (Figure 19).

To precicely determine the *Atspo11-1-2* genotype within a given generation, another PCR-mediated genotype determination assay had been designed (Krsicka, 2007). To avoid the amplification of transgenic *At*SPO11 sequences, oligonucleotide primer *spo11-1 allele_new* and *spo11-1 pin_up* were designed. As the *spo11-1 allele_new* binding site was located upstream of the cloned AtSPO11-1 region, a PCR amplicon was only yielded from the endogenous *AtSPO11-1* locus and not from an integrated *AtSPO11-1-CSR1-ZF* transgene. Again, the *Atspo11-1-2* genotype was assessed after *Vsp*I RE digestion of the oligonucleotide primer *spo11-1 allele_new* and *spo11-1 pin_up* generated PCR amplicon, resulting in distinguishable fragments, thereby allowing to clearly delineate the *Atspo11-1-2* genotype and to identify *Atspo11-1-2* homozygous mutant plants within the same generation (Figure 19).

As the latter „PIN PCR“ mediated *Atspo11-1-2* genotype determination was not robust due to lack of optimization, the *Atspo11-1-2* genotype of the majority of transformed lines was determined using the former described „CAPS PCR“.

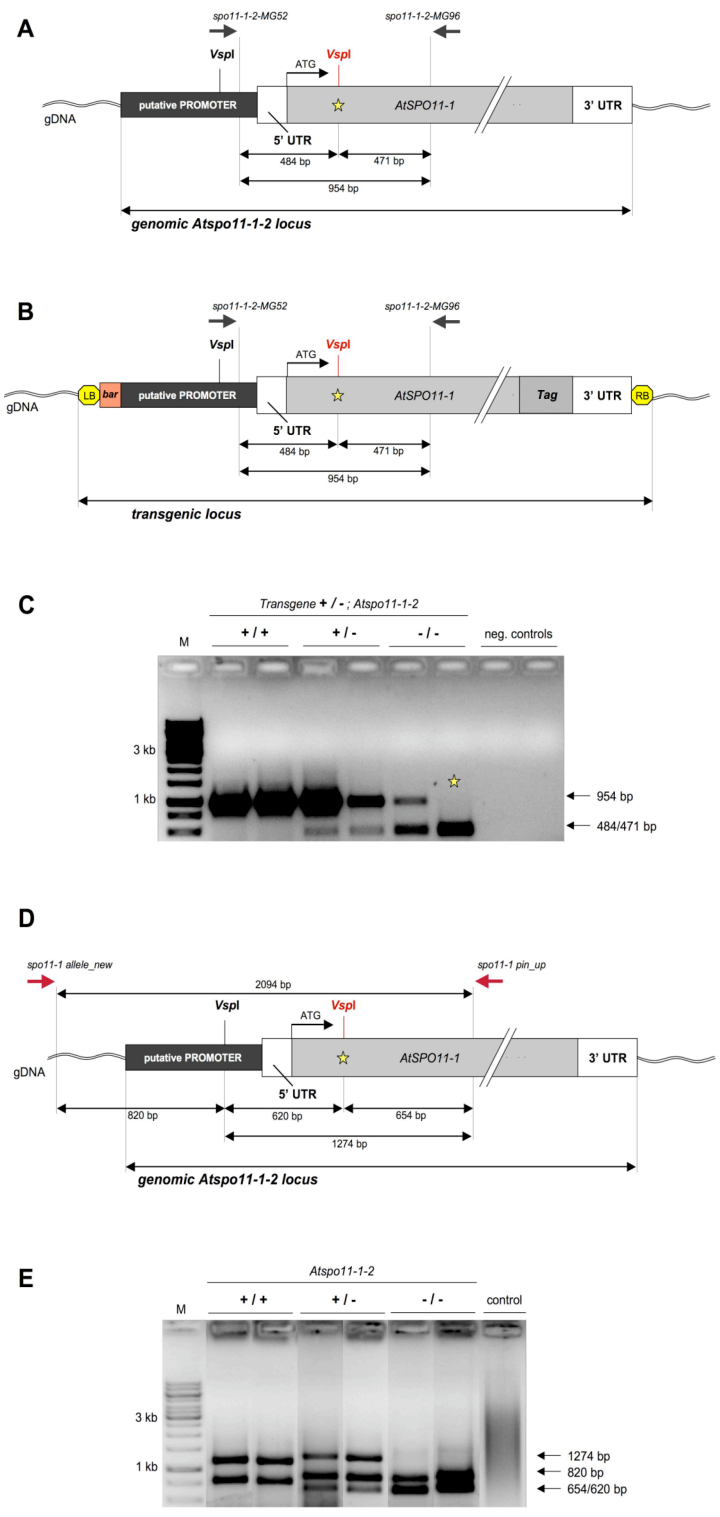

Figure 19 | *Atspo11-1-2* Genotype Determination. Two different strategies for *Atspo11-1-2* genotype determination were performed. The *Atspo11-1-2* locus was amplified by „CAPS PCR“ using oligonucleotide primers *spo11-1-2-MG52* / *spo11-1-2-MG96,* and the genotype was assessed after *Vsp*I RE digest. Thereby an *AtSPO11-1* allele yields a full-length 954 bp amplicon, while a CAPS marker within the *Atspo11-1-2* allele forms an additional *Vsp*I RE site, leading to the formation of 471 bp and 484 bp fragments, respectively. Both full length and cleaved amplicons can be visualized after agarose gel electrophoresis, thereby allowing to distinguish between *AtSPO11-1* and *Atspo11-1-2* alleles (panels A and C).

The occurrence of a CAPS marker signal, lacking the WT-specific amplicon might be due to absence of transgene integration and low-stringency BASTA selection in the previous generation (panel C, slot 7, yellow asterisk).

As both oligonucleotide primers bind within the cloned region used for *At*SPO11-1-CSR1-ZF transgene construction, the integrated transgene always gives rise to a WT-like specific full-length amplicon, leaving heterozygous and homozygous *Atspo11-1-2* genotype indistinguishable, thereby delaying complementation analyses by one generation (panel B)

The „PIN PCR“ was designed to presicely determine the *Atspo11-1-2* genotype within a given generation. As one oligonucleotide primer was placed outside the cloned *AtSPO11-1* region, a PCR amplicon was only yielded from the genomic *AtSPO11-1-2* locus but not from an integrated *AtSPO11-1-CSR1-ZF* transgene. The *Atspo11-1-2* locus was amplified using oligonucleotide primers *spo11-1 allele_new* / *spo11-1 pin_up,* and the genotype again assessed after *Vsp*I RE digest. As a second *Vsp*I RE site is present within the PCR amplicon besides the *Atspo11-1-2* related CAPS marker, the 2094 bp amplicon gives rise to different band patterns of 1234/820 bp, 820/654/620 bp and 654/620 bp in case of *ATSPO11-1*, *Atspo11-1-2* heterozygous and *Atspo11-1-2* homozygous plants, respectively (panels D and E).

Though needing further optimization, the „PIN PCR“ successfully distinguishes *Atspo11-1-2* heterozygous and homozygous genotypes. Same samples of individual *AtSPO11-1* and *Atspo11-1-2* heterozygous and homozygous T_0 transformants were subjected to *Atspo11-1-2* genotype determination using both previously described „CAPS PCR“ and „PIN PCR“ strategies. Both strategies distinguished *Atspo11-1-2* heterozygous and homozygous plants, respectively. Data from both genotyping strategies together revealed that the second *Atspo11-1-2* proposed homozygous sample was lacking the transgene-specific 954 bp band, indicating that this plant has bypassed herbicide resistance screening due to low-stringency conditions (panels C and E, slot 7).

As previously described, for each transformed construct *AtSPO11-1.CSR1-ZFP-F* and *AtSPO11-1.CSR1-ZFP-F.18xMyc*, 96 individual BASTA resistant transformants were selected, representing the successfully transformed T_0 generation. *Atspo11-1-2* genotype determination was performed using both „CAPS PCR“ and „PIN PCR“ strategies as described previously. For each construct *AtSPO11-1.CSR1-ZFP-F* and *AtSPO11-1.CSR1-ZFP-F.18xMyc*, 12 individual *Atspo11-1-2* heterozygous or homozygous, fully fertile plant lines were selected and propagated by selfing, giving rise to the T_1 generation, which was used for subsequent transgene segregation analysis (Table 2).

Table 2 | Initial *AtSPO11-1.CSR1-ZFP-F* and*18xMyc* T_0 Plant Lines used for Segregation Analysis.

Transformed Construct	Plant Line	Atspo11-1-2 Genotype “PIN PCR”	Atspo11-1-2 Genotype “CAPS PCR”
AtSPO11-1.CSR1-ZFP-F	8	-/-	+/-
	10	+/-	+/-
	15	+/-	+/-
	25	NA	+/-
	46	NA	+/-
	52	NA	+/-
	53	NA	+/-
	56	NA	+/-
	71	NA	+/-
	97	NA	+/-
	101	NA	+/-
	106	NA	+/-
AtSPO11-1.CSR1-ZFP-F.18xMyc	5	NA	+/-
	10	-/-	+/-
	11	-/-	+/-
	16	-/-	+/-
	17	-/-	+/-
	30	NA	+/-
	37	NA	+/-
	39	NA	+/-
	57	NA	+/-
	73	NA	+/-
	90	NA	+/-
	95	NA	+/-

Individual *AtSPO11-1.CSR1-ZFP-F* and *AtSPO11-1.CSR1-ZFP-F.18xMyc* transformants were selected for subsequent transgene segregation analysis. *Atspo11-1-2* genotype determination was performed using both „CAPS PCR“ and „PIN PCR“ strategies. *NA* indicates the lack of exact *Atspo11-1-2* genotype estimation, due to „PIN PCR“ failure as a consequence of lacking PCR optimization.

3.3.1. Segregation Analysis

Agrobacterium mediated *in-planta* transformation is generally characterized by low efficiency. More importantly, transgene integration is taking place at random within the *Arabidposis* genome, considerably often going along with multiple, inverted or partial insertion of the T-DNA region. For those reasons T_1 plant lines had to be identified, that harbour the transgene as single-locus insertion and gave rise to fully fertile progeny.

Single-locus transgene integration was addressed by segregation analysis of the BASTA resistance phenotype. Thereby single-locus integration of the dominant marker would result in a segregation pattern of about 3:1 herbizide resistant vs. sensitive plants, in accordance with mendelian segregation rules. Transgene insertion at two, three or more non-linked loci would lead to an elevated pattern of herbizide resistance segregation ratio of 15:1, 63:1 and higher, respectively (Figure 20).

A

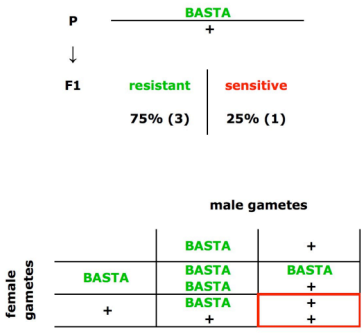

B

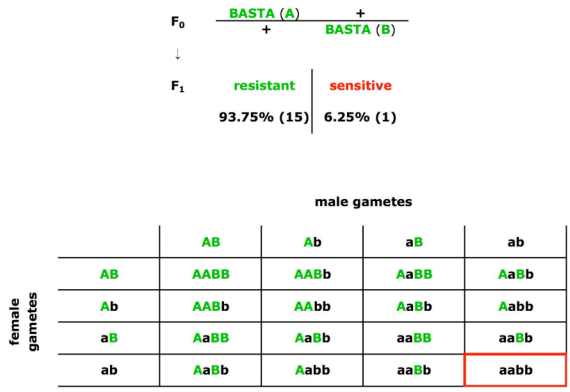

Figure 20 | Herbizide Resistance Segregation Patterns depend on Number and Position of Transgene Integration Sites. (A) Segregation patterns of BASTA resistance can be used to delineate the kind of transgene integration. According to mendelian segregation rules a single locus insertion would give rise to 3:1 segregation ratio and yield about 75% herbizide resistant plants in the next generation.

(B) Multiple non-linked insertions segregate independently and elevate the ratio of resistant plants to 15:1, and 64:1 in case of presence of two or three integration loci, repectively. In the scheme a transgene insertion at two independent loci a and b is assumed, where A and B refer to T-DNA imediated herbizide resistance, while a and b describe the non-resistant WT-like alleles at corresponding integration loci (panel B).

In general, successful complementation of the *At*SPO11-1-PZF constructs is expected to rescue the previously discussed low-fertility phenotype in transgenic *Atspo11-1-2* homozygous plants. Successfully transformed, BASTA resistant *Atspo11-1-2* mutant T_0 individuals, displaying WT-like fertility were selected and propagated by selfing for further analysis (Table 2). To address successful *At*SPO11-1-PZF complementation, the *Atspo11-1-2* genotype of T_1 individuals was determined by the previously discussed „CAPS PCR“ strategy.

Atspo11-1-2 heterozygous and homozygous lines could be deduced through presence of 75 % or 100 % mutant allele-specific CAPS fragments per investigated T_1 plant line. As individual segregation of the recessive *Atspo11-1-2* allele and the dominant resistance marker of the single-locus-integrated transgene were taking place, a sterility phenotype resulting from transgene non-complementation would be visible at different ratios, dependend on whether an *Atspo11-1-2* heterozygous or homozygous situation was investigated.

In general, 25% of all plants would be BASTA sensitive due to segregation of the herbizide resistance marker. In case of *Atspo11-1-2* heterozygous T_0 plants, independent segregation of the *Atspo11-1-2* allele occurs within the surviving transgenic population, yielding 25% *Atspo11-1-2*$^{-/-}$ plants that would display an *Atspo11-1-2* sterility phenotype in case of non-complementation.

In case of *Atspo11-1-2* homozygous T_0 plants, 100 % of transgenic T_1 individuals were expected to display the *Atspo11-1-2* sterility phenotype, as the Atspo11-1-2 allele does not segregate. Therefore complementation analysis of the introduced *AtSPO11-1-CSR1-ZF* and *AtSPO11-1-CSR1-ZF-18xMyc* transgenes could be addressed by monitoring the fertility levels within selected T1 lines (Figure 21).

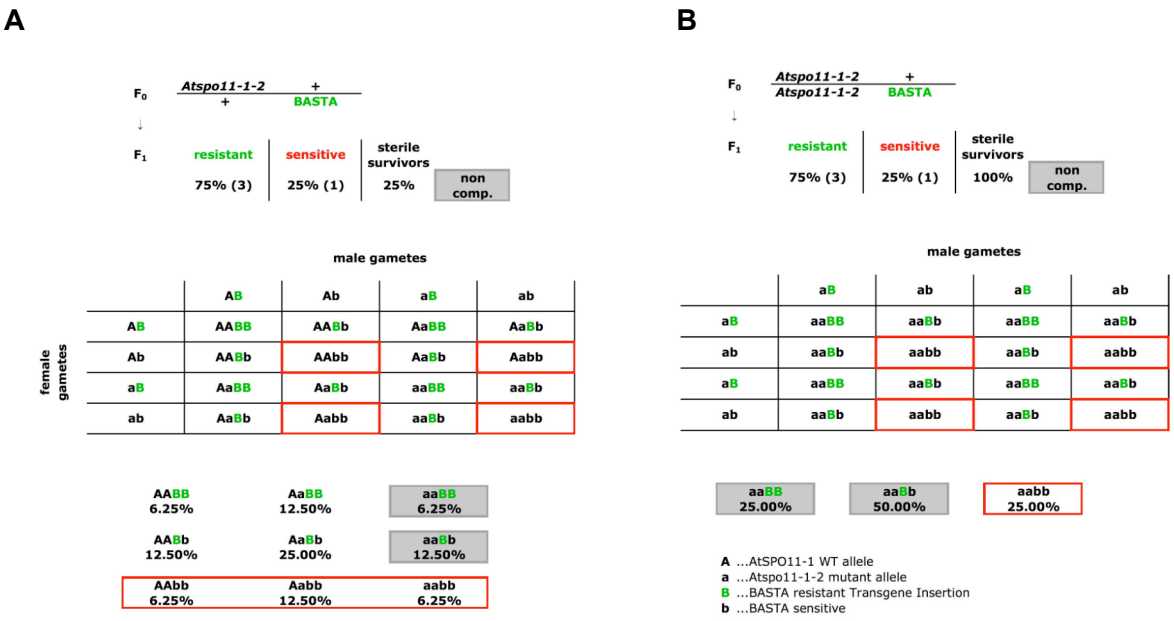

Figure 21 | Transformant Sterility due to Transgene non-Complementation. Segregation patterns of T_1 plant sterility can be used to delineate transgene non-complementation. Alleles *AtSPO11-1* and *Atspo11-1-2* are depicted as A and a; Transgene insertion is depicted as B and BASTA; corresponding WT loci are depicted as b and +. Transgene bearing, BASTA resistant allelic compositions are labeled through green alleles, while transgene lacking allelic compositions are marked by red rectangles.

(A) According to mendelian rules, segregation of independent markers yields 25% *Atspo11-1-2*$^{-/-}$ T_1 progeny, giving rise to 25 % sterile plants in case of transgene non-complementation as both dominant allelic compositions aaBB and aaBb give rise to sterile plants (shaded grey).

(B) In *Atspo11-1-2* homozygous plants only the transgene segregates, yielding about 75 % herbizide resistant plants in the T_1 generation. Transgene non-complementation results in the formation of 100 % sterile offspring (shaded grey).

Table 3 | *Atspo11-1-2* Phenotype Complementation by *AtSPO11-1.CSR1-ZFP-F* and *18xMyc* T_1 Plant Lines.

Transformed Construct	Plant Line #	Germinated Individuals	BASTA^S Resistant Individuals	Ratio	Atspo11-1-2 Genotype ("CAPS PCR WT-like")	Phenotype (# of Plants)
AtSPO11-1	8	48	23	2.1:1	-/- (all)	pleiotrop. (4)
CSR1-ZFP-F	10	60	21	2.9:1	+/- (33%)	
	15	69	9	7.7:1	+/- (24%)	
	25	**64**	**22**	**2.9:1**	**-/- (all)**	
	46	**73**	**35**	**2.1:1**	**-/- (all)**	
	52	**65**	**20**	**3.3:1**	**-/- (all)**	
	53	65	24	2.9:1	+/- (17%)	
	56	**63**	**29**	**2.2:1**	**-/- (all)**	
	71	**57**	**26**	**2.2:1**	**-/- (all)**	
	97	41	17	2.4:1	+/- (17%)	
	101	**40**	**17**	**2.4:1**	**-/- (all)**	
	106	38	12	3.2:1	NA	
AtSPO11-1	5	57	20	2.9:1	-/- (all)	*spo11-1* (3)
CSR1-ZFP-F	10	66	8	8.3:1	-/- (all)	*spo11-1* (3)
18xMyc	11	68	27	2.5:1	-/- (all)	*spo11-1* (2)
	16	**61**	**19**	**3.2:1**	**-/- (all)**	
	17	50	8	6.3:1	-/- (all)	
	30	59	12	4.9:1	-/- (all)	*spo11-1* (3)
	37	51	23	2.2:1	+/- (33%)	
	39	**58**	**20**	**2.9:1**	**-/- (all)**	
	57	41	14	2.9:1	-/- (all)	*spo11-1* (1)
	73	**37**	**19**	**1.9:1**	**-/- (all)**	
	90	**64**	**18**	**3.6:1**	**-/- (all)**	
	95	71	6	11.8:1	NA	*spo11-1* (1)

Individual fully fertile *AtSPO11-1.CSR1-ZFP-F* and *AtSPO11-1.CSR1-ZFP-F.18xMyc* T_0 lines were selected for herbizide resistance segregation analysis. The number of germinated individuals per line (total), herbizide sensitive plant number (dead) and the ratio between resistant and sensitive plants is indicated. *Atspo11-1-2* genotype determination was performed using the „CAPS PCR" strategy. In generation T_0, preferentially *Atspo11-1-2* homozygous mutant transformant plants were selected for further propagation. Therefore, the ratio between *Atspo11-1-2* heterozygous and homozygous transformant plants is not 2:1 as expected in case of random selection of transformant T_0 lines.

The presence of the mutant allele-specific amplicon in all individuals per plant line is indicative of a non-segregating *Atspo11-1-2* homozygous genotype (depicted as -/- (all)). Detection of WT-specific amplicons in about 25 % of individuals per plant line is indicative of a segregating *Atspo11-1-2* heterozygous genotype (depicted as +/-). The percentage of WT-specific amplicons per selected line is not always 25 % as expected, due to the small number of 12 plants per line that were subjected to genotype determination analysis.

The occurence of *Atspo11-1-2* mutant phenotypes within a selected plant line is given in the rightmost column. Complex, non-WT-like phenotypes were observed in one plant line within four individual plants (depicted as *pleiotrop.*) and might result from T-DNA mediated disruption of a gene essential in plant development.

Only T_1 lines that are segregating herbicide reistance at ratios of about 3:1, display full fertility and are *Atspo11-1-2* homozygous mutant were selected as candidate lines for further evaluation (marked as bold).

To address herbizide resistance segregation, 64 T_1 seeds per peviously selected, fully viable T_0 plant line (Table 2) were sown, and the ratio between BASTA resistant and non-resistant plants was determined. In parallel, *Atspo11-1-2* „CAPS PCR“ mediated genotype determination was performed for 12 surviving plants of each line. The fertility status of each plant was monitored. Herbizide resistance segregation, *Atspo11-1-2* genotype and the ratio between fertile and sterile plants was used to address transgene complementation within the selected T_1 plant lines (Figure 21, Table 3).

Single locus transgene integration could be successfully addressed through segregation analysis of the dominant BASTA resistance marker, situated on the same T-DNA as the *AtSPO11-1-CSR1-ZF* transgene. For *AtSPO11-1.CSR1-ZFP-F*, 11 individual lines could be identified, displaying BASTA resistance segregation at ratios of about or below 3:1, going along with mendelian segregation rules. Likewise, seven individual *AtSPO11-1.CSR1-ZFP-F.18xMyc* lines were identified.

Ratios below 3:1 could be observed as some individual plants were dying due to pest-related stress. Of those single-locus insertion lines, one *AtSPO11-1.CSR1-ZFP-F* line displayed a pleiotropic phenotype, characterized by ectopic rosette formation along the elongated shoot (4 of 25 individuals, 16 %). In case of *AtSPO11-1.CSR1-ZFP-F.18xMyc*, three lines (#5, #11, and #57) displayed a reduced-fertility defect. Individual plants displayed an *Atspo11-1-2*-like phenotype (3.7 %, 4.9 % and 8.1 %, respectively).

From the remaining lines, six in case of *AtSPO11-1.CSR1-ZFP-F* (lines #25, #46, #52, #56, #71 and #101) and four in case of *AtSPO11-1.CSR1-ZFP-F.18xMyc* (lines #16, #39, #73 and #90) were in addition identified to be *Atspo11-1-2* homozygous mutants. As discussed previously, non-complementation of the *Atspo11-1-2* mutation by the transgene constructs would lead to formation of 25 and 100 % sterile T_1 individuals, originating from an *Atspo11-1-2* heterozygous or homozygous T_0 plant, respectively. As for both constructs *AtSPO11-1.CSR1-ZFP-F* and *AtSPO11-1.CSR1-ZFP-F.18xMyc* appropriate *Atspo11-1-2* homozygous T_1 lines could be identified, displaying *AtSPO11-1* WT-like fruit production and fertility rate, it could be clearly shown that both transgenic constructs complemented endogenous *AtSPO11* function *in-planta*. The successfully characterized, transgenic *AtSPO11-1.CSR1-ZFP-F* (#25, #46, #52, #56, #71 and #101) and *AtSPO11-1.CSR1-ZFP-F.18xMyc* lines (#16, #39, #73 and #90) were further propagated by selfing to generate non-segregating *Atspo11-1-2*$^{-/-}$ *; AtSPO11-1-CSR1-ZFP-F(18xMyc)*$^{+/+}$ plant lines. However their ability to induce locus-specific HR induction could not be addressed within the duration of this thesis.

3.4. Detection of 18xMyc Constructs in Cell Suspension Culture

Immunoprecipitation of 18xMyc epitope-bearing *At*SPO11-1-CSR1-ZF constructs was performed to support complementation analysis data, confirming that the transgenic construct is properly expressed *in-vivo.* Moreover, successful IP of the 18x *c-Myc* tagged fusion proteins allows future analysis of SPO11-DNA recombination intermediates and ChIP experiments to address locus-specific SPO11-ZF DNA-binding activity. To address *At*SPO11-1-CSR1-ZF-18xMyc expression, initial protein isolation was performed from *Arabidopsis thaliana* cell suspension culture (CSC), rather than from whole plants for two reasons.

Protein isolated from transformed CSC can be obtained after a few days in high quantity, while it would take more than one month and considerable growth room resources to cultivate sufficient transgenic plant material for protein isolation.

Levels of *At*SPO11-1 expression were addressed by use of the online resource Genvestigator (https://www.genevestigator.ethz.ch/gv/index.jsp, NEBION AG and ETH Zurich, Hruz *et al*. 2008). The highest levels of generally low expressed *AtSPO11-1* gene were found only in proliferative tissue and in CSC (Figure 22). Therefore, a high number of plants has to be grown to harvest inflorescences, the plant organs bearing meiotically active tissue, while the maintenance of several transformed CSCs only needs limited laboratory resources.

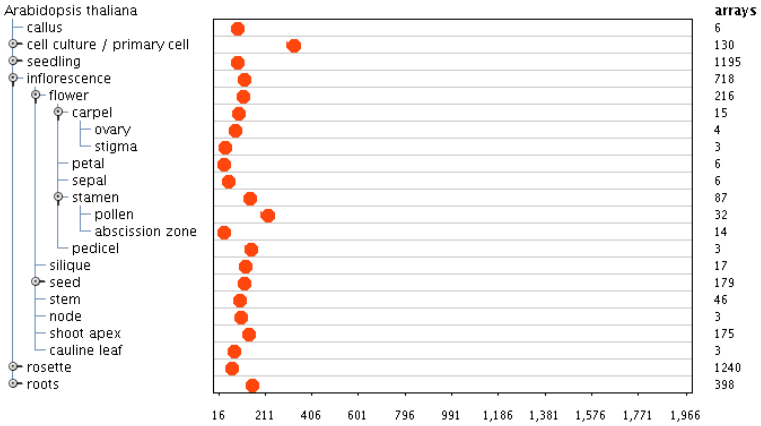

Figure 22 | *At*SPO11-1 Expression Microarray Data. Expression levels are different in various plant organs. Generally, *At*SPO11-1 expression is considerably low. Significant levels of expression can be found in generative tissue (inflorescence), being highest in pollen and cell suspension culture.

(Genvestigator, NEBION AG and ETH Zurich, Hruz *et al*. 2008)

Initially, both generated constructs *pCB302.AtSPO11-1.CSR1-ZFP-G.18xMyc* and *pCB302.AtSPO11-1.CSR1-ZFP-G.18xMyc* were used to perform *Agrobacterium*-mediated CSC transformation. In addition constructs *pCB302.AtSPO11-1.18xMyc* and *pCB302.AtSPO11-1*, giving rise to 18x *c-Myc* tagged and WT-like *At*SPO11-1 protein, were used as positive and negative control, respectively.

After five days of expression, protein extracts were prepared. IP was performed, using monoclonal mouse anti-*Myc* 9E11 antibody-coated Protein A-Sepharose (CL-4B, GE Healthcare), and proteins separated by denaturing polyacrylamide gel electrophoresis (SDS-PAGE). After protein transfer to a PVDF-membrane (Immobilon-P, Millipore), detection was performed using mouse anti-*Myc* 9E10 and goat anti-Mouse IgG + IgM (H+L), peroxidase conjugated (ImmunoPure #31444, Pierce) antibodies (both monoclonal anti-*Myc* antibodies courtesy of Kim Nasmyth's Lab; Evan *et al*., 1985).

Experiments previous to this thesis have confirmed that *At*SPO11-1.18xMyc fusion proteins could be detected by the 9E10 antibody. Thereby, a band-shift of size (93 kDa in contrast to calculated 68.7 kDa) was observed, not uncommon to *c-Myc* tagged proteins (Krsicka, 2007; Peter Schloegelhofer, MFPL, Vienna, Austria; personal communication).

As predicted, the *At*SPO11-1.18xMyc fusion protein could be detected as 93 kDa band. 25 kDa and 56 kDa bands were observed, resulting from IgG light and heavy chain fragments, respectively. Additional bands of about 30 kDa and greater than 95 kDa were observed in both tagged and untagged samples as well as in mock samples, and most probably due to an interaction of the 9E10 antibody with its own serum. For both *At*SPO11-1.CSR1-ZFP-G.18xMyc and *At*SPO11-1.CSR1-ZFP-F.18xMyc fusion proteins a calculated band size of 82 kDa is expected. Unfortunately, no clear SPO11-ZF fusion protein-specific signal could be obtained. Moreover, in both *At*SPO11-1-PZF-18xMyc fusion protein samples strong background signal between 30 and 56 kDa were detected. As these signals are neither present in the control or mock samples, they might resemble degradation products of the *At*SPO11-1-PZF-18xMyc fusion proteins (Figure 23 for further details).

These results could not confirm that the generated *At*SPO11-1-ZF-18xMyc constructs are expressed in cell culture and were most probably due to low *Agrobacterium* transformation efficiency or due to an occuring low-level infection of the CSC along transgenic protein expression. Additional experiments are needed to precicely address fusion protein expression status but could not be completed within duration of this thesis.

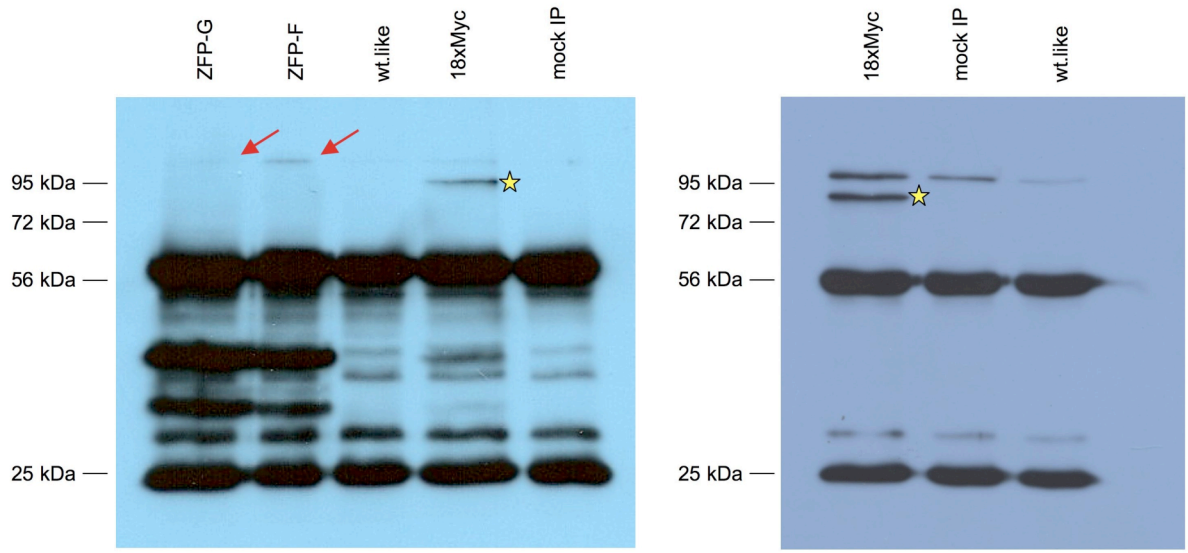

(Blot sample courtesy of Bernd Edlinger, MFPL, Vienna, Austria)

Figure 23 | Western Blot Analysis of *At*SPO11-1 Expression. The 18x *c-Myc* tagged *At*SPO11-1 positive control can be detected as 93 kDa signal (yellow asterisk, both panels). Higher molecular weight as well as 30 kDa signals are visible in tagged samples, WT-like negative control and mock samples, due to 9E10 antibody reaction to its own serum (right panel).

Generally high background signals might be due to unrecognized low-level CSC infection during transgenic protein expression. Weak signals of about 98 kDa could be detected in both *At*SPO11-ZF-18xMyc samples (red arrows, left panel). If those signals are transgenic fusion protein-specific or result from an unspecific antibody reaction remained elusive.

3.5. Generation of Test Systems to Quantify and Monitor Locus-specific Recombination Events

Fusion protein *At*SPO11-1-*CSR1*-ZF target site cleavage was previously confimed *in-vitro*. Existing test systems confirm DNA binding and cleavage in parallel, by readout of reporter gene expression within a transgene repair assay. As in our case the stimulation of HR is of interest rather than DNA cleavage activity per se, it was decided to address the ability of generated fusion protein constructs to bind and cleave respective target sites separately. Protein constructs were tested for their locus-specific nuclease activity directly by screening for site-specific recombination events *in-vivo*, and not addressed by an commonly used *in-planta* transgene repair assay. The generated fusion proteins were anticipated to induce site-specificDSBs, resulting in exchange of flanking markers following HR-mediated DSBR.

The endogenous *Arabidopsis CSR1* locus was chosen as target for PZF constructs because of its unique characteristics that allow detection and screening of HR events on the basis of plant viability. The gene product is encoded by a single exon. Two different EMS-mutagenesis derived alleles, *csr1-1* and *csr1-2* are available. The dominant point mutation in *csr1-1* is a C to T transition (Haughn *et al.* 1988) at the 5' end of the *CSR1* locus, rendering the ALS insensitive to herbizides chlorsulfuron and triazolpytimidine. The dominant point mutation in *csr1-2* is a G to A transition (Sathasivan *et al*. 1991) at the 3' end of the *CSR1* locus, rendering the ALS molecule resistant to imazapyr and pyrimidyl-oxy-benzoate. In addition *csr1-1* mutant plants were found to be sensitive to imazapyr and pyrimidyl-oxy-benzoate, and *csr1-2* mutant plants displayed sensitivity to chlorsulfuron and triazolpytimidine (Mourad and King 1992). As both alleles are spaced 1369 bp apart and confer resistance to different classes of herbizides, this locus is suited to measure and screen intragenic recombination. Test crosses between *csr1-1* and *csr1-2* determined intragenic recombination rates of 0.008 cM, corresponding to four recombination events in 100.000 crosses (Mourad *et al*., 1994) These low-level recombination events at the CSR1 locus allow the detection of even small alterations in recombination frequency, as *At*SPO11-PZF induced DSB formation between both markers is anticipated to elevate HR events within the meiotic DSBR pathway (Figure 24).

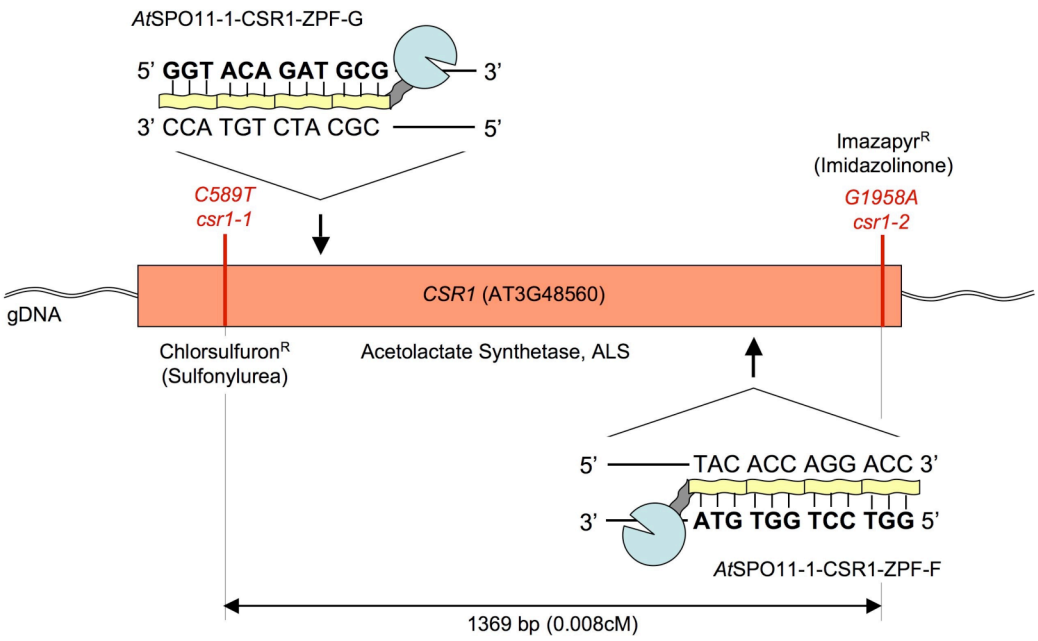

Figure 24 | Arabidopsis thaliana *CSR1* Locus. Plants harbouring different point mutations, *csr1-1* or *csr1-2* are resistant to chlorsulfuron and imazapyr, respectively. Both point mutations are spaced 1369 bp apart. Test crosses between *csr1-1* and *csr1-2* determined an intragenic recombination frequency of 0.008cM. Both generated fusion proteins *AtSPO11-1.CSR1-ZFP-G* and *AtSPO11-1.CSR1-ZFP*-F target sites downstream of *csr1-1* and upstream of *csr1-2*, prespectively. Actual Fusion protein orientation conferred by target site (bold) binding through major groove DNA interaction is indicated.

To screen for recombination events a heteroallelic F_1 *csr1-1*/*csr1-2* tester line will be generated, being homozygous for *AtSPO11-1-CSR1-ZF* constructs and harbouring both *csr1-1* and *csr1-2* markers *in trans*. With the help of this assay, recombination events can be addressed in the male and female germline as recombination between different paternal and maternal herbizide markers *in trans* will be monitored. The tester line is propagated by selfing. As *AtSPO11-1-CSR1-ZF* site-specific induced DSBs eventually are anticipated to give rise to HR, some of the progeny is anticipated to harbour both *csr1-1* and *csr1-2* alleles *in cis*. Since both point mutations are dominant and confer resistance to different herbicides, the whole F_2 progeny displays resistance to both herbizides chlorsulfuron and imazapyr. To identify recombination events, a large number of F_2 progeny is backcrossed to WT. Most progeny will display a loss of double herbizide resistance in the next F_3 generation due to segregation of the *csr1-1* and *csr1-2* alleles in a former *trans* configuration. Only F_2 progeny that harbours both alleles *in cis* due to an induced, artificial or rare, natural intragenic HR event will therefore display double herbizide resistance after a backcross with WT in the next generation.

The number of backcrossings needed is dependent on the rate of HR stimulation at the *CSR1* locus. Estimating a maximum of 50 seeds emanating from a single crossing event, about 2000 backcrossings of F_2 progeny to WT are estimated to detect the basal rate of residual HR events at the *CSR1* locus. (Figure 25).

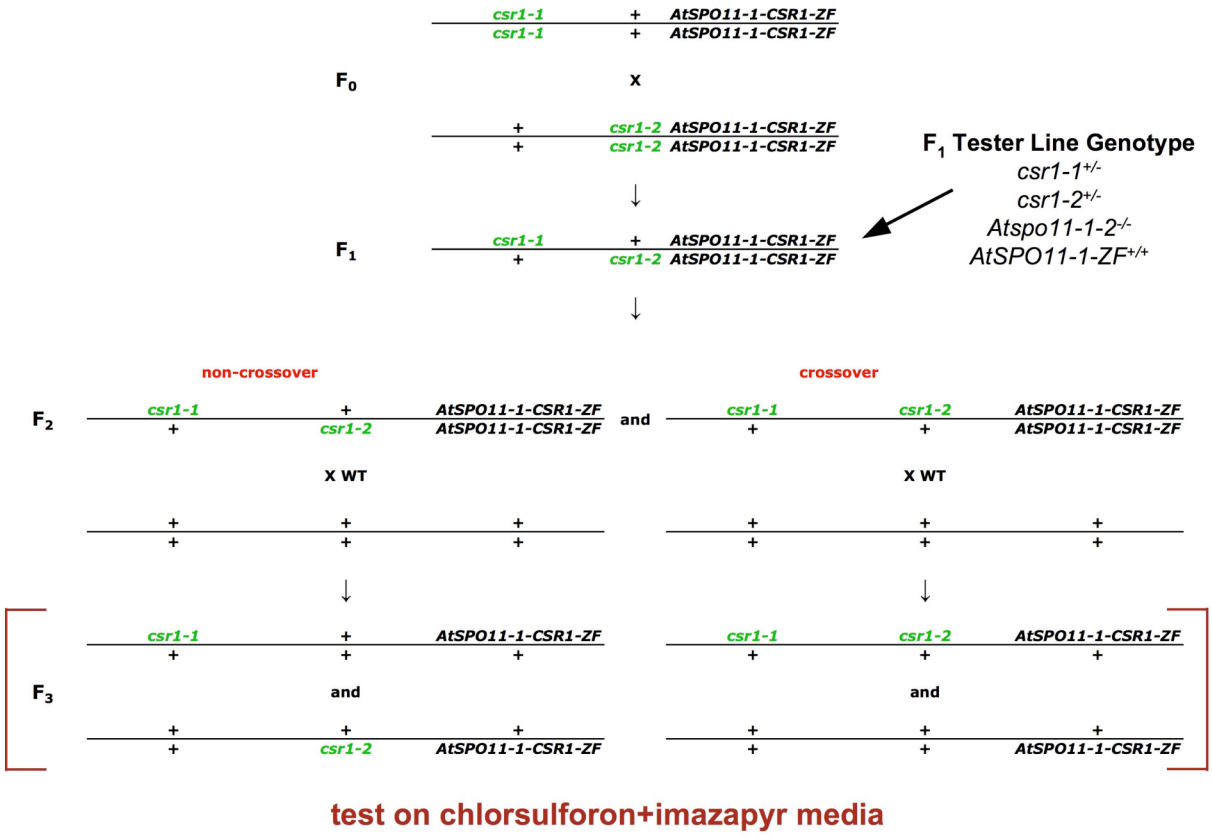

Figure 25 | Detection of HR Events by Screen for double-Herbizide Resistance. Primary F0 lines of genotype *csr1-1*$^{-/-}$; *AtSPO11-1.CSR1-ZF*$^{+/+}$ and *csr1-2*$^{-/-}$; *AtSPO11-1.CSR1-ZF*$^{+/+}$, homozygous for either *csr1-1* or *csr1-2* and the *AtSPO11-1-CSR1-ZF* construct are crossed to produce the heterolallelic F1 *csr1-1*/*csr1-2* tester line, bearing both herbizide resistance conferring mutations *in trans*.

Along propagation to F2 generation eventually induced or natural *CSR1* locus-specific HR events, lead to formation of progeny, harbouring both alleles *in cis*.

As both mutations are dominant, exchange of marker configuration can be addressed after backcrossing to WT in the subsequent F3 generation. As both markers *csr1-1* and *csr1-2* segregate being present in a *trans* configuration, double herbizide sensitive offspring is obtained.

Progeny bearing both alleles *in cis* due to an occurred HR event remain double herbizide resistant after backcrossing and can be successfully selected for.

An alternative test system will utilize a visual assay (Francis *et al*., 2007), developed by our collaborator (Gregory Copenhaver, Department of Biology, University of North Carolina, Chapel Hill, NC, USA) based on pollen-expressed fluorescent proteins. Within this assay numerous fluorescence-tagged lines (FTLs) were generated by random T-DNA mediated single-locus insertions of autofluorescent protein encoding constructs. Autofluorescent proteins are expressed under control of a pollen-specific promoter (LAT52p), giving rise to fluorescent pollen grains. Moreover, the T-DNA insertion lines were generated in the *qrt1-2* (*quarted*) background, giving rise to non-separated pollen mother cell division products, thereby resulting in the formation of pollen tetrads (Figure 26).

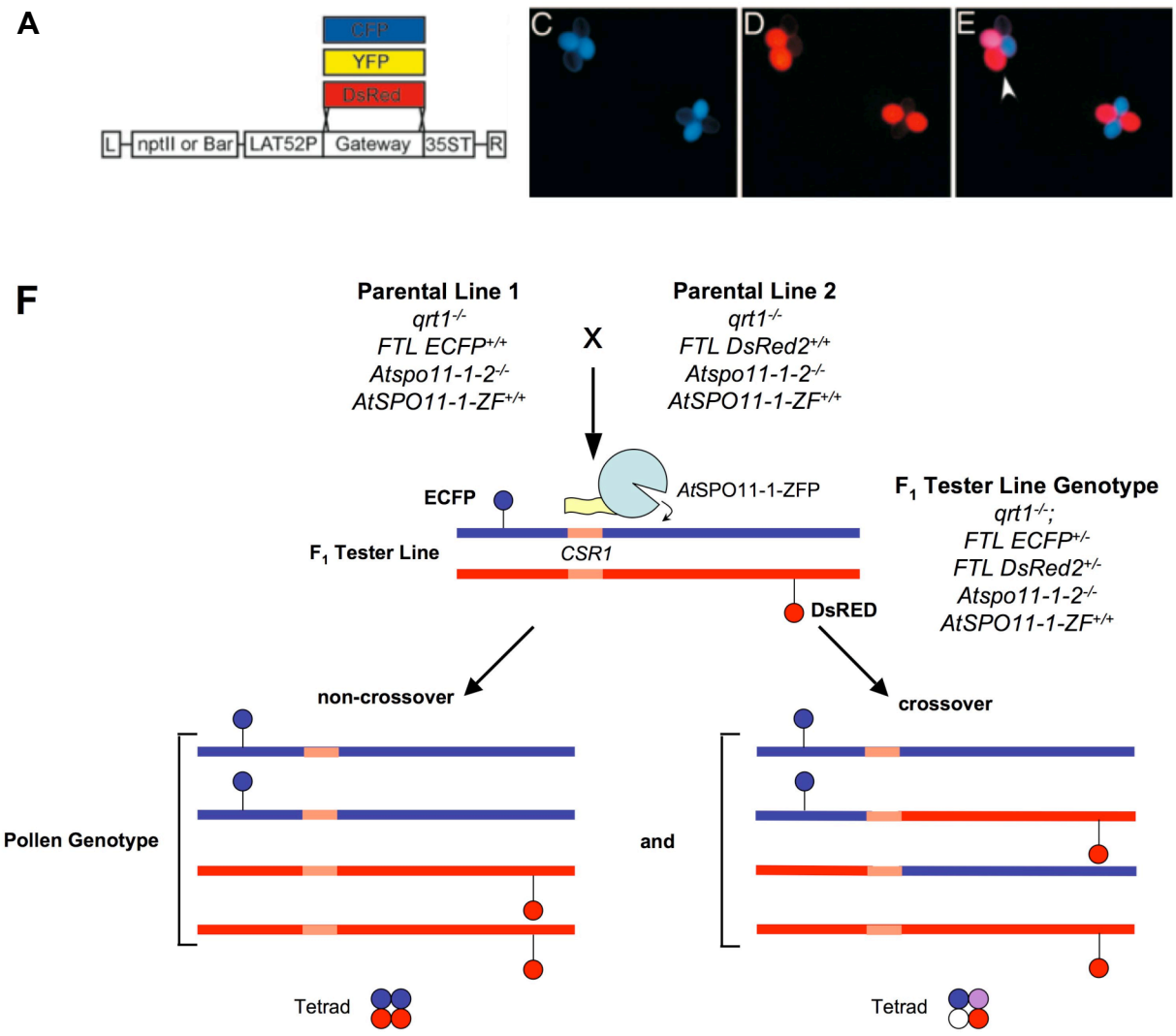

Figure 26 | Pollen-based Fluorescent Recombination Marker Exchange due to HR Events. (A to E) T-DNA constructs, bearing autofluorescent proteins under control of the LAT52 promoter have been randomly integrated into *qrt1* mutant plants. Single locus insertions are selected for by non-mendelian 2:2 segregation of fluorescent signals (blue, panel C; red, panel D; merge, panel E) and by T-DNA mediated kanamycin resistance.

(E, right) Crossing of two FTLs, bearing a T-DNA insertion within the same chromosome, but separated by a defined interval leads to generation of a hemizygous line, bearing both FTL insertions i*n trans*, thereby giving rise to bicolored pollen tetrads.

(E, left) Detection of recombination events is possible due to exchange of FTL insertions from *trans* to *cis* configuration, resulting in the formation of a double-fluorescent and a non-fluorescent pollen grain within a given tetrad.

(F) In detail, FTL lines homozygous for either *CFP* (ECFP) or *DsRed2* (DsRED) are crossed to *Atspo11-1-2*$^{-/-}$; *AtSPO11-1-ZF*$^{+/+}$ lines. Several rounds of selection and PCR based genotype determination allow for selection of *qrt1*$^{-/-}$; *Atspo11-1-2*$^{-/-}$; *AtSPO11-1-ZF*$^{+/+}$; *FTL ECFP/DsRed2*$^{+/+}$ parental lines. Selected parental lines are crossed to produce the heterolallelic F1 *CFP*$^{+/-}$*/DsRed2*$^{+/-}$ tester line, bearing both fluoprescent pollen markers *in trans.*

Along propagation to F2 induced or natural *CSR1* locus-specific HR events, result in *trans* to *cis* pollen fluorescent marker exchange and can be directly assessed by fluorescence microscopy. As a result pollen originating from a intragenic HR event do no longer show 2:2 fluorescent marker segregation, but display formation of a double-fluorescent and a non-fluorescent pollen grain within the same tetrad.

Pollen-based fluorescent recombination markers are generated by crossing of two appropriate FTLs. Thereby, a hemizygous locus is generated, harbouring both different autofluorescent protein encoding T-DNA constructs on the same chromosome in a *trans* configuration and giving rise to consistent 2:2 segregation of the fluorescent signal within the pollen tetrads. If a CO event is taking place within the interval of the two FTL T-DNA insertions, two markers are exchanged to a *cis* configuration, leading to generation of a double-fluorescent and a non-fluorescent pollen grain within the same tetrad (Francis *et al*., 2007; Figure 26).

To generate a test system for pollen fluorescence-based *CSR1* locus-specific HR detection, appropriate FTLs, bearing a single locus autofluorescent protein insertion upstream or downstream of the *CSR1* locus within a small interval (of 4.05 to 4.5 cM) are crossed, resulting in a *trans* configuration of the marker insertions, thereby creating a heteroallelic F_2 tester line. The tester line is crossed to respective lines, being homozygous for the *AtSPO11-1-CSR1-CSR1-ZF* constructs. Recombination events caused by site-specific induced DSBs result in *trans* to *cis* fluorescent pollen marker exchange and can be screened for directly in the subsequent F_3 generation by fluorescence microscopy. Though the system is advantageous over the herbicide resistance screening strategy as HR events can be directly monitored in pollen tetrads in high numbers without the need for backcrossing, it is limited to recombination event screening taking place in the male germline (Figure 26).

Background recombination rates around the *CSR1* locus are determined by crossing two target locus flanking FTLs of different autofluorescent protein color. Recombination rates are further addressed in generation F_1 by ratio-determination of non-recombinant, bicolored pollen tetrads *vs*. recombinants, characterized by the occurence of a non-colored and a mixed colored pollen grain within a given tetrad. Recombination rates determined by this strategy are comprised of extragenic recombination events within the analyzed FTL interval and intragenic, *CSR1* locus-specific recombination events.

Intragenic recombination and gene conversion events can be quantified in $FTL^{+/+}$; *csr1-1*$^{-/-}$ x *csr1-2*$^{-/-}$; $FTL^{+/+}$ crossing progeny by monitoring FTL marker exchange within a pollen tetrad in combination with double herbicide resistance segregation after backcrossing to wildtype. Thereby intragenic recombination is characterized by both FTL marker exchange and generation of double herbicide resistant plants as described previously, while gene conversion events can be identified by double herbicide resistant plant formation without FTL marker exchange.

To generate the pollen fluorescent marker test system, donated FTLs #1268 (*DsRed2*$^{+/+}$, nt pos. 17242947), #1632 (*CFP*$^{+/-}$, nt pos.17860363), both upstream of *CSR1* and FTLs #2201 (*AmCyan*$^{+/-}$ nt pos. 18319139), #2456 (*DsRed2*$^{+/-}$, nt pos. 18743679), both downstream of *CSR1* were propagated by selfing. Homozygous lines were identified by selection on kanamycin-containing plant medium plates, and subsequent fluorescence-microscopic analysis. Differing from the previously described crossing strategy it was decided to generate *FTL*$^{+/+}$; *Atspo11-1-2*$^{+/-}$ plants first, to reduce segregation of the *Atspo11-1-2* allele after subsequent crossing to *Atspo11-1-2*$^{-/-}$; *AtSPO11-1-CSR1-ZF*$^{+/+}$ lines, thereby keeping F_2 progeny smaller. *Atspo11-1-2* heterozygous plants were identified by „CAPS PCR“ mediated genotype determination, described previously. *FTL*$^{+/+}$ and *Atspo11-1-2*$^{+/-}$ individuals were selected and subjected to reciprocal crosses. Seeds were harvested and crossing progeny indentified in the next generation by selection on kanamycin and *Atspo11-1-2* genotype determination. Appropriate plants were propagated by selfing and seeds stored for further use, as generation of the test system, a double herbizide resistant hemizygous *csr1-1*/*csr1-2* line bearing an *AtSPO11-1-CSR1-ZF* construct, could not be finished within the duration of this thesis.

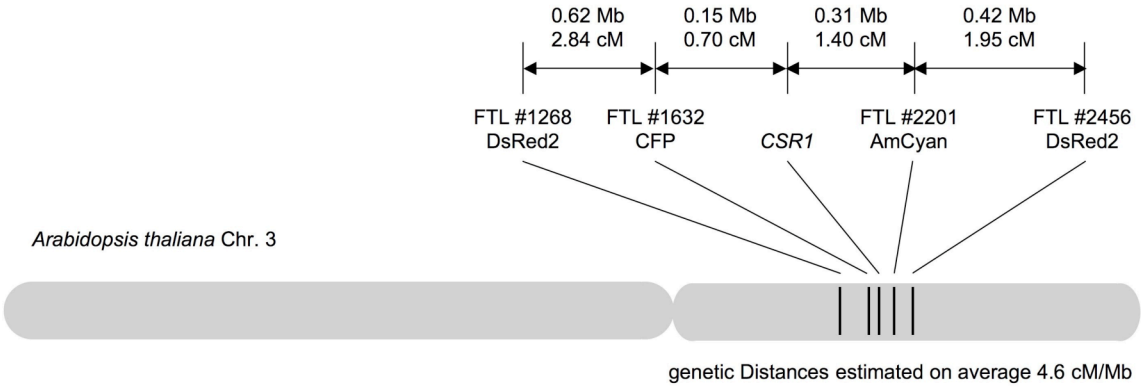

Chromosomal Positions of FTL Insertions based on TAIR Chromosome Map Tool
(The Arabidopsis Information Resource (TAIR) http://www.arabidopsis.org/jsp/ChromosomeMap/tool.jsp)

Figure 27 | Chromosomal Positions and Genetic Distances of FTL Pollen Marker Insertions. Positions of FTL pollen marker insertions on *Arabidopsis* chromosome 3 are depicted as solid lines. FTL insertion numbers and fluorescent proteins expressed within each insertion cassette are indicated. Physical distances of FTL insertions are calculated based on FTL insertion position and distance to *csr1-2* allele (FTL#1268 and FTL #1632) or *csr1-1* allele (FTL#2201 and FTL #2456), respectively. Genetic distances are calculated on an estimated *Arabidopsis* genome-wide average recombination rate of 4.6 cM/Mb. These values are subject to change (as extragenic recombination rates around the *CSR1* locus need to be experimentally addressed as described previously).

4. Discussion

Meiotic recombination during sexual reproduction is enhancing genetic diversity and ensuring the faithful chromosome segregation during meiotic divisions I and II. The initial and conserved key step of this process is the formation of DSBs mediated by *At*SPO11-1 and *At*SPO11-2. (Grelon *et al*., 2001; Hartung and Puchta, 2000, 2001; Stacey *et al*., 2006). Studies in *Saccharomyces cerevisiae, Arabidopsis thaliana, Drosophila melanogaster, Mus musculus*, and man, indicate that meiotic recombination takes place at so-called „hotspots“, while other genomic regions display a lack of recombination (Nishant and Rao, 2006; Mezard, 2006). Hotspot regions are not only defined by the chromosomal context as redirection of GAL4BD-Spo11 fusion proteins to defined genomic loci is sufficient to induce site-specific DSB formation and to elevate the rate of HR. In addition hotspots interact with each other as artificial HR induction is suppressing recombination activity at nearby natural hotspot regions (Pecina *et al*, 2002, Robine, 2007; Fukuda *et al*., 2008). Precise targeting of Spo11 to selected genomic loci thas proven to be a valuable tool for analysis of crossover interference. It is limited at present date to unicellular organisms, as GAL4 target sites need to be locus-specifically introduced by HR first.

Stimulation of HR by artificial introduction of DNA double strand-breaks is desired in plants and other higher organisms, too. Somatic DSB formation by rare-cutting homing endonucleases (Puchta *et al*., 1996; Chilton and Que, 2003) are limited to pre-existing recognition sites. Generation of *Fok*I-PZF fusion proteins, comprising of an endonuclease cleavage domain and a transcription factor-like site-specific polydactyl zinc-finger protein (Kim *et al*., 1996), allows to either mutagenize the targeted locus or to induce HR-mediated gene correction or transgene integration (Lloyd *et al*., 2005; Urnov *et al*., 2005; Wright *et al*., 2005).

4.1. Generation of *At*SPO11-PZF Fusion Proteins

The generation of an *At*SPO11-1-PZF fusion protein allows to generate artificial hotspots of recombination at will. Moreover, the stimulation of recombination at defined loci allows exchange of closely linked markers, opening up new possibilities for genome modification and crop improvement.

To analyze the relationship between PZF target site length and putative genomic binding sites, different, previously designed three-finger and de-novo designed four-finger PZF proteins were subjected to a computational binding site prediction analysis. Both 3xZF constructs were predicted to target several sites within the *Arabidopsis* genome.

As a random, nonspecific 9 bp target site sequence can be found between 15 and 38 times on every chromosome, 3xZF proteins were found to be unsuited for targeting single loci within the genome. 4xZF constructs, termed ZF-F and ZF-G, were designed to target the endogenous *CSR1* locus. ZF-G was predicted to bind five sites and ZF-F to bind four sites in addition to the *CSR1* target locus. In detail ZF-G and ZF-F were anticipated to bind twice or once, respectively, either within the *CSR1* locus or elsewhere on chromosome III. Both were chosen for construction of *At*SPO11-1-PZF fusion proteins. 4xZF proteins and target site plasmids were constructed by our collaborator (Tsvi Tzfira, Department of Molecular, Cellular and Developmental Biology, University of Michigan, Ann Arbor, MI, USA). Constructs *pET28.CSR1-ZFN-G* and *pET28.CSR1-ZFN-F* were used to express PZF-*Fok*I fusion proteins in *E.coli*. As the crude bacterial lysate could cleave corresponding target sites on plasmids *pSAT6.CSR1-ZFN-F-TS* and *pSAT6.CSR1-ZFN-G-TS*, respectively, we conclude that both 4xZF constructs could bind to their corresponding target sites.

Different from fungi and higher eukaryotes, three *AtSPO11* homologs are present in *Arabidopsis thaliana*, of which *AtSPO11-1* and *AtSPO11-2* are specific and essential for meiosis (Hartung and Puchta, 2000, 2001; Grelon *et al*., 2001; Stacey *et al*., 2006). Genomic cloning and C-terminal tagging of *At*SPO11-1 and *At*SPO11-2 was succesfully performed previous to this thesis (Krsicka, 2007; Bernd Edlinger; Peter Schlögelhofer, both MFPL, University of Vienna, Austria; personal communication). A *Sma*I restriction site was artificially introduced upstream of the *At*SPO11 stop codon for future C-terminal modification of *At*SPO11-1 and *At*SPO11-2. It was likewise decided to create C-terminal fusions of both 4xZF constructs to *At*SPO11-1. The 4xZF constructs were fitted with a short N-terminal linker sequence (encoding 1x Ala, 3x Gly; *Arabidopsis* codon usage-optimized) and introduced as blunt-ended *Sma*I/EcoRV fragments into the *Sma*I site of construct *pCB302.AtSPO11-1* (Xiang *et al*., 1999; Krsicka, 2007). Introduction of the 4xZF sequences gave rise to constructs *pCB302.AtSPO11-1.CSR1-ZFP-G* and *pCB302.AtSPO11-1.CSR1-ZFP-F*, encoding fusion proteins of 4xZF domains fused to the *At*SPO11-1 C-terminus (section 3.2.3).

*At*SPO11-1-PZF constructs were additionally tagged with 18x *c-Myc* epitopes to allow future IP or ChIP experiments. Different fusion proteins were constructed by introducing the 18x *c-Myc* epitope either at the N-terminus or at the C-terminus of the *CSR1*-PZF domain (section 3.2.4). All generated constructs were analyzed by „Colony PCR“ and RE digest to address insertion direction. Cloned PZF domains were additionally subjected to sequence verification.

4.2. Complementation Analysis of *At*SPO11-1-ZF Variants

Both *Arabidopsis* Spo11 homologs *AtSPO11-1* and *AtSPO11-2* were found to be required for meiotic recombination initiation (Grelon *et al*., 2001; Hartung and Puchta, 2000, 2001; Stacey *et al*., 2006. Homozygous single mutants displayed a severe phenotype, resulting in almost full sterility at the plant level (Grelon *et al*., 2001; Stacey *et al*., 2006). Previous studies showed that either WT-like and tagged genomic constructs of *AtSPO11-1* and *AtSPO11-2* complemented the respective *Atspo11-1* and *Atspo11-2* mutant phenotypes (Hartung *et al*., 2007; Krsicka, 2007; Bernd Edlinger, MFPL, University of Vienna, Austria; personal communication).

The EMS mutagenesis-derived *Atspo11-1-2* allele (Grelon *et al*., 2001) was used for complementation analysis of *At*SPO11-1-*CSR1*-ZF derivates. Heterozygous *Atspo11-1-2* plants were identified by "CAPS PCR" mediated genotype determination and subjected to *Agrobacterium*-mediated transformation with constructs *pCB302AtSPO11-1.CSR1-ZFP-F* and *pCB302.AtSPO11-1.CSR1-ZFP-F.18xMyc*. Transformed plants were selected for in generation T_0 by BASTA resistance. *Atspo11-1-2* mutant alleles were identified by CAPS marker analysis.

Individual T_0 lines of genotypes *Atspo11-1-2*$^{+/-\text{ or }-/-}$; *AtSPO11-1.CSR1-ZFP-F*$^{+/-}$ and *Atspo11-1-2*$^{+/-\text{ or }-/-}$; *AtSPO11-1.CSR1-ZFP-F.18xMyc*$^{+/-}$ were propagated by selfing and generation T_1 was again subjected to BASTA selection. Single-locus insertions within transgenic lines were identified by a 3:1 ratio of BASTA resistant vs. sensitive plants, caused by mendelian segregation of the dominant transgenic resistance marker. Phenotypes of BASTA resistant T_1 progeny were evaluated in combination with CAPS marker analysis to address complementation ability of selected T_1 lines. Heterozygositiy or homozygosity for the *Atspo11-1-2* allele could be deduced through presence of 75 % or 100 % mutant allele-specific fragments during CAPS marker analysis per investigated T*1* line.

Due to Iindividual segregation of *Atspo11-1-2* alleles and integrated transgene, sterility phenotypes indicative of non-complementation depended on whether an *Atspo11-1-2* heterozygous or homozygous situation was investigated. Segregation of the *Atspo11-1-2* allele in heterozygous T_0 plants leads to formation of 25% *AtSPO11-1* T_1 progeny that would be sterile in case of non-complementation. *Atspo11-1-2* homozygous T_0 plants do not display segregation, giving rise to 100% sterile T_1 progeny in case of transgene non-complementation (section 3.3.1).

For both transformed constructs, *pCB302AtSPO11-1.CSR1-ZFP-F* and *pCB302.AtSPO11-1.CSR1-ZFP-F.18xMyc*, 12 individual T_1 lines were analyzed. Single locus integration was found in several lines bearing *AtSPO11-1.CSR1-ZFP-F* (n = 11) and *AtSPO11-1.CSR1-ZFP-F.18xMyc* (n = 7). Herbizide segregation rates in remaining lines was below 3:1 or at about 16:1. The former, as some individual plants were dying rather due to pest-related pressure than because of herbizide application. The latter due to multiple transgene insertions.

One single-locus insertion line, *AtSPO11-1.CSR1-ZFP-F* (#8) displayed a pleiotropic phenotype of ectopic rosette formation on shoots (4 of 25 individuals, 16 %), and three lines *AtSPO11-1.CSR1-ZFP-F.18xMyc* (#5, #11, and #57) displayed a reduced-fertility defect similar to the *Atspo11-1-2* phenotype. The pleiotropic phenotype might have been due to T-DNA mediated disruption of an essential developmental gene. Reduced fertility defects in the three *AtSPO11-1.CSR1-ZFP-F.18xMyc* lines could be caused by transgene silencing effects.

Remaining lines *AtSPO11-1.CSR1-ZFP-F* (n=6; #25, #46, #52, #56, #71 and #101) and *AtSPO11-1.CSR1-ZFP-F.18xMyc* (n=4; #16, #39, #73 and #90) were identfied to be *Atspo11-1-2* homozygous. All of those lines displayed *AtSPO11-1* WT-like fruit production and fertility rate, proving that both transgenic constructs were able to complement endogenous *AtSPO11* function *in-planta*.

4.3. Detection of 18xMyc Constructs in Cell Suspension Culture

In addition to complementation analysis, IP experiments were performed to directly address transgenic protein expression *in-vivo*. An available anti-*At*SPO11-1 antibody (Courtesy of Chris Franklin, School of Biosciences, University of Birmingham, United Kingdom) failed to pull down *At*SPO11-1 previous to this thesis. However, a C-terminal tagged *At*SPO11-1.18xMyc fusion protein was successfully detected by a monoclonal anti-*c-Myc* antibody (Krsicka, 2007).

*At*SPO11-1-CSR1-ZF-18xMyc protein isolation was performed from *Arabidopsis* CSC. Constructs *pCB302.AtSPO11-1.CSR1-ZFP-F*(and *ZFP-G*)*.18xMyc* were transformed to address transgene expression while previously tested constructs *pCB302.AtSPO11-1.18xMyc* and *pCB302.AtSPO11-1* were used as positive and negative controls, respectively.

Monoclonal mouse anti-*c-Myc* antibodies 9E11 and 9E10 were used for IP and Western Blot detection (both monoclonal anti-Myc antibodies courtesy of Kim Nasmyth's Lab, Evan *et al*., 1985). The *At*SPO11-1.18xMyc positive control was detected at 93 kDa in contrast to calculated 68.7 kDa, displaying a band-shift of size not uncommon to *c-Myc* tagged proteins (Krsicka, 2007).

Additional bands of about 30 kDa and greater than 95 kDa were observed in all samples as well as in a mock control, most probably due to an interaction of the 9E10 antibody with its own serum, but no *At*SPO11-1-PZF specific signals were detected (82 kDa calculated and about 106 kDa expected size). As the 18xMyc-mediated band shift of transformed constructs resulted in an altered but unpredictable SDS-PAGE migration pattern, protein constructs might have migrated along with an about 98 kDa unspecific background signal, thereby beeing virtually undetectable.

In addition, *At*SPO11-1-PZF-18xMyc sample-specific strong background signals between 30 and 56 kDa were detected. These signals were not present in control or mock samples, and might arise due to degradation of the *At*SPO11-1-PZF-18xMyc fusion proteins.

Summarized, PZF-bearing constructs might be expressed at lower level, indicative of poor *Agrobacterium* transformation efficiency. Expression rates were eventually further decreased due to an unrecognized low-level CSC contamination. These results did not successfully confirm *At*SPO11-1-PZF-18xMyc protein expression. However, obtained segregation analysis data was clearly indicating successful complementation of an *Atspo11-1-2* mutant phenotype. Additional experiments are needed to precicely address fusion protein expression status.

4.4. Experimental Outlook

Several single-locus insertion transgenic *At*SPO11-1.*CSR1*-ZFP-F and *At*SPO11-1.*CSR1*-ZFP-F.18xMyc lines were identified being able to fully complement an *Atspo11-1-2* homozygous mutant background. The identification of non-segregating *Atspo11-1-2*$^{-/-}$; *AtSPO11-1-CSR1-ZFP-F(18xMyc)*$^{+/+}$ T_2 lines will provide the basis for a series of experiments to address open questions discussed below. Prevously discussed and future experiments will apply to already generated constructs *At*SPO11-1.*CSR1*-ZFP-G, *At*SPO11-1.*CSR1*-ZFP-G.18xMyc and *At*SPO11-1.18xMyc.*CSR1*-ZFP-F (and ZFP-G) as well and are described in detail in further sections.

4.4.1. Detection of *At*SPO11-1-PZF Fusion Protein Expression

Generated *At*SPO11-1.*CSR1*-ZFP-F(18xMyc) lines successfully complemented an *Atspo11-1-2* homozygous mutant sterility phenotype. Unexpectedly, tagged constructs *At*SPO11-1.*CSR1*-ZFP-G.18xMyc and *At*SPO11-1.*CSR1*-ZFP-F.18xMyc could not be detected by immunoblotting within transformed CSCs, probably due to weak expression or due to contamination issues. A possible interaction between the PZF domain and the 18x *c-Myc* epitope cannot be ruled out. As well degradation of *At*SPO11-1-PZF fusion proteins migh occur as *At*SPO11-1-PZF-18xMyc samples displayed strong background signals between 30 and 56 kDa.

Future IP experiments will therefore be performed directly from inflorecence tissue. Floral buds of *Atspo11-1-2*$^{-/-}$ plants, homozygous for an *AtSPO11-1-ZF-18xMyc* or *AtSPO11-1-18xMyc-ZF* transgene will be harvested, serving as source for meiotic protein isolation. By this strategy, error-prone CSC maintenance will be bypassed and *At*SPO11-1-PZF fusion proteins isolated from meiotic instead of somatic tissue. Thereby transgene expression will be addressed on mRNA level. RNA will be isolated from meiotic tissue of *Atspo11-1-2*$^{-/-}$; *AtSPO11-PZF*$^{+/+}$ plants. RT-PCR mediated cDNA synthesis and subsequent *AtSPO11-1*-specific RealTime PCR amplification will allow to detect and quantify expression of all generated *At*SPO11-1-PZF derivates, independent of 18xMyc presence.

4.4.2. Extended Analysis of *At*SPO11-1-PZF Variants

Selected transgenic lines will be further evaluated after successful expression analysis to obtain additional information on transgene integration and function. Southern Blot analysis and transgene-specific PCR amplification will be performed to precicesly identify single-copy insertion lines. T-DNA left border- and right border-specific oligonucleotide primers will be used to amplify T-DNA flanking genomic regions. Further sequence determination of genomic DNA regions will allow to identify the region of transgene integration within the *Arabidopsis* genome.

Complementation analysis of an *Atspo11-1-2* homozygous sterility phenotype indicated WT-like levels regarding plant fertility and fruit production rate. Seed per silique counts will be performed to quantify the level of *Atspo11-1-2* complementation. To address transgene complementation in addition to fertility, antibodies against *At*SPO11-1 were produced and will be tested in cytological experiments for their ability to detect either *At*SPO11-1 or *At*SPO11-1 fusion proteins during meiosis. These experiments will provide insight in *At*SPO11-1 fusion protein distribution, and thereby address the transgene functionality at an additional level. Moreover anti-*At*SPO11-1 antibodies might be successfully used in future IP experiments, eliminating the need for generation of tagged *At*SPO11-1 proteins.

4.4.3. Confirmation of DNA binding activity of *At*SPO11-1-PZF Fusion Proteins

PZF-*Fok*I fusion proteins bearing N-terminal fusions of *de-novo* designed 4xZF *ZF-G* and *ZF-F* to catalytical *Fok*I restriction endonuclease domains were found to successfully bind and cleave their corresponding target site sequences in a plasmid-embedded context *in-vitro*. DNA binding activity of *At*SPO11-*CSR1*-ZF constructs will be addressed *in-vivo* by parallel strategies.

DNA bound, 18xMyc-tagged *At*SPO11-1-*CSR1*-ZF fusion proteins will be crosslinked to DNA by treatment of meiotic cell extracts with formaldehyde. Thereby, *At*SPO11-1-PZF derivates will be attached to DNA regardless of DSB induction. Genomic DNA will be sheared by sonication and *At*SPO11-1-*CSR1*-ZF-DNA complexes will be subjected to ChIP using either an anti-*c-Myc* or an anti-*At*SPO11-1 antibody. Protein-DNA interactions will be reversed and proteins degraded. Enriched genomic DNA will be subjected to RealTime PCR-mediated amplification of *CSR1* locus flanking regions to address *At*SPO11-1-*CSR1*-ZF DNA binding specificity *in-planta*.

As steady-state levels of DNA-bound *At*SPO11-1 protein are considerably low, an enrichment of 18xMyc-tagged, DNA-bound *At*SPO11-*CSR1*-ZF fusion proteins might be necessary. Spo11-DNA recombination intermediates were found enriched in *com1*Δ/*sae2*Δ mutant backgrounds in budding yeast (Prieler *et al*., 2005). Likewise *At*SPO11-1 foci were able to be detected using an *At*SPO11-1-specific antibody (Sanchez-Moran *et al*., 2007) in an *Atcom1-1* mutant background (Uanschou *et al*., 2007). Analogously, *Atspo11-1-2*$^{-/-}$; *AtSPO11-1.CSR1-ZFP-G* (*ZFP-F*)*.18xMyc*$^{+/+}$ plant lines will be crossed to *Atcom1-1* mutant plants. Plants homozygous for *Atspo11-1-2* and the transgene will be identified in further generations. Covalently bound *At*SPO11-1-*CSR1*-ZF-18xMyc-DNA recombination intermediates will be enriched in this mutant background as introduced DSBs remain unprocessed (Uanschou *et al*., 2007).

Genomic DNA will be subjected to ChIP analysis as previously described. Crosslinking and decrosslinking steps will be omitted, as covalent *At*SPO11-1-*CSR1*-ZF-18xMyc DNA recombination intermediates have been formed. Amplification of *CSR1* locus flanking regions will allow to directly identify *At*SPO11-1-*CSR1*-ZF DNA binding and DNA cleavage specificity *in-planta*.

4.4.4. Confirmation of DNA cleavage activity of *At*SPO11-1-PZF Fusion Proteins Quantification of Locus-specific Recombination Events

The ability of *At*SPO11-1-PZF fusion proteins to cleave DNA can be addressed by ChIP experiments in a homozygous *Atcom1-1* mutant background, as covalently bound *At*SPO11-1-PZF-DNA recombination intermediates accumulate after DSB induction. To address *CSR1* locus-specific HR events, the exchange of locus-flanking markers will be monitored by different strategies.

Male and female germline recombination events will be monitored by *trans* to *cis* marker exchange within heteroallelic F_1 *csr1-1*/*csr1-2*; *AtSPO11-1-CSR1-ZF*$^{+/+}$ tester lines. Since four residual HR events occur at the *CSR1* locus within 100.000 test crosses (Mourad *et al*., 1994), about 2000 backcrossings of F2 progeny to WT will be necessary to detect basal rates of recombination, expressed through the presence of double herbizide-resistant F3 progeny. The number of crossing progeny that has to be evaluated by backcrossing will depend on the magnitude of HR stimulation, and is anticipated to be considerably lower.

Alternatively, recombination events within the male germline will be visualized by monitoring pollen-expressed fluorescent protein signals (Francis *et al*., 2007). Homozygous FTLs, bearing an autofluorescent protein insertion upstream or downstream of the *CSR1* locus were generated. Individual homozygous FTLs #1268, DsRed2; #1632, CFP; both upstream of *CSR1*, and #2201, AmCyan; #2456, DsRed2; both downstream of *CSR1*, were generated and crossed to *Atspo11-1-2* to keep future populations small.

Atspo11-1-2$^{+/-}$; *FTL*$^{+/+}$ lines will be identified. Generated lines *Atspo11-1-2*$^{+/-}$; *DsRed2*$^{+/+}$ (#1268) and *Atspo11-1-2*$^{+/-}$; *AmCyan*$^{+/+}$ (#2201) as well as *Atspo11-1-2*$^{+/-}$; *CFP*$^{+/+}$ (#1632) and *Atspo11-1-2*$^{+/-}$; *DsRed2*$^{+/+}$ (#2456) will be crossed to create heteroallelic FTL tester lines in *trans* configuration. Progeny of these crossings will be used to determine the endogenous HR rate within the generated *CSR1* flanking FTL interval, resulting in *trans* to *cis* fluorescent pollen marker exchange. In parallel, generated heteroallelic tester lines will be crossed to selected *Atspo11-1-2*$^{-/-}$; *AtSPO11-1-CSR1-ZF*$^{+/+}$ lines to monitor and quanitify *At*SPO11-1-PZF mediated *CSR1* locus targeting.

4.4.5. Generation of further *At*SPO11-PZF Fusion Proteins

With the successful verification of *At*SPO11-1-PZF-mediated locus-specific DSB formation and subsequent HR, a novel method to stimulate germ line recombination will be generated, targeting *At*SPO11-1 to a single locus by simple modification of the protein.

In-silico binding prediction analysis of *CSR1*-specific 4xZF constructs has identified not more than one additional ectopic target site per *Arabidopsis* chromosome. To test if an extension of the target site sequence is inversely corellating with off-target site binding, additional *AtSPO11-6xZF* constructs will be generated. A series of three different 6xZF constructs were provided by our collaborator (Bert J. van der Zaal, Institute of Biology Leiden, Department of Molecular and Developmental Genetics, Leiden University, The Netherlands) and will be used in *At*SPO11-6xZF generation. The *PTF1* 6xZF was successfully used in targeting a transcriptional activator domain in yeast (Neuteboom *et al*., 2006) and is targeting in addition exon one of the *Arabidopsis PINOID* gene, involved in auxin transport. Another 6xZF *Sp1* resembles a mammalian TF DNA binding domain (Beerli *et al*., 1998).

As this 6xZF protein is not anticipated to bind within the *Arabidopsis* genome, it might serve as negative control in future experiments and help to address off-target site binding of PZF domains. The third 6xZF *HPT* will target the Hygromycin-Phosphotransferase gene. As the *hpt* gene is a common plant selectable marker, it is present in many lab internal transgenic plant lines at well-characterized positions within the *Arabidopsis* genome.

*At*SPO11-6xZF fusion proteins will be generated to test if *At*SPO11 can be targeted to several desired loci within the *Arabidopsis* genome. As *Arabidopsis thaliana* encodes for two meiosis-specific Spo11 homologs *At*SPO11-1 and *At*SPO11-2, *At*SPO11-2-PZF fusion proteins will be generated as previously discussed. Distant future experiments will involve *de-novo* design of PZF proteins to generate artificial hotspots of recombination at any chosen locus within the *Arabidopsis* genome at will.

4.4.6. Targeted Meiotic Recombination in Crop Plants

Targeted meiotic recombination could be beneficial to applied agricultural science, as the combination of certain traits with low genetic distances is extremely labor intensive, or simply impossible to be achieved by simple crossing procedures. Stimulated locus-specific HR will therefore allow the recovery of novel recombinants in the course of genetic crosses.

As SPO11 was found to be conserved and involved in meiotic DSB formation in all eukaryotic organisms studied so far, genomic cloning of SPO11 and generation of SPO11-PZF fusion proteins from various crop species will be conducted. In detail, SPO11 cloning of *Brassicacae* family members *Brassica oleracea* (cabbage) and *Brassica napus* (rape, canola) will be performed to introduce the strategy of targeted meiotic recombination to the field of agriculture as well.

5. Materials and Methods

5.1. Media and Solutions

5.1.1. Bacterial Media

LB Medium

10 g/L Tryptone; 5 g/L Yeast Extract; 10 g/L NaCl; ddH_2O ad 1 L; pH 7.0 (adjusted with 1N NaOH). For plate use the mixture was supplemented with 15 g/L Bacto Agar. The mixture was prepared and autoclaved for 20' at 121°C. For selection of transgenic plants, media were supplemented with 50 mg/L Kanamycin (Duchefa). For selection of *E.coli*, media were supplemented with antibiotics (100 mg/L Ampicillin, or 50 mg/L Kanamycin). For selection of *A.tumefaciens* GV3101, media were supplemented with 50 mg/L Gentamycin and 50 mg/L Kanamycin (all Duchefa). 1000x Stock solutions were prepared for all antibiotics and stored at -20°C. Plates were poured and stored at 4°C.

SOC Medium

10 g/L Tryptone; 5 g/L Yeast Extract; 2.5 mM KCl; 10 mM NaCl; ddH_2O ad 1 L; pH 7.6 (adjusted with 1 N NaOH). The mixture was prepared and autoclaved for 20' at 121°C. After autoclaving the medium was supplemented with 20 mM Glucose; 10 mM $MgCl_2$ and 10 mM $MgSO_4$ (all supplements autoclaved).

5.1.2. Plant Media

ARA Plates

4.33 g/L MS basal salt (Murashige and Skoog Medium w/o Vitamins, Duchefa); 0.5g/L MES (2-(N-morpholino) Ethanesulfonic Acid, Duchefa); 10 g/L Sucrose and 1x Gamborg's vitamin solution (Sigma); pH 5.8 (adjusted with 1M KOH); 6 g/L plant agar (Duchefa). The mixture was prepared and autoclaved for 20' at 121°C. For selection of transgenic plants, media were supplemented with 50 mg/L Kanamycin (Duchefa). Plates were poured and stored at 4°C.

Cell Suspension Culture Medium

4.33 g/L MS basal salt (Murashige and Skoog Medium, w/o Vitamins, Duchefa); 2x Gamborg's vitamin solution (Sigma); 30 g/L Sucrose; 0.5 mg/L 2,4-D (2,4-Dichlorophenoxyacetic Acid); 2.0 mg/L IAA (Indole-3-Acetic Acid); 0.5 mg/L 6-(γ,γ-Methylallyl Amino)-Purine Riboside (all Duchefa); pH 5.8 (adjusted with 1 M KOH). The mixture was prepared, filter sterilized into an autoclaved bottle and stored at 4°C.

5.2. Plant Work

5.2.1. Seed Sterilization

The seed sterilization solution (5 g $Ca(OCl)_2$; 0.02 % Triton X-100; ddH_2O ad 100 mL) was prepared and stirred for at least two hours at RT. Undissolved sterlilization agent was let to sediment and 1 mL of at least one day old supernatant (not older than 14 d) was added to about 50 to 100 seeds. The mixture was agitated to cover all seeds and incubated for 20 minutes on a rotating wheel at RT. Seeds were centrifugated shortly to accelerate sedimentation and washed twice with 1 mL sterile ddH_2O under sterile conditions. Sterlilized seeds were dried in open microtiter tubes in a sterile work bench for two days and stored at RT afterwards.

5.2.2. Growth Conditions

Sterilized seeds were dispersed on ARA plates under sterile conditions. Plates were sealed with microporous tape and stratified at 4°C for two days in absence of light to brake seed dormancy. Plates were then incubated in a controlled environment growth chamber under long-day conditions (21°C, 16 h light / 8 h dark photoperiod).

Alternatively, non-sterile seeds were soaked and stratified in 1 mL ddH_2O as described previously. Nine to 16 seeds per pot were sown on a soil/perlite mixture (3:1 mix) and covered upon development of four-leaf plantlets. Plants were further cultivated under long-day conditions (21°C, 60-80 % humidity, 16 h light / 8 h dark photoperiod, 5800 LUX, 4x PHILIPS TLD 36 W and 2x SYLVANIA GroLUX 36 W as light sources).

Leaf material of plants of about three to six weeks of age was harvested for DNA extraction and subsequent PCR-mediated genotype determination. Inflorescences of plants selected for propagation by selfing were wrapped in paper bags as early siliques developed a yellow color. Seeds were harvested after about 90 % of all siliques have dried and were stored in small paper bags or punctured microtiter tubes at RT in dark and dry environment.

5.2.3. Transformation of *Agrobacterium tumefaciens*

Electro-competent *Agrobacteria* (strain GV3101) were prepared as described elsewhere (Sambrook *et al*., 1989). 100 µl aliquots of electro-competent cells were thawn on ice. Cells were mixed with 10-100 ng plasmid DNA (1 µl of 1:20 dilution of Mini Prep scale plasmid DNA preparation), transferred to a pre-cooled 1 mm electroporation cuvette and incubated for one minute on ice. Cells were electroporated at 400 Ω, 25 µF and 1.8 kV (pulse lengths of 5-8 ms indicated successfull electroporation). Cells were mixed with 1 mL prewarmed LB or SOC medium immediately after electroporation and incubated for 1h at RT. 100 µl of cell suspension was spread on a LB plate containing antibiotics (50 mg/L Kanamycin and 50 mg/L Gentamycin) and incubated for two days at 28°C to 30°C or for three days at RT.

Plasmid DNA uptake was verified by *Agrobacterium* plasmid DNA isolation, *E.coli* retransformation, *E.coli* plasmid DNA isolation and restriction endonuclease digest analysis.

5.2.4. Transformation of *Arabidopsis thaliana* Cell Culture

Arabidopsis thaliana CSC establishment and maintenance was performed as described elsewhere (Marthur and Koncz, 1998). CSC aliquots were subcultured every seven days. Thereby, under sterile conditions, 5 mL of cell suspension were transferred to a 100 mL Erlenmeyer flask, containing 20 mL of cell suspension culture medium. Culture aliquots were sealed with microporous tape and incubated at 21°C in dark under constant shaking.

Transient CSC transformation was carried out according to a defined time schedule. One day after CSC propagation by subculturing, an *A.tumefaciens* GV3101 strain, harbouring the transgene to be transformed, was spread on an LB plate (supplemented with 50 mg/mL Kanamycin and 50 mg/mL Gentamycin) from a glycerol stock aliquot. The plate was incubated for two days at 28°C. 50 mL of LB liquid medium (supplemented with Kanamycin and Gentamycin at previously described concentrations) were inocluated with 2-3 single colonies and grown over night (O/N) to an optical density of OD_{600} = 1.0 (130 rpm, 28°C). Bacteria were harvested by centrifugation (10', 4000 rpm, RT) and resuspended in 1 mL CSC medium. Concentrated Agrobacteria were added to a plant CSC aliquot, supplemented with 2 µl of 0.2 M Acetosyringone (Stock Solution in sterile ddH_2O at 4°C), and cocultivated for three days under previously descibed CSC maintenance conditions.

One week after initial subcultivation, the transformed CSC aliquot was centrifugated (5', 2600 rpm w/o break, RT) and washed three times with fresh CSC medium (10-20 mL). After final centrifugation, transformed cells were resuspended in 25 mL of CSC medium. 5 mL of the suspension were subcultured as initially descibed (supplemented with 250 mg/L Amoxicillin (Duchefa) to eliminate *Agrobacterium* remainders. After additional two days of CSC propagation, cells were used for preparation of protein extracts.

5.2.5. *In-planta* Transformation

5 mL of LB liquid culture supplemented with antibiotics (50 mg/L Kanamycin and 50 mg/L Gentamycin) were inoculated with an Agrobacterium GV3101 strain single colony, harbouring the transgene to be transformed, and incubated O/N at 28°C. The over-night culture (ONC) was used to inoculate 500 mL of LB liquid culture (supplemented with the same antibiotics) and incubated again O/N at 28°C.

Cells were collected by centrifugation (25', 5000 rpm, RT) and washed with 400-500 mL infiltration medium (5% Sucrose (w/v); 10', 5000 rpm, RT). The supernatant (SN) was discarded and cells resuspended in 200 mL infiltration medium (supplemented with 0.02 % Silwet L-77 (Lehle Seeds).

Flowering stems of selected plants were removed of mature siliques and dipped for 30 seconds into the *Agrobacterium*-containing infiltration medium suspension. Plants were kept in a box sealed with saran wrap for two days, and returned to normal growth conditions afterwards. Plants were grown to maturity and transformed seeds harvested as descibed previously.

5.2.6. Selection of Transgenic Plant Seedlings

Seeds obtained from propagated in-planta transformation individuals were densely sown onto wet soil (approx. 200-300 seeds/pot), and whole pots stratified for two 2 days at 4°C in dark. Four-leaf seedlings (about 8-10 days old) were sprayed with 150 mg/L BASTA® herbizide (Glufosinate Ammonium Salt 200 g/L, Bayer Crop Science) every two days (seven sessions in total). BASTA-sensitive, non-transformed plants indicated a growth stop after the first round of selection, became chlorotic and finally died during subsequent BASTA application.

5.2.7. Crossing of Mutant *Arabidopsis* Lines

Maternal plants were grown to develop about 10 to 15 cm long primary shoots. Siliques, small secondary shoots and node meristems were removed. Large but still closed floral buds were chosen for crossing. Flowers were opened under a preparative microscope at about 12.5 to 30-fold magnification. Petals and sepals were removed and flowers emasculated by removal of stamens. Flowers displaying yellow anthers were discarded. Paternal flowers were harvested and mature pollen transferred to selected carpels of maternal plants. Silique outgrowth was monitored as indicator of successful pollination. Seeds were harvested as described previously.

5.2.8. Analysis of Fluorescent Pollen Tetrads

Plants with open flowers on the primary shoot were selected. Only flowers from number 5 to 30 were selected for analysis of fluorescent recfombination markers. Standard microscope glass slides were shortly rubbed with a cotton cloth to provide electrostatic charging of the slide. Two 10µl-drops of PGM solution (17 % sucrose (w/v); 2 mM $CaCl_2$; 1.625 mM boric acid; 0.1 % Triton X-100 (v/v)) were placed on a slide. A selected flower was harvested and placed facedown into the first drop of PGM. After 30 seconds of soaking the flower was gently moved in the PGM drop to release pollen, and the same procedure repeated in the second drop to ensure quantitative pollen release. After addition of a coverslip, samples were analyzed on a Axio Imager M1 (Zeiss) epi-fluorescence microscope under 200 to 1000-fold magnification. Filters FITC narrow and Cy3 were used to analyze CFP/AmCyan and DsRed2 fluorescence signals, respectively.

5.3. DNA Work

5.3.1. DNA Preparation from *E.coli*

Over-night cultures (ONCs) were prepared by inoculating 3-5 mL of LB liquid medium, supplemented with appropriate antibiotics (50 mg/L Kanamycin or 100 mg/L Ampicillin) with an *E.coli* single colony. ONCs were incubated at 37°C and cells were collected by subsequent centrifugation (30'', 14.000 rpm, RT) of 3 mL ONC in total. For glycerol stock production, 750 µl of 87 % glycerol were mixed with 750 µl of ONC, incubated for 1h at RT, and finally stored at -80°C.

The supernatant (SN) was discarded and cells suspended in 200 µl GTE Buffer (50 mM Glucose; 25 mM Tris-Cl pH 8.0; 10 mM EDTA pH 8.0) by vigorous mixing. 200 µl of Alkaline SDS Solution (0.2 N NaOH; 1 % SDS; prepared fresh) were added, microtiter tubes inverted several times, and incubated for 5' on ice. Cell lysis was followed by addition of 200 µl Acetate Solution (3 M KOAc pH 5.0; 11.5 % Acetic Acid (v/v)), gentle tube inversion and incubation for 5' on ice.

Samples were centrifugated (10', 14.000 rpm, RT) and the SN mixed with 1x volume of isopropanol. Plasmid DNA was precipitated, pelleted by centrifugation (15', 14.000 rpm, RT), washed with 500 µl 70 % ethanol (5', 14.000 rpm, RT), dried and resuspended in 50 µl ddH_2O. Plasmid DNA was finally resolved by incubation for 30' at 37°C and stored at -20°C.

5.3.2. High-Quality Grade DNA Preparation from *E.coli*

ONC inoculation and cell collection were prepared as described previously. The SN was discarded, cells suspended in 250 µl Resuspension Buffer (50 mM Tris-Cl pH 8.0; 10 mM EDTA pH 8.0; 200 µg/mL RNase A) by vigorous mixing. Cell lysis and neutralization were performed as described previously by adding 250 µl of Alkaline SDS Solution and 300 µl of Acetate Solution, respectively.

Samples were centrifugated (6', 14.000 rpm, 4°C) and the SN mixed with 600 µl isopropanol. Plasmid DNA was precipitated, pelleted by centrifugation (10', 14.000 rpm, 4°C), washed with 500 µl 70% ethanol (5', 14.000 rpm, 4°C), air-dried and resuspended in 50 µl ddH_2O.

30 µl PEG Solution (20 % PEG-6000 (v/v); 2.5 M NaCl) solution were added and samples incubated on ice for 1 h. Plasmid DNA was precipitated by centrifugation (15', 14.000 rpm, 4°C), washed with 200 µl 70 % EtOH (5', 14.000 rpm, 4°C), dried and resuspended in 20 µl ddH_2O. Plasmid DNA was resolved as decribed previously.

5.3.3. DNA Preparation from *Agrobacterium tumefaciens*

Agrobacterium ONCs were prepared by inoculating 3-5 mL of LB liquid medium, supplemented with appropriate antibiotics (50 mg/L Kanamycin and 50 mg/L Gentamycin) with a single colony. ONCs were incubated at 28°C and cells were collected by subsequent centrifugation (1', 10.0000 rpm, RT) of 3 mL ONC in total. The SN was discarded and cells suspended in 150 µl Solution 1 (0.5 % N-Lauroyl-Sarcosine (w/v); Proteinase K 1 mg/mL; 1x TE) and incubated for 1 h at 37°C. Cell lysis and neutralization were performed as described previously by adding 200 µl of Alkaline SDS Solution and 150 µl of Acetate Solution, respectively.

Samples were centrifugated (5', 14.000 rpm, 4°C) and the SN mixed with 1 mL 96 % ethanol. Plasmid DNA was precipitated, pelleted by centrifugation (15', 14.000 rpm, 4°C), washed with 500 µl 70 % ethanol (5', 14.000 rpm, RT), dried and resuspended in 40 µl 1x TE (10 mM Tris-Cl, pH 8.0; 1 mM EDTA, pH 8.0). Plasmid DNA was finally resolved by incubation for 30' at 37°C and stored at -20°C. Subsequent transformation of chemically-competent *E.coli* was conducted with 5 µl of this solution.

5.3.4. PCR-Grade DNA Preparation from *Arabidopsis thaliana*

One to three rosette leaves were ground with a plastic pestle (Sigma) in a microtiter tube, containing 400 µl DNA Extraction Buffer (200 mM Tris-Cl pH 7.5; 250 mM NaCl; 0.5 % SDS (v/v); 25 mM EDTA, pH 8.0). After centrifugation (5', 14.000 rpm, RT) the SN was mixed with 1x volume of isopropanol and genomic DNA precipitated by incubation for 5-10' at RT. DNA was pelleted by centrifugation (15', 14.000 rpm, RT), washed with 300 µl 70 % ethanol (5', 14.000 rpm, RT), dried, and suspended in 50 µl 1x TE. Finally, samples were incubated 10' at 65°C and stored at -20°C.

5.3.5. High-Quality Grade DNA Preparation from *Arabidopsis thaliana*

One to two inflorescences or alternatively several young cauline leafs were homogenized in 400 µl Urea Lysis Buffer (0.3 M NaCl, 30 mM Tris-Cl, pH 8.0, 20 mM EDTA, pH 8.0, 1 % N-Lauroylsarcosine (w/v), 7 M Urea) as previously described and incubated for 10' at 50°C. Samples were mixed with 400 µl PCI Solution (Phenol: Chloroform: Isoamylalcohol = 25: 24: 1) and tubes slightly flicked.

After centrifugation (5', 14.000 rpm, RT) the upper aqueous phase was recovered and mixed with 40 µl 3 M NaOAc, pH 5.2, 400 µl isopropanol and incubated 20' at RT. DNA was precipitated by centrifugation (10', 14.000 rpm, RT), washed with 70 % EtOH (5', 14.000 rpm, RT), air-dried and re-suspended in 100 µl ddH_2O.

5.3.6. Restriction Endonuclease Digest

An appropriate amount of plasmid DNA (*i.e.* 5 µl of PCR-grade DNA or 1 µl of high-quality grade DNA) was incubated in 1x Reaction Buffer together with 5 U of restriction endonucleae in a 20µl-reaction volume. In case of PCR-grade DNA, reactions were supplemented with RNase A (0.1 mg/ml final concentration). Digest reactions were performed according to the manufacturers recommendations (in general samples were incubated for 2h at 37°C).

In case of double-digest reactions, reaction conditions in terms of buffer selection and supplementation (*e.g.* with BSA) were adapted using the manufacturer's online-ressources DoubleDigest™ (www.fermentas.com/doubledigest/index.html) or Double Digest Finder (www.neb.com/nebecomm/DoubleDigestCalculator.asp?). Digested samples were directly subjected to gel-electrophoresis or stored at -20°C upon further use.

5.3.7. DNA Gel-Electrophoresis

Restriction enzyme digest fragments or PCR amplicons were separated in standard agarose gels for DNA analysis (1 % Agarose (genXpress); 1x TAE Buffer (50x TAE: 242 g/L Tris; 57.1 ml/L Glacial Acetic Acid; 100 ml/L 0,5 M EDTA, pH 8.0); Ethidiumbromide 35 µg / 100 mL). Samples were separated at field forces of about 5.0-5.5 V/cm for 30 to 80 minutes, depending on fragment size pattern or amplicon length. Fragments less than 300 bp in length were separated on 2 % 1xTAE gels. Bands were visualized on a Molecular Imager Gel Doc XR System (Bio-Rad Laboratories).

5.3.8. DNA Gel Extraction and Precipitation

Preparative agarose gels intended for extraction of DNA fragments after restriction endonuclease digest or PCR amplification were prepared as described previously. Running buffers were prepared fresh, and DNA separation was conducted in absence of excess light. Bands were excised under UV-light transillumination. DNA was eluted using the E.Z.N.A. Gel Extraction Spin Kit (Omega Bio Tek) according to the manufacturer's protocol and samples were eluted in a final volume of 20 µl ddH_2O.

Alternatively, DNA was eluted from gel slices using the Freeze 'N Squeeze DNA Gel Extraction Spin Columns (Bio-Rad Laboratories) according to the manufacturer's protocol. Eluted DNA was further concentrated by precipitation. 1/10x volume 3 M NaOAc, pH 5.2 and 2.5x volumes 96 % ethanol were added to the DNA sample and mixed vigorously. DNA was precipitated by incubation at -20°C O/N. Samples were centrifugated (15', 14.000 rpm, 4°C), washed with 200 µl 70 % ethanol (5', 14.000 rpm, 4°C), dried and resuspended in 12 µl ddH_2O.

5.3.9. DNA Quantification and Plasmid DNA Ligation

1-5 µl of eluted DNA were subjected to standard agarose gel-electrophoresis. DNA fragment concentrations were estimated by comparing fragment band intensities to DNA marker (GeneRuler™ 1 kb DNA Ladder, Fermentas) band intensities of about same sizes.

Cloning of PCR fragments was performed using the TA Cloning® Kit (Invitrogen). *Taq* polymerase-mediated amplification results in addition of an additional adenosine nucleotide to 3' ends of DNA strands. Generated single-nucleotide A-overhangs are then ligated to T-overhangs of a linearized, TA cloning-capable vector (*pCR2.1-TA*, Invitrogen). Ligation reactions were performed according to the manufacturer's protocol. In detail, a three-fold molar excess of insert DNA was ligated into 12.5 ng of vector DNA.

Prior to directional subcloning of amplicon fragments from *pCR2.1-TA* into appropriate target vectors, high-quality grade DNA preparations were made. Construct integrity was addressed by restriction endonuclease digest analysis sequence verification of selected constructs.

Vector and insert DNA were prepared for ligation by appropriate RE digest. Vector DNA was dephosphorylated by incubation with 2 units of shrimp alkaline phosphatase (SAP, Fermentas) for 45' at 37°C. SAP was inactivated by heat treatment (20' at 65°C). Vector and insert samples were subjected to agarose gel-electrophoresis and appropriate fragments were excised. Subsequent DNA gel extraction and DNA quantification was performed as previously described. Ligation reactions were performed in 15-18 µl reaction volumes (1x T4 Ligase Buffer; 1 or 5 units T4 Ligase, Fermentas). In detail a 3-6-fold molar excess of insert DNA was ligated into 100 ng of vector DNA. Reactions were incubated at RT O/N.

5.3.10. Transformation of chemically-competent *E. coli*

Chemically-competent *E.coli* strains (XL1-Blue, Stratagene; TOP10F', Invitrogen; or DH5α, BioDynamics Laboratory Inc.) were prepared as described elsewhere (Sambrook *et al*., 1989). 100 µl aliquots of competent cells were thawn on ice. Cells were mixed with 10-100 ng plasmid DNA and incubated for 30' on ice. Cell suspensions were transformed by heat shock (90'' at 42°C) and immediately put back on ice. After addition of 1 mL prewarmed LB or SOC medium, cells were incubated on a thermomixer (1 h, 37°C, 300 rpm). Cells were centrifugated (3' at 3000 rpm), most of the SN discarded. Cells were resuspended in remaining about 100 µl medium, spread on LB plates containing antibiotics (50 mg/L Kanamycin or 100 mg/L Ampicillin) and incubated at 37°C O/N. Construct integrity was addressed by restriction endonuclease digest analysis and sequence verification of selected constructs.

5.3.11. PCR Conditions

Standard PCR reactions were performed in a 20 µl reaction volume, containing 1x PCR buffer (50 mM KCl; 10 mM Tris-Cl, pH 9.0; 0.1 % Triton X-100), 1.5 mM $MgCl_2$, 0.2 mM dNTPs, 10 pmoles of each primer and 0.2 µl of purified *Taq* polymerase dilution (prepared by former lab member Claudia Kerzendorfer). Dependend on the context of the PCR reaction, different amplification conditions and amounts of template DNA were used (Tables 4 and 5).

If not otherwise stated, PCR programs comprised of one cycle of initial denaturation (94°C for 1'), 30 cycles of amplification (denaturation, 94°C, 15''; annealing Tm-5°C, 15''; elongation 72°C, 1' per 1 kb amplicon length) and one cycle of final elongation (72°C for 5'). Samples were cooled to 8°C after completion of the amplification reaction and stored at -20°C upon further analysis.

Preparative PCR amplifications for cloning experiments were performed using proofreading high-fidelity *Ex Taq* Polymerase (TaKaRa Bio Inc.) in a 50 µl reaction volume containing 1x Ex Taq Buffer (supplied), 2 mM $MgCl_2$ (supplied); 0.2 mM dNTPs (supplied); 10 pmoles of each primer, 1.25 units Ex Taq polymerase and 1 µl template DNA dilution.

The PCR program comprised of one cycle of initial denaturation (94°C for 30''), 30 cycles of amplification (denaturation, 94°C, 30''; annealing Tm-5°C, 20''; elongation 72°C, 1' per 1 kb amplicon length) and one cycle of final elongation (72°C for 5'). Samples were cooled to 8°C after completion of the amplification reaction and directly used for further experiments.

Table 4 | Overview of PCR Conditions.

PCR	Type	Initial Denat.	Denaturation	Annealing	Elongation	Cycles
ZFP-F/G	HiFi	94°C, 30''	94°C, 30''	55°C, 20''	72°C, 25''	30
ZFP-F/G	Colony	94°C, 15''	94°C, 15''	55°C, 15''	72°C, 25''	30
SPO11-ZFP(Myc)	Colony	94°C, 15''	94°C, 15''	55°C, 15''	72°C, 45''	30
SPO11-(Myc)ZFP	Colony	94°C, 15''	94°C, 15''	60°C, 15''	72°C, 1'10''	30
spo11-1-2 CAPS	Genotype	94°C, 2'	94°C, 20''	60°C, 20''	72°C, 1'	25
spo11-1-2 PIN	Genotype	94°C, 15''	94°C, 15''	57°C, 15''	72°C, 2'	40

Table 5 | Overview of Amplicon Lengths.

PCR	Primer 1	Primer 2	Template	Amplicon Length
ZFP-F/G	4xZFN FW1	4xZFN REV1	1µl Plasmid DNA (1:1000)	368 bp
SPO11-1-ZFP(Myc)	SpoSeq5dn	4xZFN REV1	single colony	760 bp
SPO11-1-(Myc)ZFP	c-myc_new_dn	4xZFN REV1	single colony	1103 bp
spo11-1-2 CAPS	spo11-1-2-MG52	spo11-1-2-MG96	1-2 µl gDNA	954 bp
spo11-1-2 PIN	spo11-1 allele_new	spo11-1 pin_up	1 µl gDNA	2094 bp

5.3.12. *Atspo11-1-2* Genotype Determination

Genotype determination determination was performed, utilizing a CAPS marker within the *Atspo11-1-2* EMS-allele in form of a newly formed *Vsp*I RE site. 2 µl of PCR-grade gDNA were subjected to oligonucleotide primer *spo11-1-2-MG52* and *spo11-1-2-MG96* mediated „CAPS PCR“ amplification as described previously. The *Atspo11-1-2* genotype was assessed after *Vsp*I RE digestion of the generated PCR amplicon. 15 µl of PCR amplicon were digested in a 20 µl reaction volume, containing 1x Buffer O+BSA and 3-5 units *Vsp*I (both Fermentas) by incubation for 2 h at 37°C. Restriction digest fragment patterns were used to identify the *Atspo11-1-2* genotype. AtSPO11-1 WT plants lacked the CAPS marker, resulting in an uncleaved full-length 955 bp PCR amplicon. Homozygous *Atspo11-1-2* plants were characterized by PCR amplicon cleavage, yielding co-migrating 484 and 471 bp digest fragments. Heterozygous Atspo11-1-2 plants were identified by presence of both WT and mutant allele-specific DNA fragments of 955, 481 and 471 bp, respectively.

Alternatively 1 µl of PCR-grade gDNA was amplified by the „PIN PCR“ strategy, using oligonucleotide primers *spo11-1 allele_new* and *spo11-1 pin_up.* The *Atspo11-1-2* genotype was assessed after *Vsp*I RE digestion as described. *AtSPO11-1* WT plants were characterized by 1274 and 820 bp cleavage products, while *Atspo11-1-2* homozygous plants yielded fragments of 820, 654 and 620 bp of size, respectively. Heterozygous *Atspo11-1-2* plants were identified by presence of both WT and mutant allele-specific DNA fragments.

5.3.13. Sequencing Reactions

High-quality grade plasmid DNA was subjected to restriction endonuclease digest and agarose gel-electrophoresis. Plasmid DNA concentration estimation was performed by DNA band intensity comparison as described. 300 to 500 ng of plasmid DNA were used in a 10 µl cycle sequencing reaction, containing 1.5 µl 2.5x sequencing buffer (supplied), 1 µl Terminator Ready Reaction Mix (both part of Big Dye Terminator Cycle Sequencing Kit, Applied Biosystems) and 2 µl of 2 µM oligonucleotide primer. Reaction preparation was performed on ice under light protection.

The cycle sequencing reaction comprised of 25 cycles (denaturation, 96°C for 10’’; annealing, 45°C for 15’’; elongation, 60°C for 4’) after inintial denaturation (96°C for 2’). Reaction mixes were precipitated by addition of 1 µl 3 M NaOAc, pH 5.2 and 25 µl 96 % ethanol, followed by incubation at -20°C O/N. DNA was precipitated by centrifugation (15’, 14.000 rpm, 4°C), washed with 100 µl 70 % ethanol (5’, 14.000 rpm, 4°C), dried and resuspended in 10 µl ddH_2O. DNA sequence readout was perfomed external on an ABI Prism 377 DNA Sequencer (Applied Biosystems) at the Institute of Botany, 1030 Vienna.

5.4. Generation of *At*SPO11-1-PZF Fusion Proteins

The cloning procedure of *At*SPO11-1-PZF constructs is depicted in sections 3.2.3 and 3.2.4 in detail. Oligonucleotide primers and vectors used for cloning are listed in sections 6.1 and 6.2.

PZF DNA fragments were amplified using high-fidelity proofreading *Ex Taq DNA* Polymerase (TaKaRa Bio Inc.) and ligated into *pCR2.1-TA* (Invitrogen) after gel-electrophoresis of PCR amplicons, excision of fragments and purification. After transformation into *E.coli*, high-quality grade plasmid DNA was prepared and PZF fragments were sequenced using oligonucleotide primers *M13 forward (-20)* and *M13 reverse.* PZF fragments were mobilized after *Sma*I/*Eco*RV restriction enzyme digest, and ligated into *Sma*I linearized, dephosphorylated *pCB302.AtSPO11-1* derivates. High-quality plasmid DNA preparations of subcloned *pCB302.AtSPO11-1.PZF* derivates were screened by „Colony PCR" for PZF presence. Appropriate clones were isolated and analyzed by restriction endonuclease digest. PZF presence was verified by sequencing and constructs were transformed into *Agrobacterium tumefaciens*. *Agrobacterium* plasmid DNA preparation, retransformation into *E.coli* and plasmid DNA preparation from *E.coli* were performed. Restriction endonuclease digest analysis was performed to rule out *Agrobacterium*-mediated construct recombination events, and constructs finally used for transient CSC and stable *in-planta* transformation.

5.4.1. Fusion of *At*SPO11-1 with 4xZF DNA Binding Motifs

ZF-F and *ZF-G* encoding regions were amplified from templates *pET.CSR1-ZFN-F* and *pET.CSR1-ZFN-F*, respectively, using oligonucleotide primers *4xZFN FW1* and *4xZFN REV1* (PCR „ZFP-F/G", Tables 4 and 5). 368 bp PCR amplicons were ligated into *pCR2.1-TA*, giving rise to constructs *pCR2.1-TA.CSR1-ZFP-F* and *pCR2.1-TA.CSR1-ZFP-G.* Cloned *ZF-F* and *ZF-G* sequences were verified by cycle sequencing using primers *M13 forward (-20)* and *M13 reverse*.

Fragments *ZF-F* and *ZF-G* were subjected to a RE double-digest and released as 354 bp *Sma*I/*EcoR*V fragments from their respective vectors. *ZF-F* and *ZF-G* fragments were ligated into *Sma*I digested, linearized 9262 bp *pCB302.AtSPO11-1* vector. Insert orientation was identified by „Colony-PCR" using oligonucleotide primer pairs *4xZFN REV1* and *SpoSeq5dn*. (PCR „SPO11-1-ZFP(Myc)", Tables 4 and 5). Verified constructs were termed *pCB302.AtSPO11-1.CSR1-ZFP-F* and *pCB302.AtSPO11-1.CSR1-ZFP-G. ZF-F* and *ZF-G* sequences were again verified by cycle sequencing using primers *4xZFN FW1, 4xZFN REV1 and Spo11Seq5dn.*

5.4.2. Fusion of *At*SPO11-1-*CSR1*-ZFP Constructs with 18xMyc Protein Tags

Fragments *ZF-F* and *ZF-G* were subjected to a RE double-digest and released as 354 bp *Sma*I/*EcoR*V fragments from their respective vectors *pCR2.1-TA.CSR1-ZFP-F* and *pCR2.1-TA.CSR1-ZFP-G.* Processed blunt-ended *ZF-F* and *ZF-G* fragments were ligated into *Sma*I digested, linearized 9997 bp *pCB302.AtSPO11-1.18xMyc* vector. Insert orientation was identified by „Colony PCR" using oligonucleotide primer pairs *4xZFN REV1* and *SpoSeq5dn* (PCR „SPO11-1-ZFP(Myc)", Tables 4 and 5). Constructs were termed *pCB302.AtSPO11-1.CSR1-ZFP-F.18xMyc and pCB302.AtSPO11-1.CSR1-ZFP-G.18xMyc.*

In parallel, the 18x *c-Myc* Epitope encoding region was subjected to a RE double-digest and released as 735 bp *Sma*I/*EcoR*V fragment from the respective vector *pCR2.1-TOPO.18xMyc.* The processed blunt-ended 18xMyc fragment was ligated into *Sma*I digested, linearized 9997 bp *pCB302.AtSPO11-1.CSR1-ZFP-F* and *pCB302.AtSPO11-1.CSR1-ZFP-G* vectors. Insert orientation was identified by „Colony PCR" using oligonucleotide primer pairs *c-myc_new_dn* and *4xZFN REV1* (PCR „SPO11-1-(Myc)ZFP", Tables 4 and 5). Constructs were termed *pCB302.AtSPO11-1.18xMyc.CSR1-ZFP-F and pCB302.AtSPO11-1.18xMyc.CSR1-ZFP-G.*

ZF-F and *ZF-G* sequences were again verified by cycle sequencing using primers *4xZFN FW1, 4xZFN REV1* and *Spo11Seq5dn.*

5.5. Protein Work

5.5.1. Protein Isolation from *Arabidopsis thaliana* Cell Suspension Culture

One day prior to scheduled IP experiments 25 µl aliquots of protein-A sepharose beads (CL-4B, GE Healthcare) were washed three times (30'', max 500x g, RT) with 500 µl NET-2 buffer (50 mM Tris-Cl, pH 7.5; 150 mM NaCl; 0.05 % NP-40 (v/v)). 600 µl NET-2 buffer and 600 µl 9E11 antibody (monoclonal mouse anti-*c-Myc* cell culture SN; Courtesy of Kim Nasmyth's Lab; Evan *et al.*, 1985). Tubes were sealed with microporous tape and incubated on a rotating wheel at 4°C O/N.

Cells of transformed CSC aliquots were collected by centrifugation (5', 2600 rpm w/o break, RT) and resuspended in 4 mL of ddH_2O. Subsequent experimental steps were performed on ice. Cells were transferred to a 2 mL screw cap tube, and the SN discarded (30'', 8000 rpm, RT). 2x protein extraction buffer (100 mM Tris-Cl, pH 7.5; 20 % glycerol (v/v); 0.2 % NP-40 (v/v); 2 mM EDTA, pH 8.0; 1 mM DTT, sterile filtered) was supplemented with 1/5x volume of protein inhibitor (Complete PI Mini Kit, Roche) / pepstatin A solution (2x PI; 100 µg/mL pepstatin A final concentration).

A final volume of about 400-600 µl of cell concentrate was mixed with the same volume of supplemented 2x protein extraction buffer . Cells were lysed with the help of steal beads (3 mm in diameter, stainless NIRO steel, KÖBO) in a Multi Bead Shocker (Yasui Kikai) (10' incubation, 2500 rpm, 0°C, 30'' shocks, 30'' cooling intervals). Cell debris was collected by centrifugation (10', 14.000 rpm, 4°C). In parallel, antibody-coated protein-A sepharose beads were washed three times with 500 µl NET-2 buffer (30'', 500x g, 4°C). The clear protein SN was added to the washed beads, and NET-2 buffer added to a final volume of 1.5 mL. A mock control was prepared, using an equal amount of 2x protein extraction buffer instead of cell lysate, filled with NET-2 buffer to 1.5 mL. anti-*c-Myc* IP was performed by incubating samples on a rotating wheel for 3h at 4°C.

IP samples were washed three times with 500 µl NET-2 buffer (30'', max. 500x g, 4°C), all liquid was removed and samples were mixed with 22 µl of 2x Laemmli Sample Buffer (50 % Glycerol; 2 % SDS; 125 mM Tris-Cl, pH 6.8; 20 mM DTT; 0.003 % Bromophenol Blue). Proteins were denatured by incubation for 10' at 96°C. Denatured samples were kept at RT and warmed 5' at 37°C prior to SDS-Polyacrylamide gel loading.

5.5.2. Protein Gel

A 10% SDS-PAGE separation gel was prepared (for one gel: 2.325 mL ddH_2O; 1.275 mL 40 % acrylamide/bisacrylamide mix; 1.3 mL 1.5 M Tris-Cl, pH 8.8; 50 µl 10 % SDS; 50 µl 10% ammonium persulfate; 3 µl TEMED) using a Ready Gel System (Bio-Rad Laboratories) and overlaid with isopropanol. After polymerization and isopropanol removal the separation gel was overlaid with a stacking gel (for 2 ml: 1.48 mL ddH_2O; 0.247 mL 40 % acrylamide/bisacrylamide mix; 0.25 mL 1.5 M Tris-Cl, pH 6.8; 20 µl 10 % SDS; 20 µl 10% ammonium persulfate; 2 µl TEMED). After polymerization, slots were rinsed with ddH_2O and the gel placed in 1x PAGE buffer (10x buffer: 72.1 g Glycine, 15.14 g Tris, 5 g SDS, 500 mL ddH_2O). 20 µl of protein samples were loaded and separated at a constant current of 35 mA until the blue loading dye migrated out of the gel.

5.5.3. Western Blot

The protein gel was shortly rinsed with with ddH_2O and equilibrated in 1x transfer buffer (190 mM Glycine; 25 mM Tris; 20 % Methanol (v/v)) for about 10'. The PVDF membrane (Immobilon-P, Millipore) was activated in methanol for 1' and incubated in 1x transfer buffer for 10'. Membrane and gel were placed on each other and embedded between 2 layers of Whatman paper (3MM) and 1 layer of sponge on each side. The membrane/gel sandwhich was inserted into a transfer apparatus (Mini Trans-Blot®, Biorad) and overlaid with 1x transfer buffer. Protein transfer was performed at 380 mA within about 1 h. The membrane was allowed to dry on Whatman paper O/N.

The dried membrane was moistened in methanol again, rinsed with ddH_2O and blocked in 1x TBS-T (150 mM NaCl; 10 mM Tris-Cl, pH 7.5, 0.2 % Tween-20) / 3 % Milk (non-fat instant dry milk) for 1 h at RT. All incubation steps were performed under constant shaking. The membrane was washed three times for 5' in 1x TBS-T / 3 % Milk and incubated with the primary 9E10 antibody 1:3 dilution (3 mL monoclonal mouse anti-*Myc* cell culture SN; Courtesy of Kim Nasmyth's Lab; and 6 mL 1x TBS-T / 3 % Milk) for 2-3 h at RT. The membrane was washed 3x for 10' in 1x TBS-T and incubated with the secondary antibody diluted 1:100.000 in 1x TBS-T (1 µl of 1:10 working dilution of ImmunoPure goat anti-mouse IgG+IgM (H+L) peroxidase conjugated (Pierce #31444) per 10 mL 1x TBS-T) for 1.5 h at RT.

After washing the membrane 3x 5' with 1x TBS-T, protein-antibody interactions were finally visualized by incubation with 1.5 ml of chemiluminescent ECL substrate (Pierce, #32109) for 5' at RT and subsequent exposure to an X-ray film (KODAK) for 60-90'.

6. Supplementary Information

6.1. Oligonucleotide Primer

c-myc_new_dn	5'- ATC CAT GGC TCC CGG GTC CGG TTC TGC TGC TAG TGG -3'
M13 forward (-20)	5'- GTA AAA CGA CGG CCA G -3'
M13 reverse	5'- CAG GAA ACA GCT ATG AC -3'
spo11-1 allele_new	5'- GGT TTC GTC TAC CAT CAT CCC AGG C -3'
spo11-1 pin_up	5'- CAC GGT CCA CAA TGG ATT GTG CTG -3'
spo11-1-2-MG52	5'- GGA TCG GGC CTA AAA GCC AAC G -3'
spo11-1-2-MG96	5'- CTT TGA ATG CTG ATG GAT GCA TGT AGT AG -3'
SpoSeq5dn	5'- GAC AGA AGA AGG TAA GAG ATC -3'
4xZFN FW1	5' - ATT ACC CGG GGC TGG TGG AGG TGA AAA ACC TTA CAA GTG TCC TGA ATG T - 3'
4xZFN REV1	5' - TAT AGA TAT CGC CCG TAT GCG TCC TCT GAT - 3'

6.2. Vectors and Construct Maps

pCB302.AtSPO11-1 and pCB302.AtSPO11-1.18xMyc

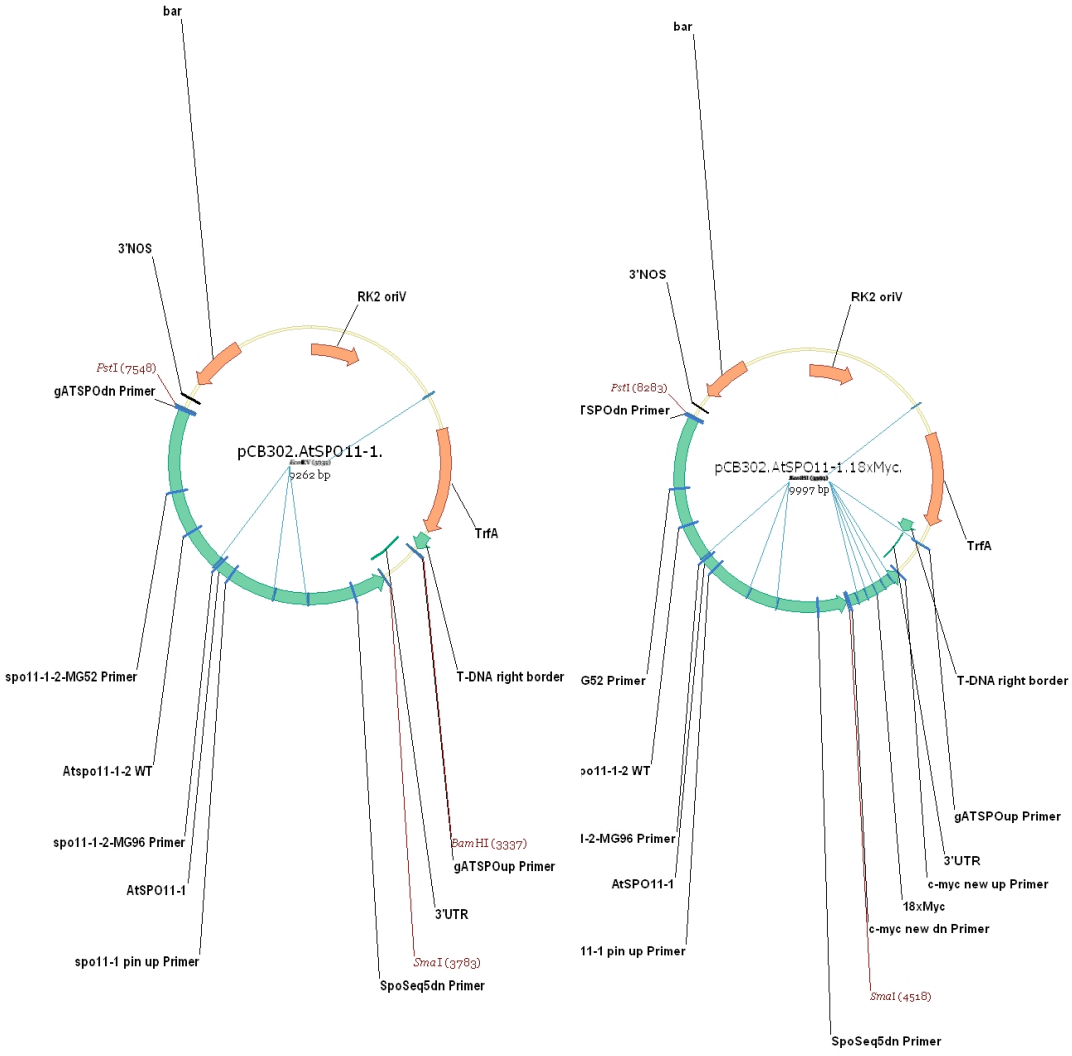

pET28.CSR1-ZFN-F and pET28.CSR1-ZFN-G

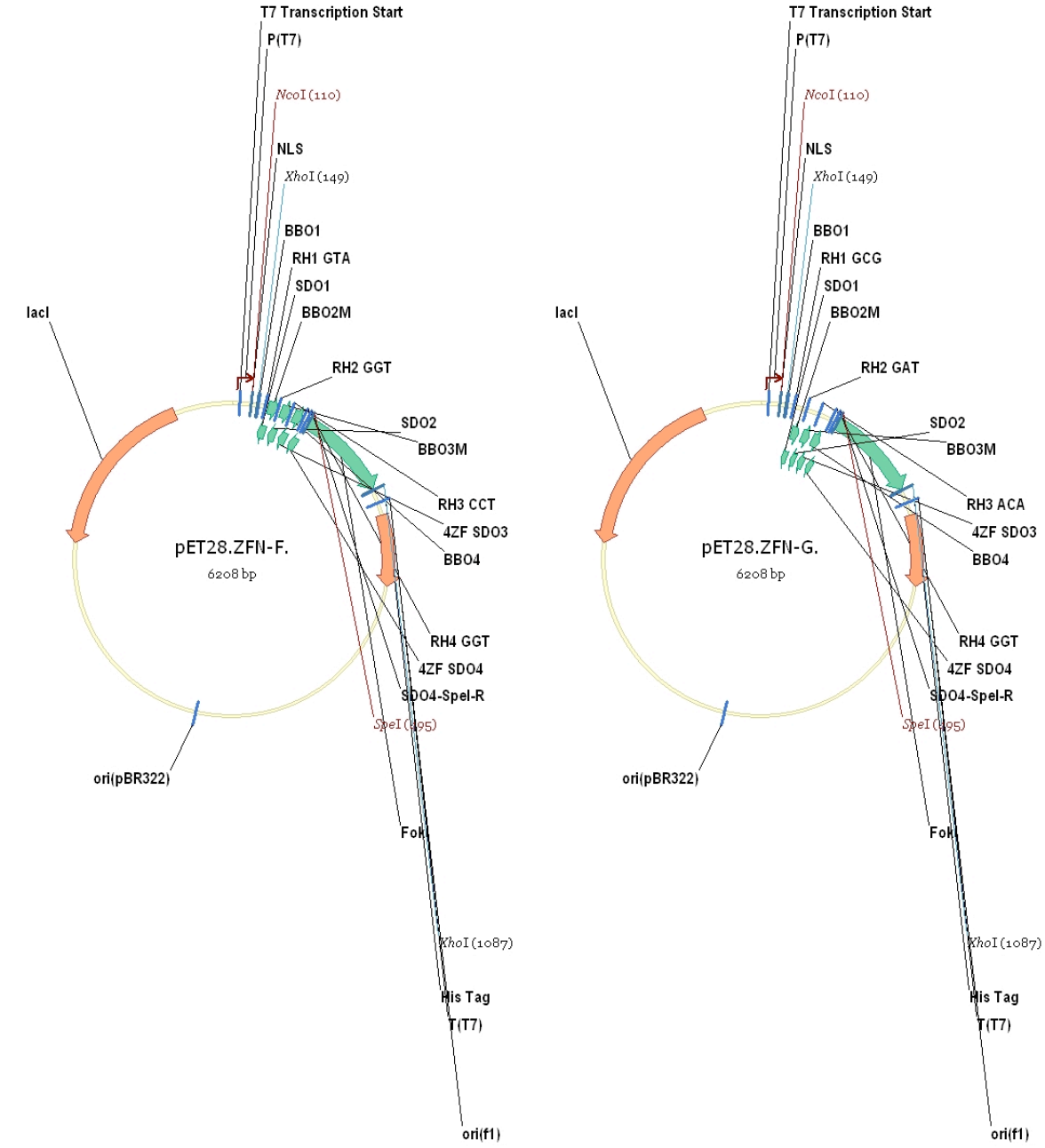

pCR2.1.CSR1-ZFP-F and pCR2.1.CSR1-ZFP-G

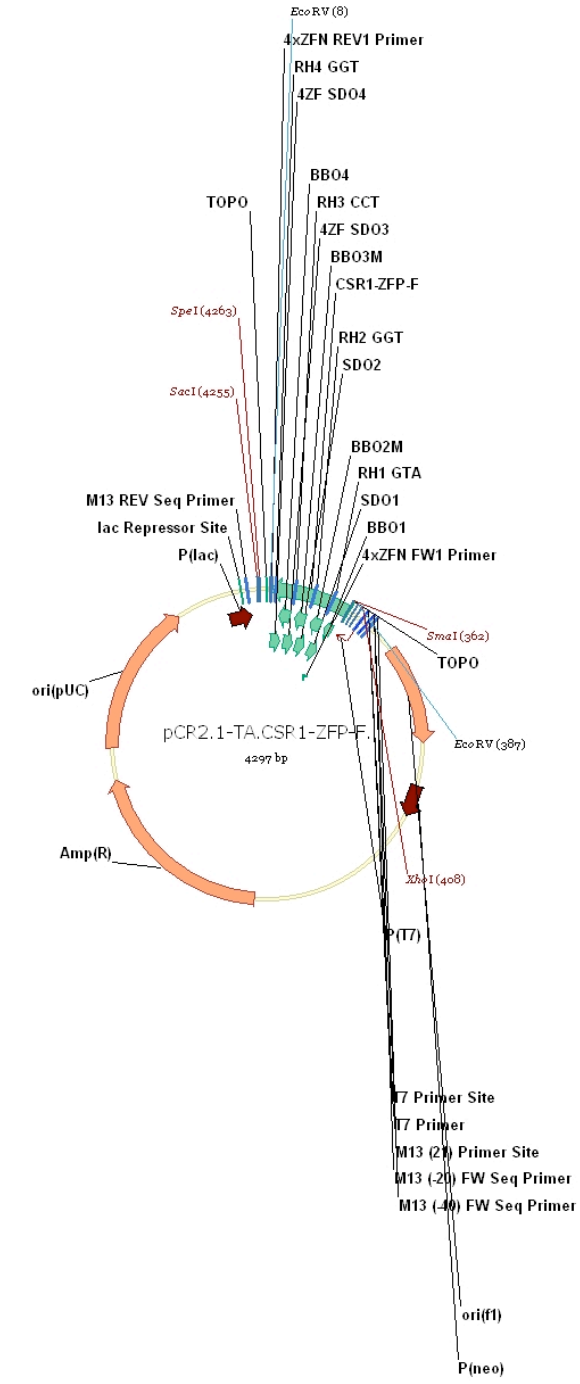

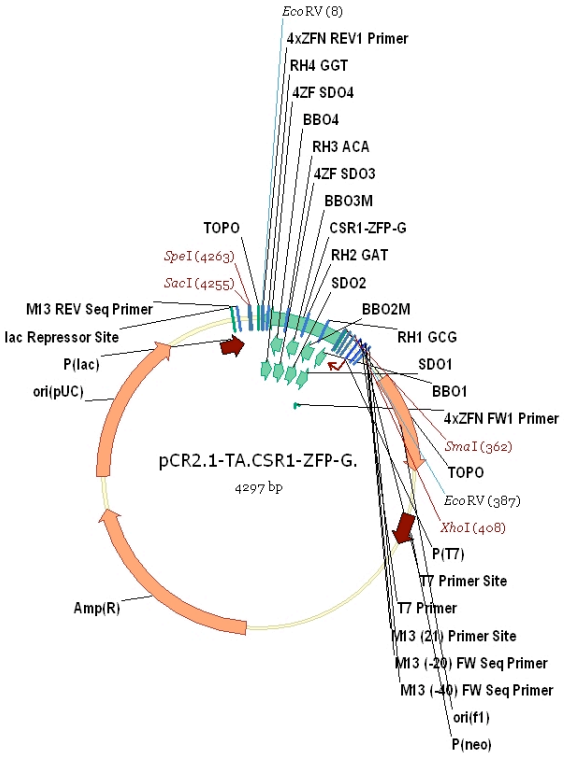

pCB302.AtSPO11-1.CSR1-ZF-F / ZF-G

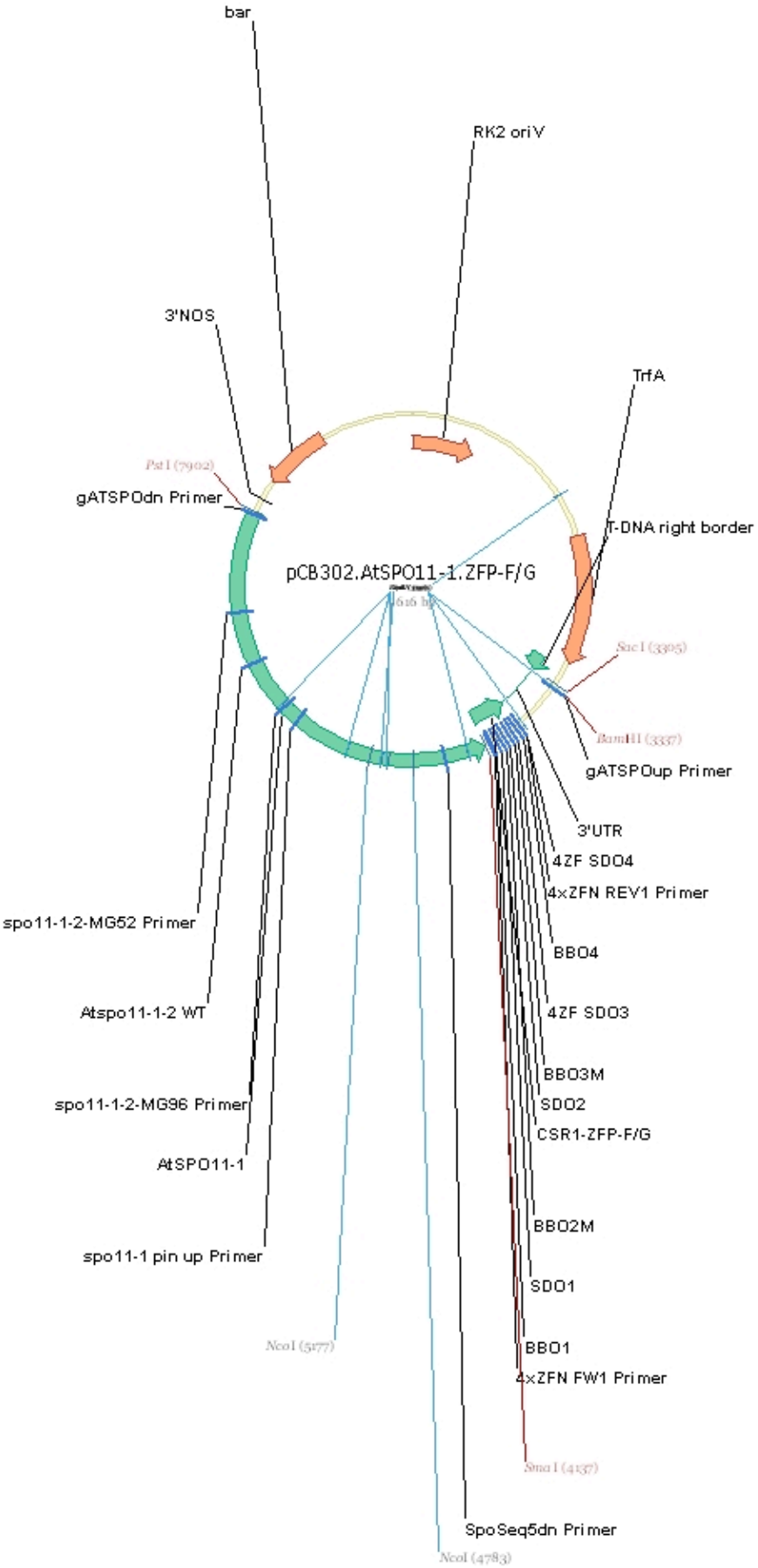

pCB302.AtSPO11-1.CSR1-ZF-F.18xMyc and pCB302.AtSPO11-1.CSR1-ZF-G.18xMyc

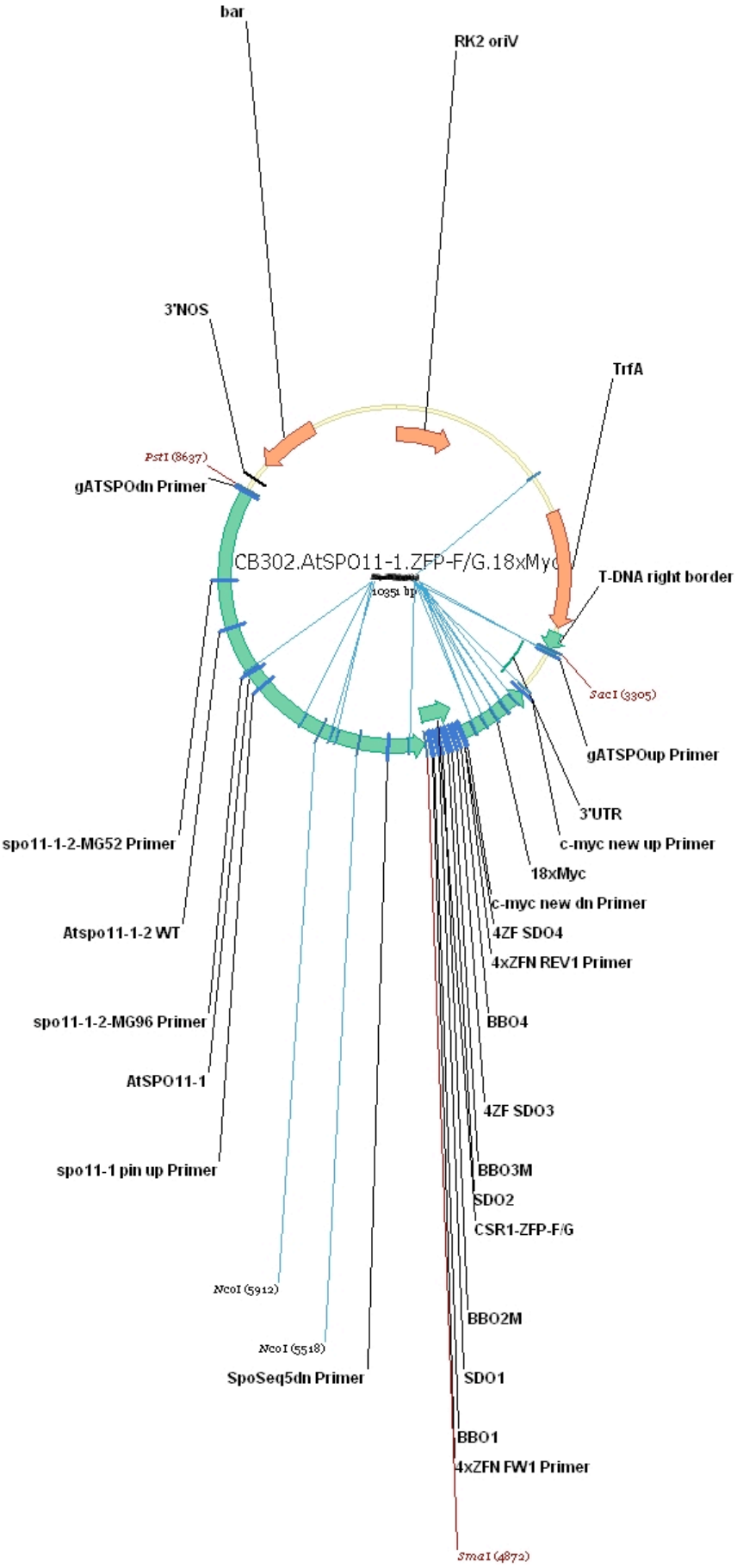

pCB302.AtSPO11-1.18xMyc.CSR1-ZF-F and pCB302.AtSPO11-1.18xMyc.CSR1-ZF-G

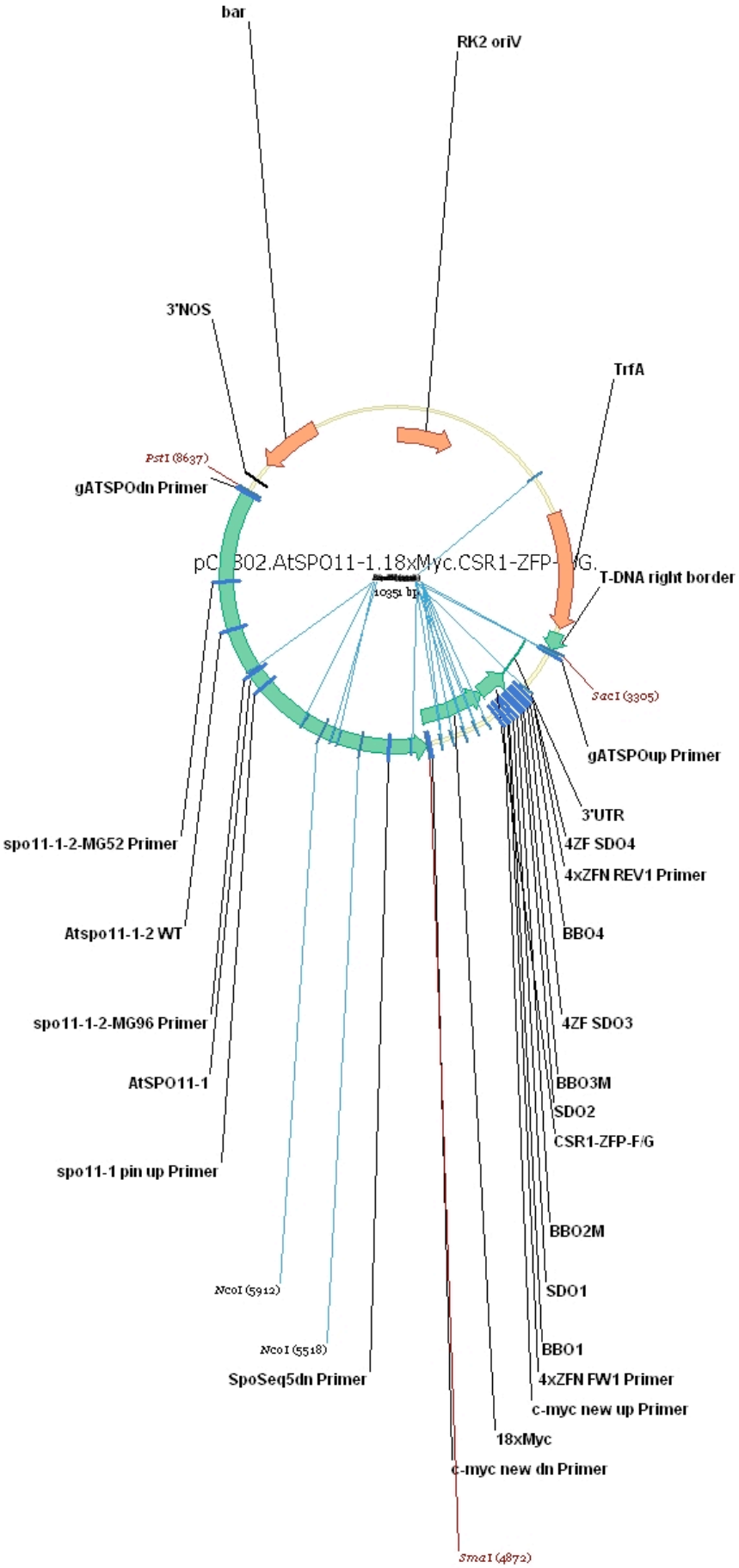

6.3. Sequence Information

Alignment of pCR2.1.CSR1-ZF-F (clone #MJ3B)

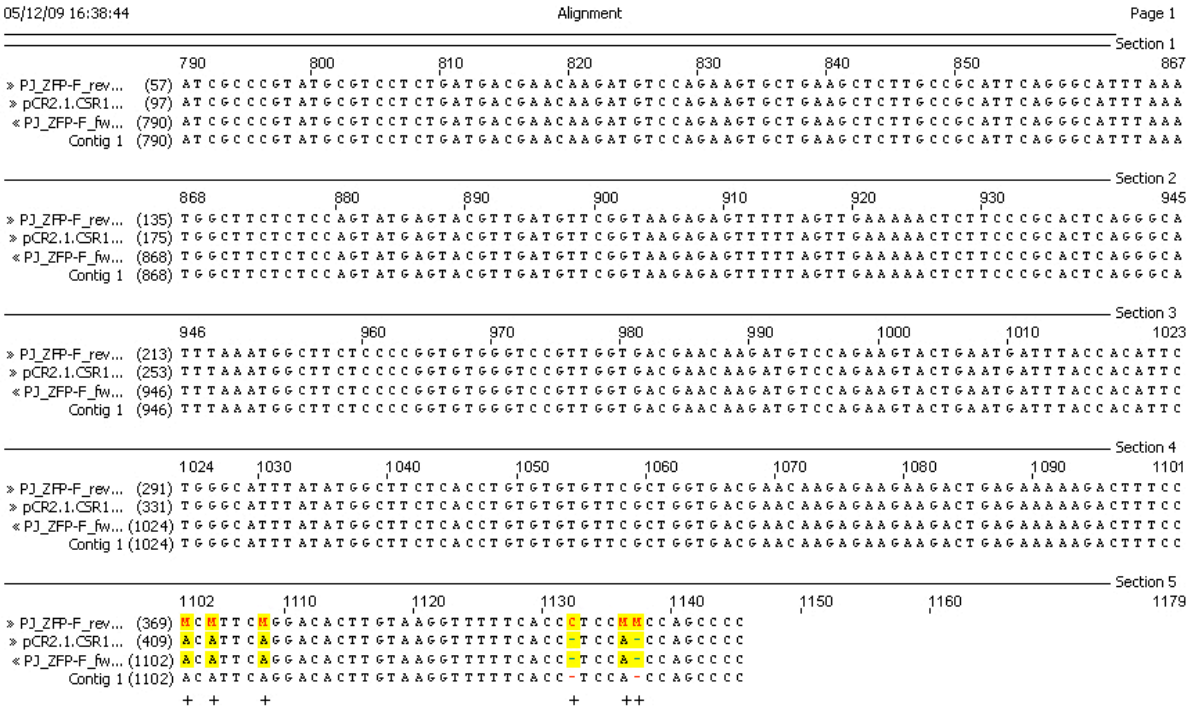

Alignment of pCR2.1.CSR1-ZF-G (clone #MJ5B)

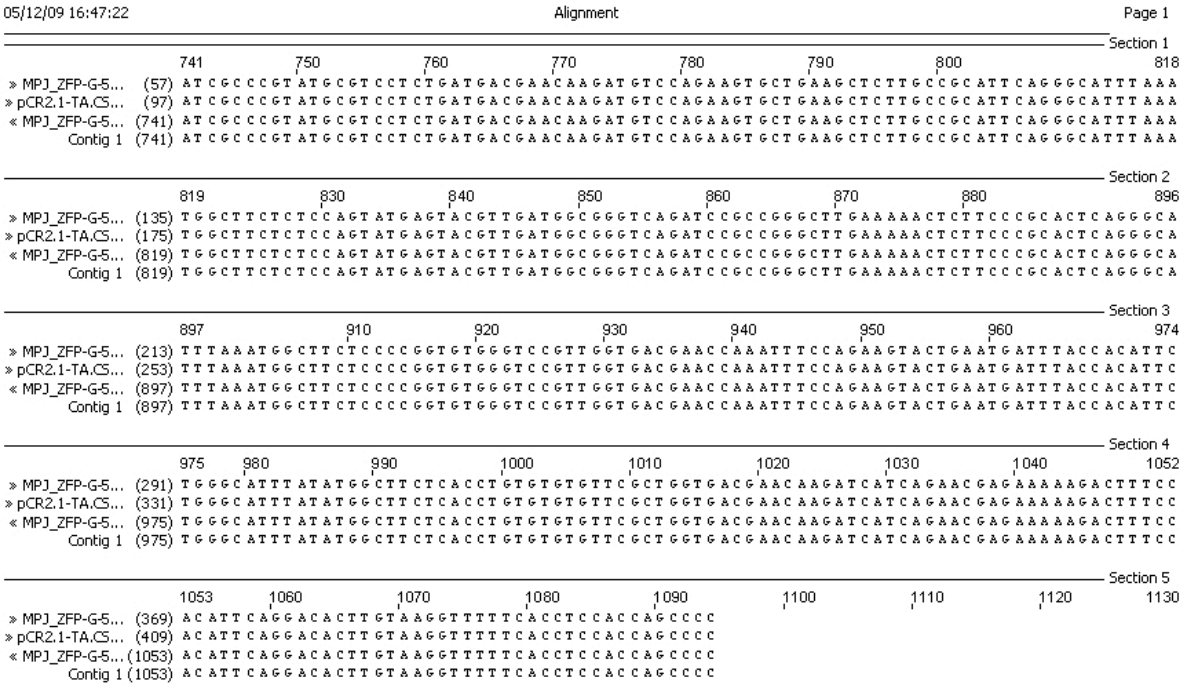

7. References

A. G. Initiative (2000). "Analysis of the genome sequence of the flowering plant Arabidopsis thaliana." Nature **408**(6814): 796-815.

Akutsu, N., K. Iijima et al. (2007). “Characterization of the plant homolog of Nijmegen breakage syndrome 1: Involvement in DNA repair and recombination.” Biochem Biophys Res Commun **353**(2): 394-8.

Alani, E., R. Padmore, et al. (1990). "Analysis of wild-type and rad50 mutants of yeast suggests an intimate relationship between meiotic chromosome synapsis and recombination." Cell **61**(3): 419-36.

Alberts, B., et al. (2002). “Molecular Biology of the Cell.” 4th edition. Garland Science.

Allers, T. and M. Lichten (2001). "Differential timing and control of noncrossover and crossover recombination during meiosis." Cell **106**(1): 47-57.

Alonso, J. M. and A. N. Stepanova (2003). "T-DNA mutagenesis in Arabidopsis." Methods Mol Biol **236**: 177-88.

Argueso, J. L., J. Wanat, et al. (2004). "Competing crossover pathways act during meiosis in Saccharomyces cerevisiae." Genetics **168**(4): 1805-16.

Armstrong, S. J., F. C. Franklin, et al. (2001). "Nucleolus-associated telomere clustering and pairing precede meiotic chromosome synapsis in Arabidopsis thaliana." J Cell Sci **114**(Pt 23): 4207-17.

Ayele, M., B. J. Haas, et al. (2005). "Whole genome shotgun sequencing of Brassica oleracea and its application to gene discovery and annotation in Arabidopsis." Genome Res **15**(4): 487-95.

Azumi, Y., D. Liu, et al. (2002). "Homolog interaction during meiotic prophase I in Arabidopsis requires the SOLO DANCERS gene encoding a novel cyclin-like protein." EMBO J **21**(12): 3081-95.

Baudat, F. and S. Keeney (2001). "Meiotic recombination: Making and breaking go hand in hand." Curr Biol **11**(2): R45-8.

Bechtold, N., J. Ellis, and G. Pelletier (1993). “*In-planta Agrobacterium* mediated gene transfer by infiltration of adult Arabidopsis thaliana plants.” C R Acad Sci Paris **316**: 1194-9.

Beerli, R. R., D. J. Segal, et al. (1998). “Toward controlling gene expression at will: specific regulation of the erbB-2/ HER-2 promoter by using polydactyl zinc finger proteins constructed from modular building blocks.” Proc Natl Acad Sci USA **95**(1998): 14628-33.

Bell, C. J. and J. R. Ecker (1994). "Assignment of 30 microsatellite loci to the linkage map of Arabidopsis." Genomics **19**(1): 137-44.

Bennett, C. B., A. L. Lewis, et al. (1993). "Lethality induced by a single site-specific double-strand break in a dispensable yeast plasmid." Proc Natl Acad Sci USA **90**(12): 5613-7.

Berchowitz, L. E., K. E. Francis, et al. (2007). "The role of AtMUS81 in interference-insensitive crossovers in A. thaliana." PLoS Genet **3**(8): e132.

Bergerat, A., B. de Massy, et al. (1997). "An atypical topoisomerase II from Archaea with implications for meiotic recombination." Nature **386**(6623): 414-7.

Bishop, D. K. and D. Zickler (2004). "Early decision; meiotic crossover interference prior to stable strand exchange and synapsis." Cell **117**(1): 9-15.

Bleuyard J. Y., M. E. Gallego, and C. I. White. (2004). “Meiotic defects in the Arabidopsis rad50 mutant point to conservation of the MRX complex function in early stages of meiotic recombination.” Chromosoma **113**: 197–203.

Bleuyard, J. Y. and C. I. White (2004). "The Arabidopsis homologue of Xrcc3 plays an essential role in meiosis." EMBO J **23**(2): 439-49.

Bleuyard, J. Y., M. E. Gallego, et al. (2005). "Differing requirements for the Arabidopsis Rad51 paralogs in meiosis and DNA repair." Plant J **41**(4): 533-45.

Boavida, L. C., J. D. Becker, et al. (2005). "The making of gametes in higher plants." Int J Dev Biol **49**(5-6): 595-614.

Borde, V., T. C. Wu, and M. Lichten. (1999). „Use of a recombination reporter insert to define meiotic recombination domains on chromosome III of Saccharomyces cerevisiae.“ Mol Cell Biol **19**(7):4832-42.

Borde, V., A. S. Goldman, et al. (2000). "Direct coupling between meiotic DNA replication and recombination initiation." Science **290**(5492): 806-9.

Borde, V. (2007). "The multiple roles of the Mre11 complex for meiotic recombination." Chromosome Res **15**(5): 551-63.

Borde, V., N. Robine, et al. (2009). "Histone H3 lysine 4 trimethylation marks meiotic recombination initiation sites." EMBO J **28**(2): 99-111.

Börner, G. V., N. Kleckner, et al. (2004). "Crossover/noncrossover differentiation, synaptonemal complex formation, and regulatory surveillance at the leptotene/zygotene transition of meiosis." Cell **117**(1): 29-45.

Bozza, C. G. and W. P. Pawlowski (2008). "The cytogenetics of homologous chromosome pairing in meiosis in plants." Cytogenet Genome Res **120**(3-4): 313-9.

Britt, A. B. and G. D. May (2003). "Re-engineering plant gene targeting." Trends Plant Sci **8**(2): 90-5.

Cai, X., F. Dong, et al. (2003). "The Arabidopsis SYN1 cohesin protein is required for sister chromatid arm cohesion and homologous chromosome pairing." J Cell Sci **116**(Pt 14): 2999-3007.

Carroll, D., J. J. Morton, et al. (2006). "Design, construction and in vitro testing of zinc finger nucleases." Nature protocols **1**(3): 1329-41.

Chang, C., J. L. Bowman, et al. (1988). "Restriction fragment length polymorphism linkage map for Arabidopsis thaliana." Proc Natl Acad Sci USA **85**(18): 6856-60.

Chelysheva, L., et al. (2005). AtREC8 and AtSCC3 are essential to the monopolar orientation of the kinetochores during meiosis. J. Cell Sci. 118, 4621-4632.

Chen, C., W. Zhang, et al. (2005). "The Arabidopsis ROCK-N-ROLLERS gene encodes a homolog of the yeast ATP-dependent DNA helicase MER3 and is required for normal meiotic crossover formation." Plant J **43**(3): 321-34.

Cheng, X., J. L. Boyer, and R. L. Juliano. (1997). "Selection of peptides that functionally replace a zinc finger in the Sp1 transcription factor by using a yeast combinatorial library." Proc Natl Acad Sci USA **94**: 14120-5.

Chilton, M.-D. and Q. Que (2003). "Targeted integration of T-DNA into the tobacco genome at double-stranded breaks: new insights on the mechanism of T-DNA integration." Plant Physiol **133**, 956-65.

Ciftci-Yilmaz, S. and R. Mittler (2008). "The zinc finger network of plants." Cell Mol Life Sci **65**(7-8): 1150-60.

Clough, S. J. and A. F. Bent (1998). "Floral dip: a simplified method for Agrobacterium-mediated transformation of Arabidopsis thaliana." Plant J **16**(6): 735-43.

Coelho, S. M., A. F. Peters, et al. (2007). "Complex life cycles of multicellular eukaryotes: new approaches based on the use of model organisms." Gene **406**(1-2): 152-70.

Copenhaver, G. P., E. A. Housworth, et al. (2002). "Crossover interference in Arabidopsis." Genetics **160**(4): 1631-9.

Couteau, F., F. Belzile, et al. (1999). "Random chromosome segregation without meiotic arrest in both male and female meiocytes of a dmc1 mutant of Arabidopsis." Plant Cell **11**(9): 1623-34.

Cromie, G. A., C. A. Rubio, et al. (2005). "A natural meiotic DNA break site in Schizosaccharomyces pombe is a hotspot of gene conversion, highly associated with crossing over." Genetics **169**(2): 595-605.

Cromie, G. A. and G. R. Smith (2007). "Branching out: meiotic recombination and its regulation." Trends Cell Biol **17**(9): 448-55.

D'Halluin, K., C. Vanderstraeten, et al. (2008). "Homologous recombination: a basis for targeted genome optimization in crop species such as maize." Plant Biotechnol J **6**(1): 93-102.

De Muyt A, D. Vezon et al. (2007). "AtPRD1 is required for meiotic double strand break formation in Arabidopsis thaliana." EMBO J **26**: 4126-37.

De Veylder, L., J. Joubès, et al. (2003). "Plant cell cycle transitions." Curr Opin Plant Biol **6**(6): 536-43.

de los Santos, T., N. Hunter, et al. (2003). "The Mus81/Mms4 endonuclease acts independently of double-Holliday junction resolution to promote a distinct subset of crossovers during meiosis in budding yeast." Genetics **164**(1): 81-94.

Daoudal-Cotterell et al. The plant Rad50-Mre11 protein complex. FEBS Lett (2002) vol. 516 (1-3) pp. 164-6.

Decordier, I., E. Cundari, et al. (2008). "Mitotic checkpoints and the maintenance of the chromosome karyotype." Mutat Res **651**(1-2): 3-13.

Diaz R. L., A. D. Alcid, et al. (2002). "Identification of residues in yeast Spo11p critical for meiotic DNA double-strand break formation." Mol Cell Biol **22**(4): 1106-15.

Dion, S., M. V. Demattéi, et al. (2007). "[Zinc finger proteins: tools for site-specific correction or modification of the genome]." Med Sci (Paris) **23**(10): 834-9.

Dong F., X. Cai and C. A. Makaroff (2001) "Cloning and characterization of two Arabidopsis genes that belong to the RAD21/REC8 family of chromosome cohesin proteins." Gene **271**(1): 99-108.

Drouaud, J., C. Camilleri, et al. (2006). „Variation in crossing-over rates across chromosome 4 of Arabidopsis thaliana reveals the presence of meiotic recombination "hot spots"." Genome Res **16**(1), 106-14.

Durai S., M. Mani, et al. (2005). "Zinc finger nucleases: custom-designed molecular scissors for genome engineering of plant and mammalian cells." Nucleic Acids Res **33**(18): 5978-90.

Durrant, W. E., S. Wang, et al. (2007). "Arabidopsis SNI1 and RAD51D regulate both gene transcription and DNA recombination during the defense response." Proc Natl Acad Sci USA **104**(10): 4223-7.

Elrod-Erickson, M., M. A. Rould, et al. (1996) "Zif268 protein-DNA complex refined at 1.6 A: a model system for understanding zinc finger-DNA interactions." Structure **4**(10): 1171-80.

Elrod-Erickson, M., T. E. Benson and C. O. Pabo (1998). "High-resolution structures of variant Zif268-DNA complexes: implications for understanding zinc finger-DNA recognition." Structure **6**(4), 451-64.

Englbrecht, C. C., H. Schoof and S. Bohm (2004). "Conservation, diversification and expansion of C2H2 zinc finger proteins in the Arabidopsis thaliana genome." BMC Genomics **5**(1): 39.

Evan, G. I., G. K. Lewis, et al. (1985). "Isolation of monoclonal antibodies specific for human c-myc proto-oncogene product." Mol Cell Biol **5**(12): 3610-6.

Feldmann, K. A. (1991). T-DNA insertion mutagenesis in Arabidopsis: mutational spectrum. Plant J. **1:** 71-82.

Forsburg, S. L. (2002). "Only connect: linking meiotic DNA replication to chromosome dynamics." Mol Cell **9**(4): 703-11.

Francis, D. (2007). "The plant cell cycle--15 years on." New Phytol **174**(2): 261-78.

Francis, K. E., S. Y. Lam, et al. (2007). "Pollen tetrad-based visual assay for meiotic recombination in Arabidopsis." Proc Natl Acad Sci USA **104**(10): 3913-8.

Franklin, A. E., J. McElver, et al. (1999). "Three-dimensional microscopy of the Rad51 recombination protein during meiotic prophase." Plant Cell **11**(5): 809-24.

Fu, F., J. D. Sander, et al. (2008). “Zinc Finger Database (ZiFDB): a repository for information on C2H2 zinc fingers and engineered zinc-finger arrays.” Nucleic Acids Res 37: D279-83.

Fukuda, T., S. Nogami, et al. (2003). "VDE-initiated intein homing in Saccharomyces cerevisiae proceeds in a meiotic recombination-like manner." Genes Cells **8**(7): 587-602.

Fukuda, T., Y. Ohya and K. Ohta (2007). “Conditional genomic rearrangement by designed meiotic recombination using VDE (PI-SceI) in yeast.” Mol Genet Genomics **278**(4):467–478.

Fukuda, T. K. Kugou, et al. (2008). “Targeted induction of meiotic double-strand breaks reveals chromosomal domain-dependent regulation of Spo11 and interactions among potential sites of meiotic recombination.” Nucleic Acids Res **36**(3): 984-97.

Fung, J. C., B. Rockmill, et al. (2004). "Imposition of crossover interference through the nonrandom distribution of synapsis initiation complexes." Cell **116**(6): 795-802.

Gepstein, S. and B. A. Horwitz (1995). "The impact of Arabidopsis research on plant biotechnology." Biotechnol Adv **13**(3): 403-14.

Gerton, J. L., J. DeRisi, et al. (2000). “Global mapping of meiotic recombination hotspots and coldspots in the yeast Saccharomyces cerevisiae”. Proc Natl Acad Sci USA **97**(21): 11383-90.

Gerton, J. L. and R. S. Hawley (2005). "Homologous chromosome interactions in meiosis: diversity amidst conservation." Nat Rev Genet **6**(6): 477-87.

Grelon, M., D. Vezon, et al. (2001). "AtSPO11-1 is necessary for efficient meiotic recombination in plants." EMBO J **20**(3): 589-600.

Greisman, H. A. and C. O. Pabo (1997). “A general strategy for selecting high-affinity zinc finger proteins for diverse DNA target sites.” Science **275**(5300): 657-61.

Gutiérrez, R. A., G. C. MacIntosh, et al. (1999). "Current perspectives on mRNA stability in plants: multiple levels and mechanisms of control." Trends Plant Sci **4**(11): 429-438.

Haber, J. E., G. Ira, et al. (2004). "Repairing a double-strand chromosome break by homologous recombination: revisiting Robin Holliday's model." Philos Trans R Soc Lond, B, Biol Sci **359**(1441): 79-86.

Hamant, O., H. Ma, et al. (2006). "Genetics of meiotic prophase I in plants." Annu Rev Plant Biol **57**: 267-302.

Hanin, M. and J. Paszkowski (2003). “Plant genome modification by homologous recombination.” Curr Opin Plant Biol **6**(2): 157-62.

Hartung, F. and H. Puchta (2000). "Molecular characterisation of two paralogous SPO11 homologues in Arabidopsis thaliana." Nucleic Acids Res **28**(7): 1548-54.

Hartung, F. and H. Puchta (2001). "Molecular characterization of homologues of both subunits A (SPO11) and B of the archaebacterial topoisomerase 6 in plants." Gene **271**(1): 81-6.

Hartung, F., S. Suer, et al. (2006). “The role of AtMUS81 in DNA repair and its genetic interaction with the helicase AtRecQ4A.” Nucleic Acids Res **34**(16): 4438-48.

Hartung, F., R. Wurz-Wildersinn, et al. (2007). "The catalytically active tyrosine residues of both SPO11-1 and SPO11-2 are required for meiotic double-strand break induction in Arabidopsis." Plant Cell **19**(10): 3090-9.

Hauf, S., E. Roitinger, et al. (2005). "Dissociation of cohesin from chromosome arms and loss of arm cohesion during early mitosis depends on phosphorylation of SA2." PLoS Biol **3**(3): e69.

Hauge, B. M., S. M. Hanley, et al. (1993). "An integrated genetic/RFLP map of the Arabidopsis thaliana genome." The Plant Journal.

Haughn, G. W., J. Smith, et al. (1988). "Transformation with a mutant Arabidopsis acetolactate synthase gene renders tobacco resistant to …." Molecular and General Genetics MGG.

Haughn, G. W. and C. R. Somerville (1990). "A Mutation Causing Imidazolinone Resistance Maps to the Csr1 Locus of Arabidopsis thaliana." Plant Physiol **92**(4): 1081-1085.

Hays, J. B. (2002). "Arabidopsis thaliana, a versatile model system for study of eukaryotic genome-maintenance functions." DNA Repair (Amst) **1**(8): 579-600.

Higgins, J. D., S. J. Armstrong, et al. (2004). "The Arabidopsis MutS homolog AtMSH4 functions at an early step in recombination: evidence for two classes of recombination in Arabidopsis." Genes Dev **18**(20): 2557-70.

Higgins, J. D., E. Sanchez-Moran, et al. (2005). “The Arabidopsis synaptonemal complex protein ZYP1 is required for chromosome synapsis and normal fidelity of crossing over.” Genes Dev **19**(20): 2488-500.

Hirano, T. (2006). "At the heart of the chromosome: SMC proteins in action." Nat Rev Mol Cell Biol **7**(5): 311-22.

Hughes, M. D., Z. R. Zhang, et al. (2005). “Discovery of active proteins directly from combinatorial randomized protein libraries without display, purification or sequencing: identification of novel zinc finger proteins.” Nucleic Acids Res **33**(3): e32.

Hunter, N. and N. Kleckner (2001). "The single-end invasion: an asymmetric intermediate at the double-strand break to double-holliday junction transition of meiotic recombination." Cell **106**(1): 59-70.

Hurt, J. A., S. A. Thibodeau, et al. (2003). “Highly specific zinc finger proteins obtained by directed domain shuffling and cell-based selection.” Proc Nat Acad Sci USA **100**(21): 12271-6.

Hruz T., O. Laule, et al. (2008). “Genevestigator V3: A Reference Expression Database for the Meta-Analysis of Transcriptomes.” Adv Bioinformatics DOI: 10.1155/2008/420747.

Isalan, M. D., Y. Choo and A. Klug (1997). “Synergy between adjacent zinc fingers in sequence-specific DNA recognition.” Proc Natl Acad Sci USA **94**(11): 5617-21.

Isalan, M., A. Klug, et al. (1998). "Comprehensive DNA recognition through concerted interactions from adjacent zinc fingers." Biochemistry **37**(35): 12026-33.

Isalan, M., A. Klug, et al. (2001). "A rapid, generally applicable method to engineer zinc fingers illustrated by targeting the HIV-1 promoter." Nat Biotechnol **19**(7): 656-60.

Ishiguro, K. and Y. Watanabe (2007). "Chromosome cohesion in mitosis and meiosis." J Cell Sci **120**(Pt 3): 367-9.

Ivanov, D. and K. Nasmyth (2005). "A topological interaction between cohesin rings and a circular minichromosome." Cell **122**(6): 849-60.

Iyer, V. and K. Struhl (1995). “Poly(dA:dT), a ubiquitous promoter element that stimulates transcription via its intrinsic DNA structure.” EMBO J **14**(11): 2570-9.

Jarvis, P., C. Lister, et al. (1994). Integration of CAPS markers into the RFLP map generated using recombinant inbred lines of Arabidopsis thaliana. Plant Mol Biol. **24:** 685-687.

Jolivet, S., D. Vezon, et al. (2006). “Non conservation of the meiotic function of the Ski8/Rec103 homolog in Arabidopsis.” Genes Cells **11**(6): 615–22.

Joung, J. K., E. I. Ramm and C. O. Pabo (2000). „A bacterial two-hybrid selection system for studying protein–DNA and protein–protein interactions“. Proc Natl Acad Sci USA **97**(13), 7382-87.

Keeney, S. and N. Kleckner (1995). "Covalent protein-DNA complexes at the 5' strand termini of meiosis-specific double-strand breaks in yeast." Proc Natl Acad Sci USA **92**(24): 11274-8.

Keeney, S., C. N. Giroux, et al. (1997). "Meiosis-specific DNA double-strand breaks are catalyzed by Spo11, a member of a widely conserved protein family." Cell **88**(3): 375-84.

Keeney, S. (2001). „Mechanism and control of meiotic recombination initiation.“ Curr Top Dev Biol **52**: 1-53.

Kim, Y. G., J. Cha and S. Chandrasegaran (1996). „Hybrid restriction enzymes: zinc finger fusions to FokI cleavage domain.“ Proc Natl Acad Sci USA **93**(3): 1156-60.

Kim, S., V. Plagnol, et al. (2007). "Recombination and linkage disequilibrium in Arabidopsis thaliana." Nat Genet **39**(9): 1151-5.

Kirkpatrick, D. T., Y. H. Wang, et al. (1999). „Control of meiotic recombination and gene expression in yeast by a simple repetitive DNA sequence that excudes nucleosomes.“ Mol Cell Biol **19**(11): 7661-71.

Kleckner, N. (2006). "Chiasma formation: chromatin/axis interplay and the role(s) of the synaptonemal complex." Chromosoma **115**(3): 175-94.

Klekowski, E. J. Jr. (1997). „Somatic mutation theory of clonality.“ The Ecology and Evolution of Clonal Plants.

Klug, A. and J. W. Schwabe (1995). „Protein motifs 5. Zinc fingers.“ FASEB J **9**(8): 597-604.

Koncz, C., R. Mayerhofer, et al. (1990). "Isolation of a gene encoding a novel chloroplast protein by T-DNA tagging in Arabidopsis thaliana." EMBO J **9**(5): 1337-46.

Koncz, C., N. H. Chua and J. Schell (1992). "Methods in Arabidopsis Research.“ World Scientific, Singapore: ISBN 9810209045, 9789810209049.

Koornneef, M., L. W. Dellaert, et al. (1982). "EMS- and radiation-induced mutation frequencies at individual loci in Arabidopsis thaliana (L.) Heynh." Mutat Res **93**(1): 109-23.

Koornneef, M., J. vanEden, et al. (1983). Linkage map of Arabidopsis thaliana. J Hered. **74:** 265-272.

Koornneef, M., P. Fransz, et al. (2003). "Cytogenetic tools for Arabidopsis thaliana." Chromosome Res **11**(3): 183-94.

Krsicka, O. (2007). „Generation of molecular tools for the analysis of meiotic recombination in *Arabidopsis thaliana*.“ Diploma Thesis, University of Vienna, Austria: 1-75.

Kuromori, T., Hirayama, T., Kiyosue, Y., Takabe, H., Mizukado, S., Sakurai, T., Akiyama, K., Kamiya, A., Ito, T. and Shinozaki, K. (2004) A collection of 11,800 single-copy Ds transposon insertion lines in Arabidopsis. Plant J. 37(6), 897–905.

Laity, J. H., B. M. Lee and P. E. Wright (2001). „Zinc finger proteins : New insights into structural and functional diversity.“ Curr Opin Struct Biol **11**(1): 39-46.

Lee, M. S., G. P. Gippert, et al. (1989). „Three-dimensional solution structure of a single zinc finger DNA-binding domain.“ Science **245**(4918):635–637.

Lee, J. Y. and T. L. Orr-Weaver (2001). "The molecular basis of sister-chromatid cohesion." Annu Rev Cell Dev Biol **17**: 753-77.

Li, W., C. Chen, et al. (2004). "The Arabidopsis AtRAD51 gene is dispensable for vegetative development but required for meiosis." Proc Natl Acad Sci USA **101**(29): 10596-601.

Lim, G. A., E. G. Jewell, et al. (2007). "A comparative map viewer integrating genetic maps for Brassica and Arabidopsis." BMC Plant Biol **7**: 40.

Lloyd, A., C. L. Plaisier, et al. (2005). "Targeted mutagenesis using zinc-finger nucleases in Arabidopsis." Proc Natl Acad Sci USA **102**(6): 2232-7.

Lynn, A., R. Soucek, et al. (2007). "ZMM proteins during meiosis: crossover artists at work." Chromosome Res **15**(5): 591-605.

Ma, H. (2006). "A Molecular Portrait of Arabidopsis Meiosis." The Arabidopsis Book: 1-39.

Mackay, J. P. and M. Crossley (1998). „Zinc fingers are sticking together.“ Trends Biochem Sci **23**(1): 1-4.

Maeder, M. L., S. Thibodeau-Beganny, et al. (2008). “Rapid "open-source" engineering of customized zinc-finger nucleases for highly efficient gene modification.” Mol Cell **31**(2): 294-301.

Maloisel, L., J. Bhargava, et al. (2004). "A role for DNA polymerase delta in gene conversion and crossing over during meiosis in Saccharomyces cerevisiae." Genetics **167**(3): 1133-42.

Mandell, J. G. and C. F. Barbas (2006) “Zinc Finger Tools: custom DNA-binding domains for transcription factors and nucleases.” Nucleic Acids Res **34**(Web Server issue): W516-23.

Mani, M., K. Kandavelou, et al. (2005). "Design, engineering, and characterization of zinc finger nucleases." Biochem Biophys Res Commun **335**(2): 447-57.

Marthur, J. and C. Koncz (1998). „Establishment and maintainance of cell suspensions.“ Methods in Molecular Biology **82:** 27-30.

Mazina, O. M., A. V. Mazin, et al. (2004). "Saccharomyces cerevisiae Mer3 helicase stimulates 3'-5' heteroduplex extension by Rad51; implications for crossover control in meiotic recombination." Cell **117**(1): 47-56.

McMahill, M. S., C. W. Sham, et al. (2007). "Synthesis-dependent strand annealing in meiosis." PLoS Biol **5**(11): e299.

Meinke, D. W., J. M. Cherry, et al. (1998). "Arabidopsis thaliana: a model plant for genome analysis." Science **282**(5389): 662, 679-82.

Melamed-Bessudo, C., E. Yehuda, et al. (2005). "A new seed-based assay for meiotic recombination in Arabidopsis thaliana." Plant J **43**(3): 458-66.

Mercier, R., S. J. Armstrong, et al. (2003). "The meiotic protein SWI1 is required for axial element formation and recombination initiation in Arabidopsis." Development **130**(14): 3309-18.

Mercier, R., S. Jolivet, et al. (2005). "Two meiotic crossover classes cohabit in Arabidopsis: one is dependent on MER3,whereas the other one is not." Curr Biol **15**(8): 692-701.

Mercier, R. and M. Grelon (2008). "Meiosis in plants: ten years of gene discovery." Cytogenet Genome Res **120**(3-4): 281-90.

Meyerowitz, E. M. (1989). "Arabidopsis, a useful weed." Cell **56**(2): 263-9.

Mézard, C. (2006). "Meiotic recombination hotspots in plants." Biochem Soc Trans **34**(Pt 4): 531-4.

Miller, J., A. D. McLachlan, and A. Klug. 1985. Repetitive zinc-binding domains in the protein transcription factor IIIA from Xenopus oocytes. EMBO J. 4(6):1609–1614.

Mimitou, E. P. and L. S. Symington (2008). "Sae2, Exo1 and Sgs1 collaborate in DNA double-strand break processing." Nature **455**(7214): 770-4.

Mourad, G., G. W. Haughn, et al. (1994). "Intragenic recombination in the CSR1 locus of Arabidopsis." Mol Gen Genet **243**(2): 178-84.

Musacchio, A. and K. G. Hardwick (2002). "The spindle checkpoint: structural insights into dynamic signalling." Nat Rev Mol Cell Biol **3**(10): 731-41.

Muyt, A. D., R. Mercier, et al. (2009). "Meiotic recombination and crossovers in plants." Genome dynamics **5**: 14-25.

Nasmyth, K. (1999). "Separating sister chromatids." Trends Biochem Sci **24**(3): 98-104.

Nasmyth, K. and C. H. Haering (2005). "The structure and function of SMC and kleisin complexes." Annu Rev Biochem **74**: 595-648.

Neale, M. J., M. Ramachandran, et al. (2002). "Wild-type levels of Spo11-induced DSBs are required for normal single-strand resection during meiosis." Mol Cell **9**(4): 835-46.

Neale, M. J., J. Pan, et al. (2005). "Endonucleolytic processing of covalent protein-linked DNA double-strand breaks." Nature **436**(7053): 1053-7.

Neuteboom, L. W., B. I. Lindhout, et al. (2006). "Effects of different zinc finger transcription factors on genomic targets." Biochem Biophys Res Commun **339**(1): 263-70.

Nishant, K. T. and M. R. Rao (2006). "Molecular features of meiotic recombination hot spots." Bioessays **28**(1): 45-56.

Oh, S. D., J. P. Lao, et al. (2007). "BLM ortholog, Sgs1, prevents aberrant crossing-over by suppressing formation of multichromatid joint molecules." Cell **130**(2): 259-72.

Orr-Weaver, T. L. (1999). "The ties that bind: localization of the sister-chromatid cohesin complex on yeast chromosomes." Cell **99**(1): 1-4.

Ow, D. W. (2007). „GM maize from site-specific recombination technology, what next?“ Curr Opin Biotechnol **18**(2): 115-20.

Pabo, C. O., E. Peisach, et al. (2001). "Design and selection of novel Cys2His2 zinc finger proteins." Annu Rev Biochem **70**: 313-40.

Papworth, M., P. Kolasinska and M. Minczuk (2006). "Designer zinc-finger proteins and their applications". Gene **366**(1): 27-38.

Pavletich, N. P. and C. O. Pabo (1991). "Zinc finger-DNA recognition: crystal structure of a Zif268-DNA complex at 2.1 A." Science **252**(5007): 809-17.

Peciña, A., K. N. Smith, et al. (2002). "Targeted stimulation of meiotic recombination." Cell **111**(2): 173-84.

Pelham, H. R. and D. D. Brown (1980). "A specific transcription factor that can bind either the 5S RNA gene or 5S RNA." Proc Natl Acad Sci USA **77**(7): 4170-4.

Petes, T. D. (2001). "Meiotic recombination hot spots and cold spots." Nat Rev Genet **2**(5): 360-9.

Petronczki, M., J. Matos, et al. (2006). "Monopolar attachment of sister kinetochores at meiosis I requires casein kinase 1." Cell **126**(6): 1049-64.

Picard, B. and M. Wegnez (1979). "Isolation of a 7S particle from Xenopus laevis oocytes : A 5S RNA-protein complex." Proc Natl Acad Sci USA **76**(1), 241-5.

Prieler, S., A. Penkner, et al. (2005). "The control of Spo11's interaction with meiotic recombination hotspots." Genes Dev **19**(2): 255-69.

Prieto, I., J. A. Suja, et al. (2001). "Mammalian STAG3 is a cohesin specific to sister chromatid arms in meiosis I." Nat Cell Biol **3**(8): 761-6.

Pruitt, R. E. and E. M. Meyerowitz (1986). "Characterization of the genome of Arabidopsis thaliana." J Mol Biol **187**(2): 169-83.

Puchta, H., B. Dujon, et al. (1993). "Homologous recombination in plant cells is enhanced by in vivo induction of double strand breaks into DNA by a site-specific endonuclease." Nucleic Acids Res **21**(22): 5034-40.

Puchta, H., B. Dujon, et al. (1996). "Two different but related mechanisms are used in plants for the repair of genomic double-strand breaks by homologous recombination." Proc Natl Acad Sci USA **93**(10): 5055-60.

Puchta, H. (2002). "Gene replacement by homologous recombination in plants." Plant Mol Biol **48**(1-2): 173-82.

Puchta, H. (2005). "The repair of double-strand breaks in plants: mechanisms and consequences for genome evolution." J Exp Bot **56**(409): 1–14.

Puizina, J., J. Siroky, et al. (2004). "Mre11 deficiency in Arabidopsis is associated with chromosomal instability in somatic cells and Spo11-dependent genome fragmentation during meiosis." Plant Cell **16**(8): 1968-78.

Ramirez, C. L., J. E. Foley, et al. (2008). "Unexpected failure rates for modular assembly of engineered zinc fingers." Nat Methods **5**(5): 374-5.

Ray, A. and M. Langer (2002). "Homologous recombination: ends as the means." Trends Plant Sci **7**(10): 435-40.

Rédei, G. P. (1992). Methods in Arabidopsis Research: 1–15.

Reiss, B., I. Schubert, et al. (2000). "RecA stimulates sister chromatid exchange and the fidelity of double-strand break repair, but not gene targeting, in plants transformed by Agrobacterium." Proc Natl Acad Sci USA **97**(7): 3358-63.

Reiss, B. (2003). "Homologous recombination and gene targeting in plant cells." Int Rev Cytol **228**: 85-139.

Revenkova, E., M. Eijpe, et al. (2001). "Novel meiosis-specific isoform of mammalian SMC1." Mol Cell Biol **21**(20): 6984-98.

Rhee, S. Y., W. Beavis, et al. (2003). "The Arabidopsis Information Resource (TAIR): a model organism database providing a centralized, curated gateway to Arabidopsis biology, research materials and community." Nucleic Acids Res **31**(1): 224-8.

Rivera, T. and A. Losada (2006). "Shugoshin and PP2A, shared duties at the centromere." Bioessays **28**(8): 775-9.

Robert, L. S., F. Robson, et al. (1998). "Conserved structure and function of the Arabidopsis flowering time gene CONSTANS in Brassica napus." Plant Mol Biol **37**(5): 763-72.

Robine, N., N. Uematsu et al. (2007). "Genome-wide redistribution of meiotic double-strand breaks in Saccharomyces cerevisiae." Mol Cell Biol **27**(5): 1868-80.

Roeder, G. S. (1990). "Chromosome synapsis and genetic recombination: their roles in meiotic chromosome segregation." Trends Genet **6**(12): 385-9.

Roeder, G.S. (1997). "Meiotic chromosomes: it takes two to tango." Genes Dev **11**(20): 2600-21.

Ross, K. J., P. Fransz, et al. (1996). "A light microscopic atlas of meiosis in Arabidopsis thaliana." Chromosome Res **4**(7): 507-16.

Rosso, M. G., Y. Li, et al. (2003). " An Arabidopsis thaliana T-DNA mutagenized population (GABI-Kat) for flanking sequence tag-based reverse genetics." Plant Mol Biol **53**(1-2): 247-259.

Sakamoto, H., K. Maruyama, et al. (2004). " Arabidopsis Cys2/His2-type zinc-finger proteins function as transcription repressors under drought, cold, and high-salinity stress conditions." Plant Physiol **136**(1): 2734-46.

Salinas, J. and J. J. Sánchez-Serrano (2006). "Arabidopsis Protocols." p.60.

Sambrook, J., E. F. Fritsch and T. Maniatis (1989). "Molecular Cloning: A Laboratory Manual." 2nd edition: 1-1669. ISBN 0-87969-309-6

Sanchez-Moran, E., J. L. Santos, et al. (2007). "ASY1 mediates AtDMC1-dependent interhomolog recombination during meiosis in Arabidopsis." Genes Dev **21**(17): 2220-33.

Sasanuma, H., H. Murakami, et al. (2007). "Meiotic association between Spo11 regulated by Rec102, Rec104 and Rec114." Nucleic Acids Res **35**(4): 1119-33.

Sathasivan, K., G. W. Haughn, et al. (1991). "Molecular Basis of Imidazolinone Herbicide Resistance in Arabidopsis thaliana var Columbia." Plant Physiol **97**(3): 1044-1050.

Schwacha, A. and N. Kleckner (1997). "Interhomolog bias during meiotic recombination: meiotic functions promote a highly differentiated interhomolog-only pathway." Cell **90**(6): 1123-35.

Segal, D. J., B. Dreier, et al. (1999). " Toward controlling gene expression at will: selection and design of zinc finger domains recognizing each of the 5′-GNN-3′ DNA target sequences." Proc Natl Acad Sci USA **96**(6): 2758-63.

Segal, D. J., and C. F. Barbas III (2000). "Design of novel sequence-specific DNA-binding proteins." Curr Opin Chem Biol **4**(1): 34-9.

Sessions, A., E. Burke, et al. (2002). "A high-throughput Arabidopsis reverse genetics system. Plant Cell **14**(12): 2985-94.

Shaked, H., C. Melamed-Bessudo, et al. (2005). "High-frequency gene targeting in Arabidopsis plants expressing the yeast RAD54 gene." Proc Natl Acad Sci USA **102**(34): 12265-9.

Shinohara, A. and M. Shinohara (2004). "Roles of RecA homologues Rad51 and Dmc1 during meiotic recombination." Cytogenet Genome Res **107**(3-4): 201-7.

Siaud, N., E. Dray, et al. (2004). "Brca2 is involved in meiosis in Arabidopsis thaliana as suggested by its interaction with Dmc1." EMBO J **23**(6): 1392-401.

Singer, T., Y. Fan, et al. (2006). "A high-resolution map of Arabidopsis recombinant inbred lines by whole-genome exon array hybridization." PLoS Genet **2**(9): e144.

Smith, G. P. (1985). "Filamentous fusion phage: novel expression vectors that display cloned antigens on the virion surface." Science **228**(4705): 1315-17.

Snowden, T., S. Acharya, et al. (2004). "hMSH4-hMSH5 recognizes Holliday Junctions and forms a meiosis-specific sliding clamp that embraces homologous chromosomes." Mol Cell **15**(3): 437-51.

Somerville, C. and M. Koornneef (2002). "A fortunate choice: the history of Arabidopsis as a model plant." Nat Rev Genet **3**(11): 883-9.

Srivastava, V. and D. W. Ow (2004). "Marker-free site-specific gene integration in plants." Trends Biotechnol **22**(12): 627-9.

Stacey, N. J., T. Kuromori, et al. (2006). "Arabidopsis SPO11-2 functions with SPO11-1 in meiotic recombination." Plant J **48**(2): 206-16.

Sullivan, M. and D. O. Morgan (2007). "Finishing mitosis, one step at a time." Nat Rev Mol Cell Biol **8**(11): 894-903.

Szostak, J. W., T. L. Orr-Weaver, et al. (1983). "The double-strand-break repair model for recombination." Cell **33**(1): 25-35.

Takatsuji, H. (1999). "Zinc-finger proteins : The classical zinc finger emerges in contemporary plant science." Plant Mol Biol **39**(6): 1073-78.

Terada, R., H. Urawa, et al. (2002). "Efficient gene targeting by homologous recombination in rice." Nat Biotechnol **20**(10): 1030-4.

Terada, R., Y. Johzuka-Hisatomi, et al. (2007). "Gene targeting by homologous recombination as a biotechnological tool for rice functional genomics." Plant Physiol **144**(2): 846-56.

Tovkach, A., V. Zeevi and T. Tzfira (2009). "A toolbox and procedural notes for characterizing novel zinc finger nucleases for genome editing in plant cells." Plant J **57**(4): 747-57.

Tzfira, T., J. Li, et al. (2004). "Agrobacterium T-DNA integration: molecules and models." Trends Genet **20**(8): 375-83.

Tzfira, T., G. W. Tian, et al. (2005). "pSAT vectors: a modular series of plasmids for autofluorescent protein tagging and expression of multiple genes in plants." Plant Mol Biol **57**(4): 503-16.

Tzfira, T. and C. White (2005). "Towards targeted mutagenesis and gene replacement in plants." Trends Biotechnol **23**(12): 567-9.

Uanschou, C., T. Siwiec, et al. (2007). "A novel plant gene essential for meiosis is related to the human CtIP and the yeast COM1/SAE2 gene." EMBO J **26**(24): 5061-70.

Uhlmann, F. and K. Nasmyth (1998). "Cohesion between sister chromatids must be established during DNA replication." Curr Biol **8**(20): 1095-101.

Urnov, F.D., J. C. Miller, et al. (2005). "Highly efficient endogenous human gene correction using designed zinc-finger nucleases." Nature **435**(7042): 646-51.

Watanabe, Y. (2004). "Modifying sister chromatid cohesion for meiosis." J Cell Sci **117**(Pt 18): 4017-23.

Watanabe, Y. (2005). "Shugoshin: guardian spirit at the centromere." Curr Opin Cell Biol **17**(6): 590-5.

Waterworth, W. M., C. Altun, et al. (2007). "NBS1 is involved in DNA repair and plays a synergistic role with ATM in mediating meiotic homologous recombination in plants." Plant J **52**(1): 41-52.

Whitby, M. C. (2005). "Making crossovers during meiosis." Biochem Soc Trans **33**(Pt 6): 1451-5.

Wolfe, S. A., L. Nekludova, et al. (2000). "DNA recognition by Cys2His2 zinc finger proteins." Annual review of biophysics and biomolecular structure **29**: 183-212.

Wright, D. A., J. A. Townsend, et al. (2005). "High-frequency homologous recombination in plants mediated by zinc-finger nucleases." Plant J **44**(4): 693-705.

Wright, D. A., S. Thibodeau-Beganny, et al. (2006). "Standardized reagents and protocols for engineering zinc finger nucleases by modular assembly." Nature protocols **1**(3): 1637-52.

Wu, J., K. Kandavelou, et al. (2007). "Custom-designed zinc finger nucleases: what is next?" Cell Mol Life Sci **64**(22): 2933-44.

Xiang, C., P. Han, et al. (1999). "A mini binary vector series for plant transformation." Plant Mol Biol **40**(4): 711-7.

Yamagishi, Y., T. Sakuno, et al. (2008). "Heterochromatin links to centromeric protection by recruiting shugoshin." Nature **455**(7210): 251-5.

Yin, Y., H. Cheong, et al. (2002). "A crucial role for the putative Arabidopsis topoisomerase VI in plant growth and development." Proc Natl Acad Sci USA **99**(15): 10191-6.

Zickler, D. and N. Kleckner (1999). "Meiotic chromosomes: integrating structure and function." Annu Rev Genet **33**: 603-754.

8. Abbreviations

18xMyc	18x *c-Myc* Epitope
AA	Amino Acid
AE	SC Axial Element
AGI	the Arabidopsis Genome Initiative
ALS	Acetolactate Synthase
APC/C	Anaphase Promoting Complex /Cyclosome
bp	Base Pairs
CAPS	Cleaved Amplified PolymorphicSequence (Marker)
CDK	Cyclin-Dependent Kinase
CDS	Coding Sequence
CE	SC Central Element
ChIP	Chromatin-Immunoprecipitation
cM	centi-Morgan
CO	Crossover
Col-0	*A.thaliana* ecotype Columbia
CSC	Cell Suspension Culture
DAPI	4',6-Diamidino-2'-Phenylindole
dHJ	Double Holliday Junction
D-Loop	Displacenment-Loop
DSB	DNA Double-Strand Break
DSBR	Double Stranded Break Repair (Model)
EMS	Ethylmethanesulfonate
FTL	Fluorescence-tagged Lines
FRT	FLP Recombinase Target
G1	Gap Phase 1
G2	Gap Phase 2
gDNA	Genomic DNA
GUS	β-Glucuronidase
HJ	Holliday Junction
HR	Homologous Recombination
IP	Immunoprecipitation
Kb	Kilo Base Pairs
LE	Synaptonemal Complex Lateral Element
M	Mitotic / Meiotic Phase
Mb	Mega Base Pairs
MCC	Mitotic Checkpoint Complex

MCS	Multiple Cloning Site/Polylinker
MRN	MRE11-RAD50-NBS1 Complex
MRX	Mre11-Rad50-Xrs2 Complex
NCO	Non-Crossover
NHEJ	non-Homologous End Joining
ONC	Over-Night Culture
ORF	Open Reading Frame
PAGE	Polyacrylamide Gel Electrophoresis
PCR	Polymerase Chain Reaction
PLK	Polo-Like Kinase
poly(A) site	Polyadenylation Site
PZF	Polydactyl Zinc-Finger
RACE	Rapid Amplification of cDNA End
RE	Restriction Endonuclease
RFLP	Restriction Fragment Length Polymorphism (Marker)
S	DNA Synthesis phase
SAP	Shrimp Alkaline Phosphatase
SC	Synaptonemal Complex
SCC	Sister Chromatid Cohesion (Protein)
SDSA	Synthesis-Dependent Strand Annealing (Model)
SEI	Single End Invasion
SIC	Synapsis Inititation Complex
SMC	Structural Maintenance of Chromosomes (Protein)
SN	Supernatant
ssDNA	Single-Stranded DNA
T-DNA	transferred DNA (of the tumor-inducing (Ti) plasmid of *Agrobacterium tumefaciens*)
TF	Synaptonemal Complex Transverse Filament
TF	Transcription Factor
TSO	Target Site Overlap
TOPVIA	Archaeal Toposiomerase II Subunit VIA (Protein)
UAS	Upstream Activation Sequence
UTR	Untranslated Region
XPF	*Xeroderma Pigmentosum* Complementation Group F
ZF	Zinc-Finger
ZFN	Zinc-Finger Nuclease
ZMM	Zip, Mer, Msh (Protein Family Homolog)

9. Acknowledgments

First of all I want to thank my supervisor Dr. Peter Schlögelhofer. Thank you, Peter, for giving me the opportunity to work on this very interesting project. Thank you for your patience and motivation, and for your catching passion for science. Most of all, I am deeply grateful to be able to continue working on this project.

I want to thank Prof. Dr. Dieter Schweizer for fueling the interest of many students, including myself, in the field of plant genetics, for his lively and highly interesting lectures and for the examination of this thesis.

My thank goes to our external collaborators. I want to thank Andriy Tovkach and Tsvi Tzfira (Department of Molecular, Cellular and Developmental Biology, University of Michigan, Ann Arbor, MI, USA) for generation and *in-vitro* testing of 4x ZF domains, as well as for providing pSAT and pRCS2 vectors. I want to thank Maria Novatchkova (Bioinformatics unit, IMP - Research Institute of Molecular Pathology, Vienna, Austria) for her PZF binding prediction analysis. I want to thank Greg P. Copenhaver (Department of Biology, University of North Carolina, Chapel Hill, NC USA) for providing pollen based fluorescent recombination markers and Bert van der Zaal (Institute of Biology Leiden, Department of Molecular and Developmental Genetics, Leiden University, The Netherlands) for providing 6x ZF constructs.

Thank you, dear former and present colleagues for initial and ongoing scientific advice, for hours of scientific discussions, for your support, for competent cell aliquots, for the chocolate, for lessons in bavarian dialect, for your community and last but not least for the great time in our lab. Thank you Bernd, Clemens, Tesi, Tanja, Lisi, Stefan, Fritz, René, Ahmed, Connie, Dominik, Sandy, Wojtek, Drasko and all the other “Chromosomes”. Special thanks, Sveta for providing numerous *Arabidopsis* cell suspension culture aliquots.

Nicht zuletzt möchte ich meiner Familie für Ihr Verständnis und Ihre Unterstützung während meines gesamten Studiums danken. Mein größter Dank geht an Eva, Josef, Marieluise und Eugen. Vielend Dank für Eure Freundschaft, Motivation und Unterstützung in absolut jeder Lebenslage!

10. Curriculum vitae

Personal Information	
First name(s) / Surname	**Michael Peter Janisiw**
Address	Stavangergasse 2/1/54, A1220, Vienna, Austria
Telephone	+43(0)699/19465968 (mobile)
E-mail	Michael.Peter.Janisiw@univie.ac.at
Nationality	Austrian
Date of birth	November 10, 1974
Gender	Male
Marital Status	Single
Education	
June 2007 – August 2008	**Diploma Thesis** "Targeted Meiotic Recombination in *Arabidopsis thaliana*" (Dr. Peter Schloegelhofer) Department of Chromosome Biology University of Vienna, Austria
March 2002 – January 2008	**Study of Molecular Biology** Principal subjects Genetics, Cell Biology and Developmental Biology University of Vienna, Austria
October 1998 – March 2002	**Study of Chemistry** (1st part undergraduate courses) University of Vienna, Austria
September 1994 – June 1997	**Chemical and Environmental Engineering** (Kolleg für Technische Chemie und Umwelttechnik) Principal subjects Process and Environmental Engineering, Immission and Water Pollution Control, Analytical Chemistry Diploma examination June 2, 1997 (good pass) HBLVA for Chemical Industry XVII, Rosensteingasse, Vienna, Austria
September 1985 - June 1994	**A-Levels (Matura)** Bundesrealgymnasium II, Vereinsgasse, Vienna, Austria

Employment and Training

September 2001 – June 2005	**Research assistant** Multilocus SNP Genotyping, DNA Hybridization and Detection Techniques, Gene Expression Analysis Univ. Prof. Dipl-Ing. Dr. Christine Mannhalter Medical University of Vienna, Austria Clinical Institute of Medical and Chemical Laboratory Diagnostics
March 2001 – August 2001	**Research assistant** SNP Genotyping Dr. Anahit Anvari Medical University of Vienna, Austria Univ. Clinic of Neurology
October 1998 – January 2001	**Research assistant** Cell Surface Antigen Typing, Antibody Detection Techniques, Cell Sorting, Coagulation Assays Univ. Prof. Dr. Simon Panzer Medical University of Vienna, Austria Univ. Clinic of Blood Group Serology and Transfusion Medicine
September 1997 – September 1998	**Alternative Civilian Service** Vienna General Hospital, Austria
August 1996	**Internship at the Municipality of Vienna, Division of Environmental Protection** Training in sampling and trace analysis of water and air samples
July 1996	**Internship at the Vienna General Hospital, Clin. Department of Blood Group Serology** Training in thrombocyte surface antigen determination techniques

Authorships and Publications

Greisenegger S, Zehetmayer S, Bauer P, Endler G, Ferrari J, Lang W, Janisiw M, Steiner L, Cheng S, Lalouschek W, Mannhalter C. Polymorphisms in inflammatory genes and the risk of ischemic stroke and transient ischemic attack: results of a multilocus genotyping assay. *Clin Chem* (2009). vol. **55** (1) pp. 134-8.

Hsieh K, Lalouschek W, Schillinger M, Endler G, Reisinger M, Janisiw M, Lang W, Cheng S, Wagner O, Mannhalter C. Impact of alphaENaC polymorphisms on the risk of ischemic cerebrovascular events: a multicenter case-control study. *Clin Chem* (2005) vol. **51** (6) pp. 952-6.

Hsieh K, Funk M, Schillinger M, Endler G, Janisiw M, Reisinger M, Unger P, Greisenegger S, Lang W, Lalouschek W, Mannhalter C. Vienna Stroke Registry. Impact of the platelet glycoprotein Ib alpha Kozak polymorphism on the risk of ischemic cerebrovascular events: a case-control study. *Blood Coagul Fibrinolysis* (2004) vol. **15** (6) pp. 469-73.

Woelfer B, Schuchter K, Janisiw M, Hafner E, Philipp K, Panzer S. Postdelivery levels of anti-D IgG prophylaxis in D- mothers depend on maternal body weight. *Transfusion* (2004) vol. **44** (4) pp. 512-7.

Jilma-Stohlawetz P, Hergovich N, Homoncik M, Dzirlo L, Horvath M, Janisiw M, Panzer S, Jilma B. Impaired platelet function among platelet donors. *Thromb Haemost* (2001) vol. **86** (3) pp. 880-6.

Panzer S, Janisiw M, Fischer G, Jilma B. The platelet alpha2-integrin (GPIa) nucleotide-807 polymorphism is not associated with a risk for maternal-fetal human platelet antigen-5 incompatibility. *Ann Hematol* (2000) vol. **79** (6) pp. 296-8.

Anvari A, Janisiw M, Türel Z, Huber K, Fischer G, Panzer S. Platelet glycoprotein Ia gene dimorphism alpha2-807 in malignant arrhythmia in coronary artery disease. *Thromb Res* (2000) vol. **98** (4) pp. 281-6.

Vogelsang H, Suk EK, Janisiw M, Stain C, Mayr WR, Panzer S. Calcaneal ultrasound attenuation and vitamin-D-receptor genotypes in celiac disease. *Scand J Gastroenterol* (2000) vol. **35** (2) pp. 172-6.

Janisiw M, Eichelberger B, Koren D, Panzer S. Screening for platelet auto-antibodies by flow cytometry and their evaluation by the MAIPA technique. *Wien Klin Wochenschr* (1998) vol. **110** (15) pp. 531-4.

Sperr WR, Huber K, Roden M, Janisiw M, Lang T, Graf S, Maurer G, Mayr WR, Panzer S. Inherited platelet glycoprotein polymorphisms and a risk for coronary heart disease in young central Europeans. *Thromb Res* (1998) vol. **90** (3) pp. 117-2.

11. Zusammenfassung

Die sexuelle Reproduktion diploider Organismen benötigt Mechanismen zur korrekten Verteilung der paternalen und maternalen Chromosomen in den zu bildenden Keimzellen. Dieser Prozess findet im Rahmen der Meiose statt. Nach Replikation der Chromosomen führen zwei Schritte von Chromosmensegregationen zur Bildung von vier haploiden Gametenvorläufer-Zellen. Durch Rekombination von paternalen und maternalen Chromosomen wird während der Meiose die genetische Diversität erhöht. Dieser Prozess führt auch zur Ausbildung von Chiasmata, welche aus reziproken Rekombinationsereignissen hervorgehen, und ist essentiell für die korrekte Chromosomensegregation während der ersten meiotischen Teilung.

Das Schlüsselereignis dieses Prozesses, die kontrollierte Ausbildung von DNA Doppelstrangbrüchen, ist eine Voraussetzung für die nachfolgend stattfindende homologe Rekombination. Die Verteilung der DNA Doppelstrangbrüche ist nicht zufällig, da diese an diskreten Loci im Genom konzentriert sind – den ‚Hotspots' der meiotischen Rekombination. Das zentrale Protein im Rahmen der Induktion von Doppelstrangbrüchen ist das konservierte Enzym SPO11. In *Arabidopsis thaliana* wurden drei *SPO11* Gene identifiziert, von welchen *AtSPO11-1* und *AtSPO11-2* für die gezielte Einführung von DNA Doppelstrangbrüchen verantwortlich sind.

Das Hauptziel dieser Studie war, die Rekombinationsmaschinerie zu spezifischen Loci im Arabidopsis Genom zu dirigieren. Die dabei gewählte Strategie beinhaltet die Erzeugung verschiedener Fusionsproteine, in welchen *At*SPO11 N-terminal an Zink-Finger (ZF) DNA-Bindungsdomänen fusioniert wurde. Dadurch ist zu erwarten, dass induzierte DNA Doppelstrangbrüche verstärkt in der Region der spezifischen Zink-Finger DNA-Bindungsstelle erfolgen. Weiters auch, dass die nachfolgende DNA Reparatur zum Austausch von paternaler und maternaler genetischer Infomation an dem gewählten Locus führt

Es wurden verschiedene Zink-Finger Konstrukte hergestellt, welche an einen bestimmten endogenen Locus im Arabidopsis Genom binden. Die Einführung eines zusätzlichen c-*Myc* Epitops in die Konstrukte erlaubt dadurch eine biochemische Manipulation der Fusionsproteine. Die *At*SPO11-1-ZF Fusionsproteine wurden durch Komplementationsanalyse auf ihre Funktionalität getestet, und konnten die Funktion des endogenen *At*SPO11-1 Proteins übernehmen. In zukünftigen Experimenten ist weiters die Herstellung von *At*SPO11-2-ZF Fusionsproteinen geplant.

Unterschiedliche Tester-Linien welche *At*SPO11-ZF Konstrukte und gleichzeitig verschiedende Marker beinhalten, um die erwartete erhöhte Rekombinationsrate quantitativ zu bestimmen, wurden miteinander gekreuzt. Die Kreuzungsprodukte dienen der Detektion von induzierten Rekombinationsereignissen an dem ausgewählten Locus, einhergehend mit einem *trans* zu *cis* Austausch der Markerkonfiguration.